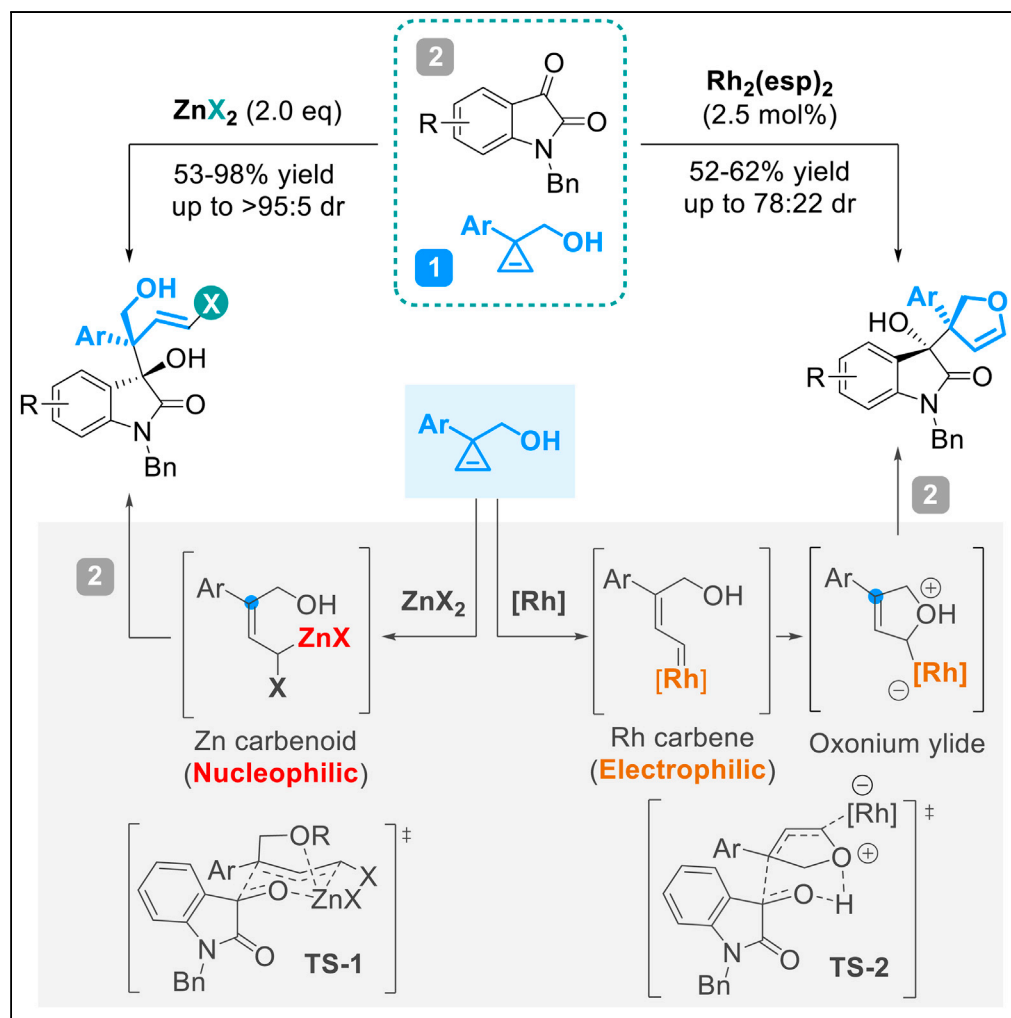


Article

Metal-Dependent Umpolung Reactivity of Carbenes Derived from Cyclopropenes



Dan Zhang,
Zhenghui Kang,
Junwen Liu,
Wenhao Hu

huwh9@mail.sysu.edu.cn

HIGHLIGHTS
Metals reverse the
reactivity of carbenes

Nucleophilic zinc
carbenoids

Reactive carbenoid and
ylide intermediates are
trapped by electrophiles

Chemodivergent
synthesis



Article

Metal-Dependent Umpolung Reactivity of Carbenes Derived from Cyclopropenes

Dan Zhang,¹ Zhenghui Kang,¹ Junwen Liu,¹ and Wenhao Hu^{1,2,*}

SUMMARY

Metal carbenes, divalent carbon species, are versatile intermediates that enable novel synthetic pathways. These species exhibit either electrophilic or nucleophilic character, depending on the carbene and metal fragments. Although the metal carbene reactivity is regulated by the metal, the umpolung of carbene reactivity by changing metal remains challenging. Here, we report a unique metal-induced *de novo* umpolung of carbene reactivity, wherein a carbene precursor can be transformed into either an electrophilic carbene or a nucleophilic carbenoid, depending on the metal promoters. Thus, a chemodivergent reaction of isatins and cyclopropenes is developed. Under the promotion of Zn²⁺ halides, a nucleophilic zinc carbenoid is formed and trapped by isatins to produce oxindole derivatives containing an alkenyl halide moiety. Using Rh₂(esp)₂ as a catalyst, the reaction delivers oxindoles carrying a dihydrofuran unit. This work provides a facile approach to harness the metal carbene reactivity and is critical for the development of diversity-oriented synthesis.

INTRODUCTION

Transition metal carbenes and carbenoids, which are highly reactive and versatile intermediates, have inspired and stimulated a number of research activities in chemistry (Dorwald, 1999; Moss and Doyle, 2014). These intermediates can participate in diverse chemical reactions, including C-H and X-H (X = O, N, Si, B, P, etc.) insertions, cyclopropanations, cycloadditions, and ylide formation and further transformations. Beyond the typical carbene reactions, many unique conversions have been reported in recent decades, for example, carbene migratory insertions (Xia et al., 2017) and gold-carbene-mediated annulations (Obradors and Echavarren, 2014). These studies can enable powerful synthetic pathways in diversity-oriented synthesis, total synthesis, and pharmaceutical process development, making this field dynamic for development purposes (Bertrand, 2002; Chiu, 2005; Bien et al., 2018).

The diverse reactivity profile of transition metal carbenes originates from their unique structures of a divalent carbon atom with two unshared valence electrons, paired or unpaired, with a broad range of different reactivities and diverse substituents (Grubbs et al., 2003). Typically, these complexes can be simply classified as Fischer carbenes and Schrock carbenes (alkylidenes), of which the former is often considered electrophilic and the latter is generally nucleophilic (Dötz and Stendel, 2009; Schrock, 2002; Mindiola and Scott, 2011). The borderline between traditional Fischer and Schrock carbenes is the non-heteroatom-stabilized carbene bound to late transition metals (Figure 1A) (de Frémont et al., 2009), which is usually electrophilic at the carbene center in contrast with the Schrock carbene. This kind of carbene, with intermediate characteristics and reactivity profiles, has emerged as one of most attractive research topics to discover new transformations (Dorwald, 1999; Moss and Doyle, 2014). Another reactive intermediate that exhibits the reaction characteristics of a carbene without the necessary divalent carbon center is the carbenoid (Figure 1B) (Closs and Moss, 1962; Gessner, 2016), which possesses a leaving group and a metal connected to the same carbon, displaying both electrophilic and nucleophilic characteristics. The unique and diverse structural characteristics of these carbene species comprises the foundation of diverse reactivity profiles.

Generally, due to the distinctly different structural features of different types of carbene and carbenoid species, it is quite challenging to generate more than one type of species from the same precursor, and different metals only modulate the level of electrophilicity (or nucleophilicity) rather than reversing the polarity (Cheng and Doyle, 2016). As an exceptional example, 3,3-diphenylcyclopropene was converted to an electrophilic rhodium carbene intermediate and a nucleophilic Schrock carbene complex by Wang (Zhang et al., 2015b) and Grubbs (Johnson et al., 1993), respectively, but the latter was not used as a synthetic intermediate for further transformations. Considering this fact, we envisioned the controllable formation of both electrophilic and nucleophilic carbene species from the same reactant via alteration of the metal,

¹Guangdong Key Laboratory of Chiral Molecule and Drug Discovery, School of Pharmaceutical Sciences, Sun Yat-Sen University, Guangzhou 510006, China

²Lead Contact

*Correspondence:
huwh9@mail.sysu.edu.cn

<https://doi.org/10.1016/j.isci.2019.04.001>



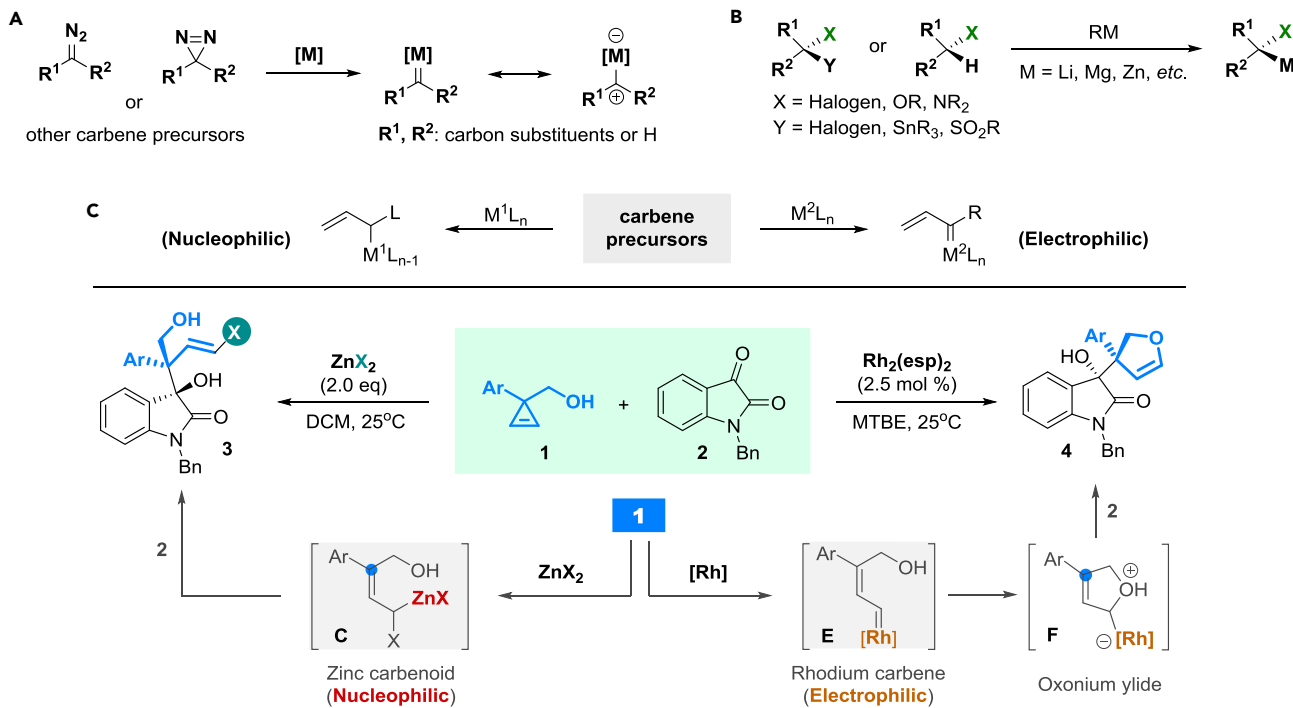


Figure 1. Metal Carbene Intermediates and Their Reactivities

(A) Non-heteroatom-stabilized carbene: electrophilic.

(B) Carbenoid: ambiphilic.

(C) This work: metal-induced *de novo* umpolung of carbene reactivity.

followed by divergent interception of these intermediates, which would enable the discovery of novel chemodivergent reactions. Herein, we report the metal-induced *de novo* umpolung of carbene reactivity (Figure 1C), in which a carbene precursor (cyclopropene) could be transformed to either an electrophilic carbene or a nucleophilic carbenoid, depending on the metal catalysts. Furthermore, trapping these electrophilic and nucleophilic carbene species affords structurally diverse molecules in a single step. This work provides an efficient strategy to harness the reactivity of metal carbenes and is critical for the development of diversity-oriented synthesis.

Diazo compounds are the most convenient and widely used carbene precursors owing to their high reactivity and diverse structural features (Zollinger, 1995; Doyle et al., 1998). However, in the absence of an electron-withdrawing group adjacent to the diazo moiety, such as diazo alkanes or alkenes, the compound suffers severe stability and safety issues (Battilocchio et al., 2016; Greb et al., 2017), which greatly limit its access and applications. As an alternative strategy, non-diazo carbene precursors have attracted considerable interest over the last decades (Jia and Ma, 2016; Ma et al., 2016; Wang and Wang, 2019). Cyclopropene, a reliable and easy-to-handle precursor, could generate vinyl carbene in a safe, mild, and practical way with a 100% atom economy via transition metal-catalyzed ring-opening rearrangement (Rubin et al., 2007; Archambeau et al., 2015; Vicente, 2016; Benitez et al., 2009). Furthermore, the unique vinyl functionality could offer new opportunities to discover new transformations. Thus, we depict here the differentiated reactivities of vinyl carbene derived from cyclopropene with zinc or rhodium complexes as promoters (Figure 1C). For the zinc halide-promoted reaction, the generated ambiphilic zinc carbenoid (Pasco et al., 2013; Nishimura et al., 2015), which is the key intermediate in the Simmons-Smith (SS) reaction (Denmark et al., 1991, 1992), shows a nucleophilic character and undergoes nucleophilic attack to isatins without elimination of the halogen atom, delivering oxindole derivatives 3 containing a synthetically valuable alkynyl halide moiety. Importantly, despite the theoretical nucleophilicity, the nucleophilic reactivity of the zinc carbenoid without elimination of halogen atoms has never been achieved (Knochel et al., 1989; Retherford et al., 1989), which provides unique access to alkynyl halides using inexpensive and non-toxic zinc halides as halogenating agents under very mild conditions. On the other hand, in the case of rhodium catalysis, the

reaction forms an electrophilic Rh-carbene, followed by an ylide formation and trapping process (Guo and Hu, 2013; Zhang et al., 2015a) to give product **4**. Remarkably, although we have developed various electrophilic trapping processes of active ylide intermediates (Guo and Hu, 2013; Zhang et al., 2015a), this is the first interception of the active ylide without an α -carbonyl group that is deemed essential for stabilization and trapping of the ylide. Overall, this controllable metal-induced *de novo* umpolung of carbene reactivity presents an efficient approach for chemodivergent synthesis.

RESULTS AND DISCUSSION

Optimization of Reaction Conditions

We commenced our study by exploring the reaction of 3-hydroxymethyl-3-phenylcyclopropene (Rubina et al., 2004; Selvaraj et al., 2014) **1a** with isatin **2a** under the activation of various metal catalysts in different reaction conditions. When the reaction was conducted with catalytic $ZnCl_2$ (0.1 equiv.) (González et al., 2015) in CH_2Cl_2 , the reaction only resulted in a trace amount of **3a** (Table 1, entries 1 and 2), but increasing the loading of $ZnCl_2$ (2.0 equiv.) gave rise to **3a** in 84% yield with a 92:8 diastereomeric ratio (dr) and complete *E*-selectivity in 10 min (Table 1, entries 3–6). Further optimizations did not improve the results (Table 1, entries 7–11). Interestingly, when catalytic $Rh_2(esp)_2$ was selected as the catalyst in CH_2Cl_2 , dihydrofuryl 3-hydroxyl oxindole **4a**, the trapping product of oxonium ylide, was obtained in 45% yield with 73:27 diastereomeric ratio (dr), whereas other metal catalysts, such as $Rh_2(OAc)_4$, $Rh(COD)Cl_2$, or $(PPh_3)AuNTf_2$, did not provide detectable amounts of product (Table 1, entries 12–15). The yield of **4a** was increased to 60% after screening the solvents, indicating methyl tert-butyl ether (MTBE) as the optimal solvent (Table 1, entries 16–20). The divergent reaction pathways switched by the catalyst or reagent will enhance the utility of this reaction in organic synthesis.

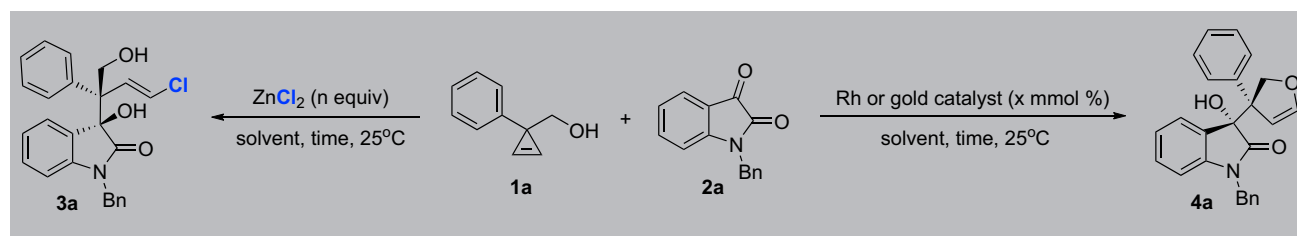
Substrate Scope

We then investigated the scope of substrates under the promotion of zinc halides (Figure 2). First, $ZnCl_2$, $ZnBr_2$, and ZnI_2 were tested, and all gave corresponding halide three-component products **3a**–**3c** in good yields (82%–89%) with dr up to 94:6. Notably, the introduction of a vinyl halide moiety greatly improved the synthetic utility of the desired products **3** because they are beneficial for further transformations through coupling reactions to prepare more functionalized molecules.

Next, we assessed the substituents on cyclopropenes. Electron-withdrawing groups at the *para*-position (4-F, 4-Cl, and 4-Br) and *meta*-position (3-Br) of the aryl group were tolerated and afforded the desired products (**3d**–**3g**, **3k**) with equally good results (76%–91%, up to 94:6 dr) except for the compound with a 2-Br functionality (**3h**). The substrates with a dichloro-substituted phenyl or *p*-Tol also worked well to provide the corresponding product **3i**–**3j** in 93%–95% yield with 95:5 diastereoselectivity. Moreover, when the free hydroxyl group of cyclopropene was capped by a methyl group, the reaction proceeded smoothly as well (**3l**). In addition, blocking the hydroxyl group with an acetyl (Ac) or removal of the oxygen functionality from cyclopropene had no deleterious effect on the yield and selectivities of **3m**–**3n**, although an extension of the reaction time to 12 h was required. The remarkable rate acceleration of alcohol and ether substrates should be attributed to a complex-induced proximity effect (CIPE) (Denmark et al., 1992; Beak and Meyers, 1986).

Subsequently, the scope of isatins was also examined. Delightedly, various substituents on the aromatic ring of isatins, regardless of whether the substituent was chloride, bromide, fluoride, methyl, or methoxyl at the C4-, C5-, C6-, or C7-positions, were tolerated to afford **3o**–**3w** in excellent yields with high diastereoselectivity (up to 94% yield and 95:5 dr, respectively). With regard to the *N*-substitution, both *N*-methyl and *N*-acetyl isatins were transformed into the corresponding halide alkenyl oxindoles **3x** or **3y** in good yield with a high dr value. Moreover, this transformation was also tolerant of the *N*-unprotected isatin to produce the desired product **3z** in 78% yield with a diminished dr of 76:24.

Finally, we also studied the scope of the $Rh_2(esp)_2$ -catalyzed reaction of cyclopropenes with isatins. As the retro-alcohol reaction of **4** occurred during silica chromatography isolation, the reaction yield was determined by crude 1H nuclear magnetic resonance imaging. As shown in Figure 2, **4a** and **4b** were obtained in moderate yields with acceptable dr values. To stabilize the product, crude **4a**, **4c**, and **4d** were methylated using Mg/NaH in a one-pot manner to provide the stable products **4a'** (52%, 73:27 dr), **4c'** (62%, 78:22 dr), and **4d'** (77%, 62:38 dr), respectively. Moreover, the relative configuration of **4** was determined by single-crystal X-ray diffraction analysis of **4b**. To examine the electrophilic reactivity of the rhodium vinyl



Entry	Metal Complex	Solvent	Time	Yield of 3a (%) ^{a,b}	dr ^c	Yield of 4a (%) ^{a,b}	dr ^c
1	ZnCl ₂ (0.1 equiv.)	CH ₂ Cl ₂	5 h	<5	—	—	—
2	ZnCl ₂ (0.5 equiv.)	CH ₂ Cl ₂	5 h	18	92:8	—	—
3	ZnCl ₂ (1.0 equiv.)	CH ₂ Cl ₂	1 h	47	92:8	—	—
4	ZnCl ₂ (1.5 equiv.)	CH ₂ Cl ₂	10 min	57	92:8	—	—
5	ZnCl ₂ (2.0 equiv.)	CH ₂ Cl ₂	10 min	87 (84 ^d)	92:8	—	—
6	ZnCl ₂ (3.0 equiv.)	CH ₂ Cl ₂	10 min	76	92:8	—	—
7	ZnCl ₂ (2.0 equiv.)	CHCl ₃	10 min	74	94:6	—	—
8	ZnCl ₂ (2.0 equiv.)	(CH ₂ Cl) ₂	10 min	71	94:6	—	—
9	ZnCl ₂ (2.0 equiv.)	toluene	10 h	41	—	—	—
10	ZnCl ₂ (2.0 equiv.)	n-hexane	10 h	<5	—	—	—
11 ^e	ZnCl ₂ (2.0 equiv.)	CH ₂ Cl ₂	10 min	67	92:8	—	—
12	Rh ₂ (OAc) ₄ (5.0 mmol%)	CH ₂ Cl ₂	12 h	—	—	<5	—
13	Rh ₂ (COD)Cl ₂ (5.0 mmol%)	CH ₂ Cl ₂	12 h	—	—	<5	—
14	Rh ₂ (esp) ₂ (5.0 mmol%)	CH ₂ Cl ₂	2 h	—	—	45	73:27
15	AuPPh ₃ NTf ₂ (5.0 mmol%)	CH ₂ Cl ₂	2 h	—	—	<5	—
16	Rh ₂ (esp) ₂ (5.0 mmol%)	CHCl ₃	2 h	—	—	38	70:30
17	Rh ₂ (esp) ₂ (5.0 mmol%)	(CH ₂ Cl) ₂	2 h	—	—	28	70:30
18	Rh ₂ (esp) ₂ (5.0 mmol%)	THF	20 h	—	—	41	75:25
19	Rh ₂ (esp) ₂ (5.0 mmol%)	MTBE	2 h	—	—	62	75:25
20	Rh ₂ (esp) ₂ (2.5 mmol%)	MTBE	3 h	—	—	60	75:25

Table 1. Optimization of Reaction Conditions for the Divergent Reaction of 1a and 2a

dr, diastereomeric ratio; COD: 1,5-cyclooctadiene; esp: $\alpha,\alpha,\alpha',\alpha'$ -tetramethyl-1,3-benzenedipropionic acid; THF, tetrahydrofuran; NMR, nuclear magnetic resonance.

^aRatio of substrates, 1a:2a = 2:1.

^bYields are determined by ¹H NMR spectroscopy using 1,3,5-trimethoxybenzene as the internal standard.

^cDetermined by ¹H NMR analysis of the crude mixture.

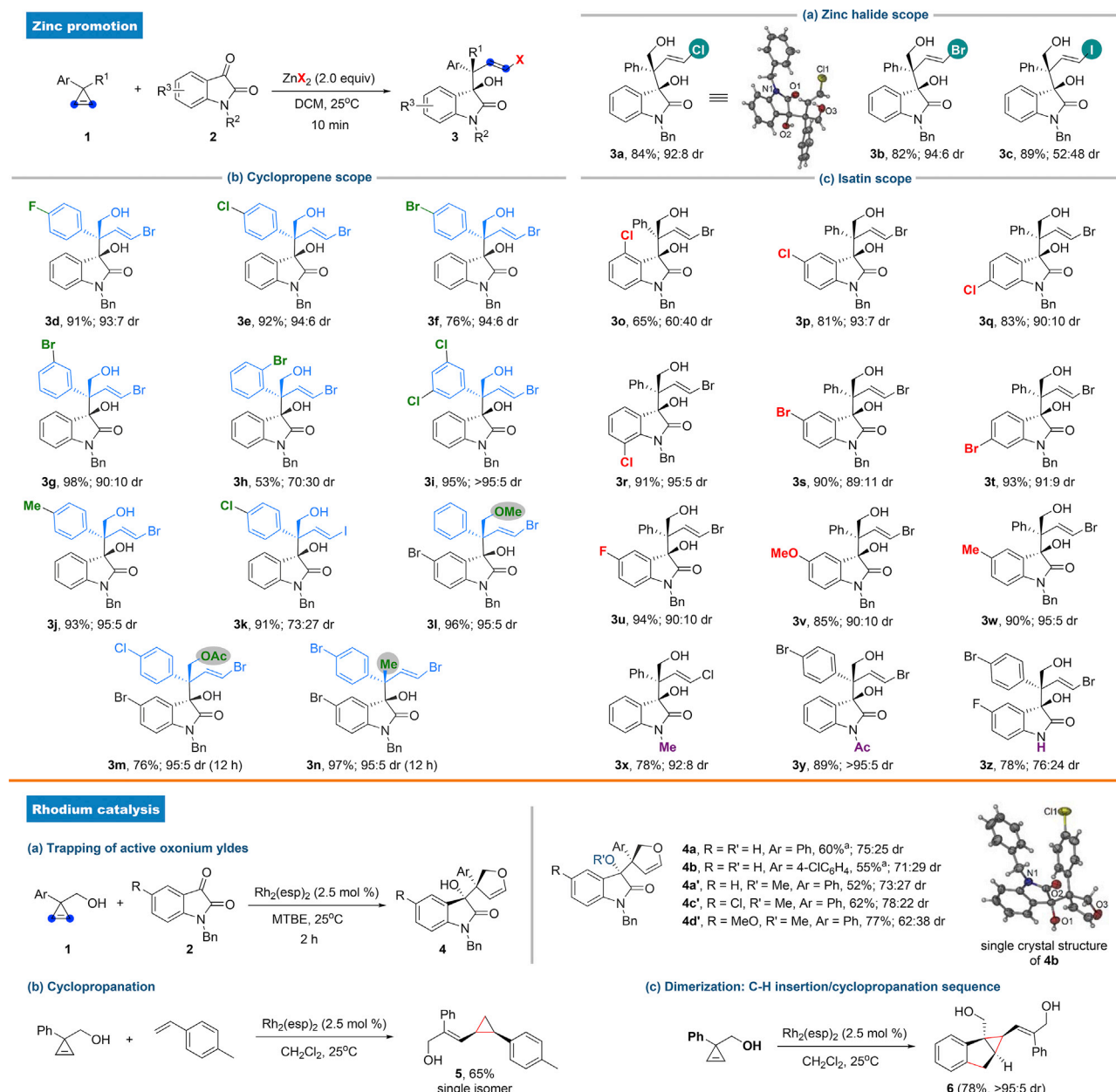
^dIsolated yield.

^eRatio of substrates, 1a:2a = 1.5:1.

carbene, cyclopropanation, a classical reaction of electrophilic metal carbenes, was conducted to afford the corresponding cyclopropane **5** in 65% yield. Furthermore, treatment of **1a** with Rh₂(esp)₂ in CH₂Cl₂ resulted in dimer **6** in 78% yield via a C-H insertion/cyclopropanation sequence, which was suppressed by using MTBE as the solvent in the reaction of **1** and **2**.

Transformation of Products

To demonstrate the synthetic utility of this reaction, a gram-scale synthesis of **3b** and **3c** was achieved in 76% (96:4 dr) and 90% yield (55:45 dr), respectively. The alkenyl halides **3b** and **3c** were then used as

**Figure 2. Scope of the Reactions Induced by Zinc Halides (top) or Rh₂(esp)₂ (bottom)**^a Yields are determined by ¹H NMR spectroscopy using 1,3,5-trimethoxybenzene as the internal standard.

coupling partners for further transformations (Figure 3). For example, Pd-catalyzed cross-coupling of 3c with 4-methoxyphenylboronic acid, *n*-C₄H₉ZnBr, TMSC≡CH, or vinyltributyltin at 25°C gave cross-coupling products 7a–7d in moderate to excellent yields of 60%–90%.

Mechanistic Discussion

In a seminal study of zinc halide-catalyzed transformations with cyclopropene by López and Vicente (González et al., 2015) and Doyle (Deng et al., 2016), an electrophilic zinc vinylcarbene A (Figure 5) was proposed as the key intermediate, whereas for the diazo-involved SS reaction (Wittig and Schwarzenbach, 1959; Goh et al., 1969; Crumrine et al., 1975; Lévesque et al., 2014) and a theoretical study by Bernardi and Bottoni (Bernardi et al., 2000), the halogen of zinc carbene would further transfer to the carbon atom to form

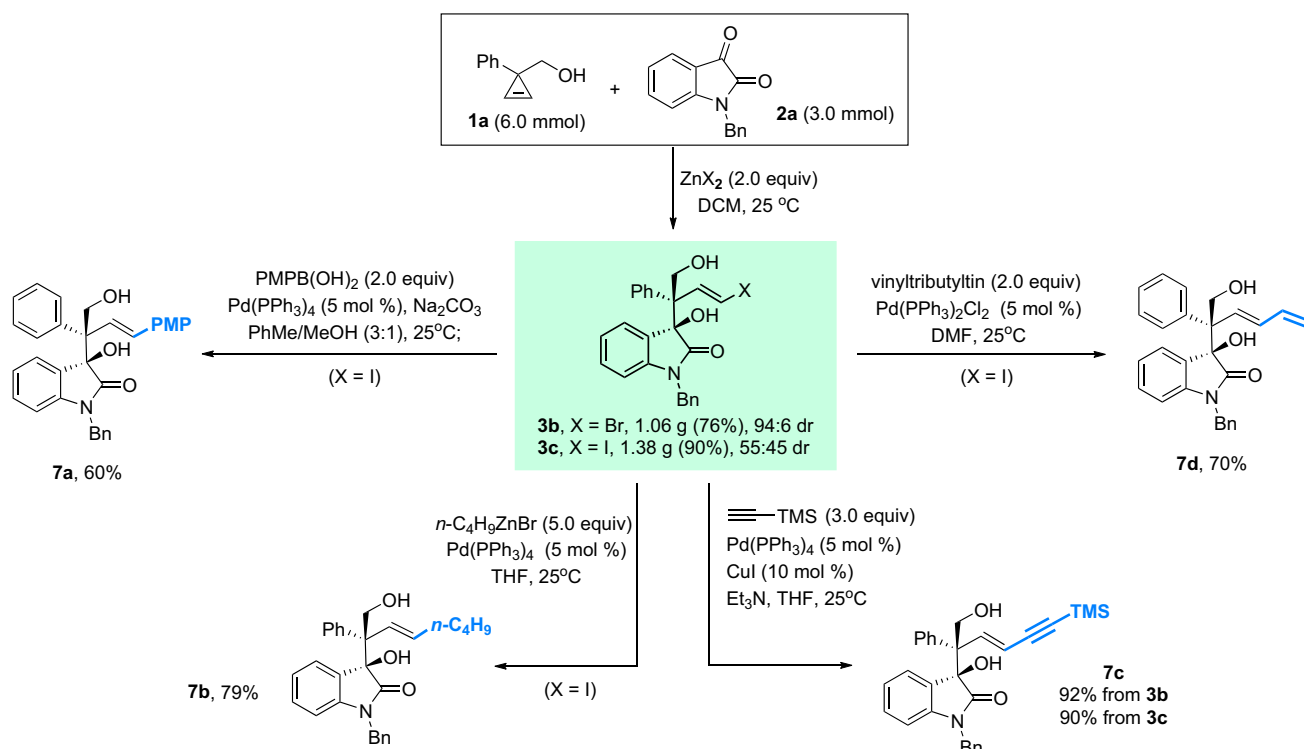


Figure 3. Gram-scale Synthesis and Derivatization of Products

ambiphilic zinc carbenoid, the actual SS reagent (Denmark et al., 1991, 1992). To obtain further insight into the properties of the proposed intermediate of our reaction, a competing reaction was conducted in which 1.0 equiv. of 4-methylstyrene was added to a mixture of **1a** and **2a** under the standard conditions of zinc catalysis (Figure 4A). The reaction yielded 63% **3b**, accompanied by 32% yield of cyclopropane **Z-5**. Although the cyclopropane product is considered to be generated from the electrophilic zinc vinylcarbene **A** according to López and Vicente (González et al., 2015), it should be the ambiphilic zinc

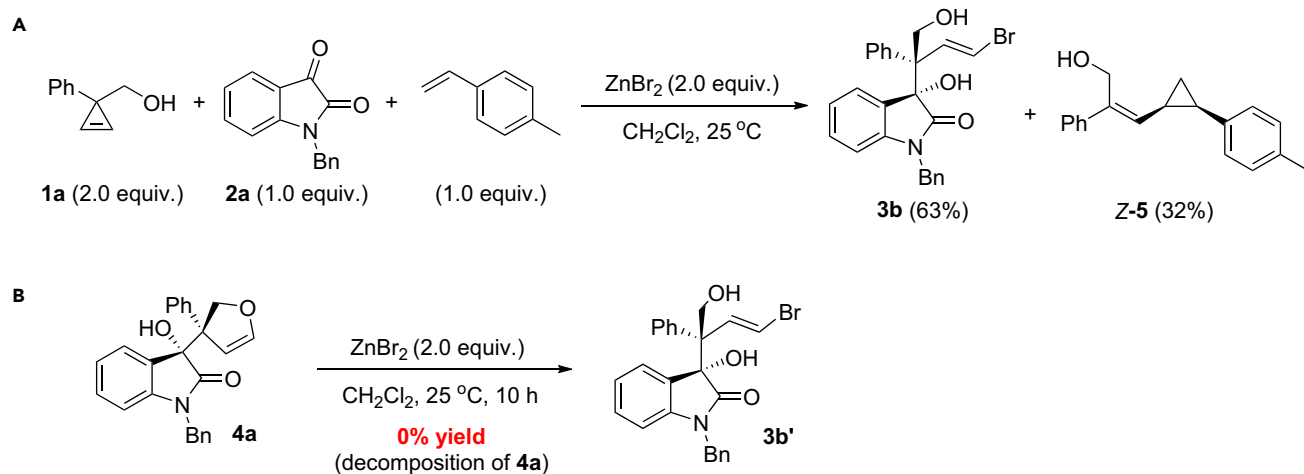
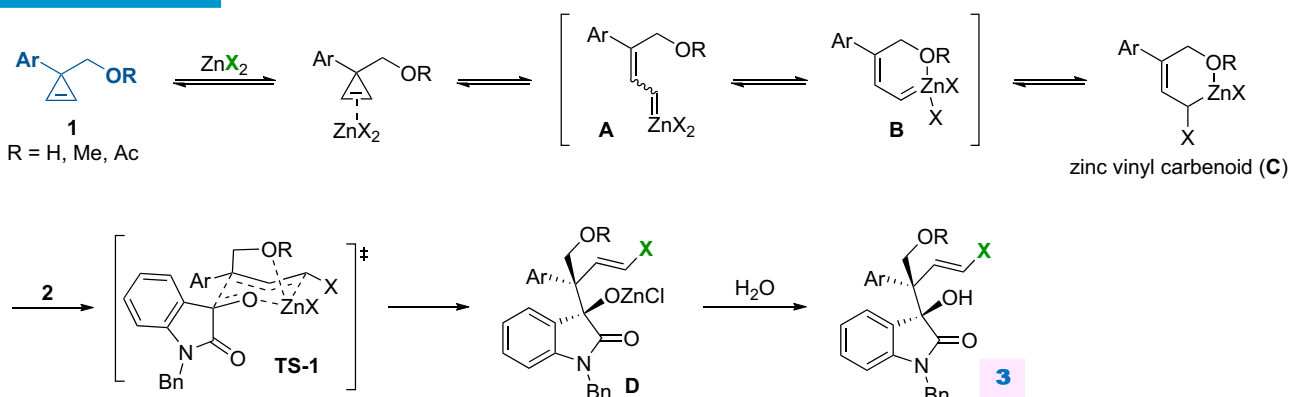
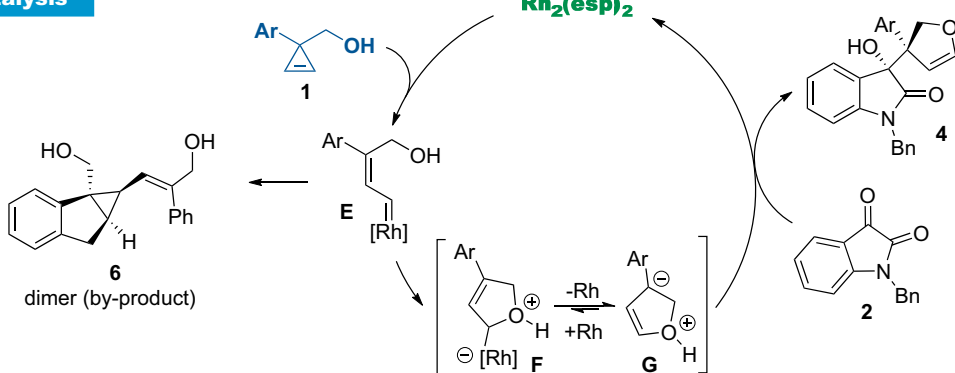


Figure 4. Control Reactions

(A) Competing reaction.

(B) Conversion of **4a** under the standard conditions of zinc catalysis.

A Zinc Promotion**B Rhodium catalysis****Figure 5. Mechanistic Proposals**

- (A) Zinc-promoted reaction.
(B) $\text{Rh}_2(\text{esp})_2$ -catalyzed reaction.

vinylcarbenoid, which presents unique nucleophilic reactivity in this reaction, that leads to adduct **3**. Furthermore, the treatment of **4a** with ZnBr_2 under the standard conditions was not able to give **3e'**, negating the possible pathway that **3** was derived from ZnBr_2 -promoted ring-opening or bromination of **4** (Figure 4B). According to this observation and the formation of **3l-3n**, we hypothesized that the ambiphilic zinc vinylcarbenoid **C** is the key intermediate in our research. As for the rhodium-catalyzed process, the formation of **5** and **6** (Figure 2), as well as the reported process by Cossy (Archambeau et al., 2015), supported rhodium vinylcarbene as the intermediate.

Mechanistic Proposal

Based on the control reactions and the discussions above, a proposed reaction pathway is depicted in Figure 5. For the zinc promotion process (Figure 5A), zinc halide coordinates to cyclopropane **1** and induces ring-opening rearrangement to generate a zinc vinyl carbene **A** or the cyclic **B**, in which the oxygen functionality coordinates to zinc(II) and greatly accelerates the rate of the subsequent process via the CIPE. Subsequently, halogen migration of **B** results in the ambiphilic zinc carbeneoid **C**, which undergoes nucleophilic addition to isatins **2** via a six-membered transition state (Vabre et al., 2015) **TS-1** to afford alkenyl halide adduct **D** that gives rise to the final product **3** during workup with water. For the rhodium-catalyzed process (Figure 5B), $\text{Rh}_2(\text{esp})_2$ promotes cyclopropane **1** to generate carbene **E**, which converts to the cyclic oxonium ylide **F** or the more stable **G**. Finally, nucleophilic addition of intermediate **G** to isatin **2** leads to trapping of the product **4** along with the regeneration of the rhodium(II) catalyst. This is the first report on the trapping of an active ylide without an α -carbonyl group that is considered indispensable for stabilizing the proposed intermediate (Guo and Hu, 2013; Zhang et al., 2015a).

Limitations of Study

Zinc fluoride is not effective for the zinc-promoted process.

Conclusion

We reveal a unique *de novo* umpolung of carbene reactivity via alteration of the metal. Based on this process, a unique chemodivergent aldol-type reaction of isatins with 3-hydroxymethyl-3-arylpropenes is achieved, wherein cyclopropene as a carbene precursor can be converted to either an electrophilic rhodium carbene or a nucleophilic zinc carbenoid. Trapping of these carbene species allows for the facile, rapid, and efficient synthesis of structurally diversified oxindole derivatives with a synthetically important alkenyl halide moiety or a dihydofuran unit in good yields with high stereo- and chemoselectivities. Significantly, the ambiphilic zinc vinyl carbenoid generated from cyclopropene and zinc halides undergoes a rare nucleophilic addition to electrophiles, which provides an efficient approach to *E*-selective alkenyl halides from inexpensive and non-toxic zinc halides under mild conditions. Moreover, electrophilic trapping of gem-halovinylzinc can extend the utilities of SS intermediates. This study provides an efficient approach to harness the reactivity of metal carbenes, therefore enriching the versatile carbene chemistry.

METHODS

All methods can be found in the accompanying [Transparent Methods supplemental file](#).

DATA AND SOFTWARE AVAILABILITY

The structures of **3a**, **3n**, **4b**, and **6** reported in this article have been deposited in the Cambridge Crystallographic Data Center under accession numbers CCDC: 1862658, 1862655, 1862657 and 1862654, respectively.

SUPPLEMENTAL INFORMATION

Supplemental Information can be found online at <https://doi.org/10.1016/j.isci.2019.04.001>.

ACKNOWLEDGMENTS

This work was supported by the Program for Guangdong Introducing Innovative and Entrepreneurial Teams (No. 2016ZT06Y337). We thank Prof. Yian Shi (Colorado State University) for helpful discussions, Yunyun Chen (Sun Yat-Sen University) for analysis of single-crystal X-ray diffraction data, and Dr. Xin Wang (Sun Yat-Sen University) for assistance in some experiments.

AUTHOR CONTRIBUTIONS

D.Z. planned, conducted, and analyzed the experiments. Z.K. and J.L. assisted with some experiments. W.H. directed the project. D.Z. and W.H. wrote the manuscript.

DECLARATION OF INTERESTS

The authors declare no competing interests.

Received: February 9, 2019

Revised: March 20, 2019

Accepted: March 30, 2019

Published: April 26, 2019

REFERENCES

- Archambeau, A., Miege, F., Meyer, C., and Cossy, J. (2015). Intramolecular cyclopropanation and C–H insertion reactions with metal carbenoids generated from cyclopropenes. *Acc. Chem. Res.* **48**, 1021–1031.
- Battilocchio, C., Feist, F., Hafner, A., Simon, M., Tran, D.N., Allwood, D.M., Blakemore, D.C., and Steven, V.L. (2016). Iterative reactions of transient boronic acids enable sequential C–C bond formation. *Nat. Chem.* **8**, 360–367.
- Beak, P., and Meyers, A.I. (1986). Stereo- and regiocontrol by complex induced proximity effects: reactions of organolithium compounds. *Acc. Chem. Res.* **19**, 356–363.
- Benitez, D., Shapiro, N.D., Tkatchouk, E., Wang, Y., Goddard, W.A., III, and Toste, F.D. (2009). A bonding model for gold(I) carbene complexes. *Nat. Chem.* **1**, 482–486.
- Bernardi, F., Bottini, A., and Mischion, G.P. (2000). Metal carbene or carbenoid complexes? A theoretical study of the active form of transition metal catalysts in cyclopropanation and olefin metathesis reactions. *Organometallics* **19**, 5529–5532.
- Bertrand, G. (2002). *Carbene Chemistry: From Fleeting Intermediates to Powerful Reagents* (CRC Press).

- Bien, J., Davulcu, A., DelMonte, A.J., Fraunhofer, K.J., Gao, Z., Hang, C., Hsiao, Y., Hu, W., Katipally, K., Littke, A., et al. (2018). The first kilogram synthesis of beclabuvir, an HCV NS5B polymerase inhibitor. *Org. Process. Res. Dev.* 22, 1393–1408.
- Cheng, Q.-Q., and Doyle, M.P. (2016). The selection of catalysts for metal carbene transformations. *Adv. Organomet. Chem.* 66, 1–31.
- Chiu, P. (2005). Application of the carbene cyclization–cycloaddition cascade in total synthesis. *Pure Appl. Chem.* 77, 1183–1189.
- Closs, G.L., and Moss, R.A. (1962). Carbenoid formation of arylcyclopropanes from olefins, benzal bromides, and organolithium compounds and from photolysis of aryl diazomethanes. *J. Am. Chem. Soc.* 86, 4042–4053.
- Crumrine, D.S., Haberkamp, T.J., and Sutherl, D.J. (1975). Arylsulfonylation of aromatic compounds. VI. Decomposition of m-trifluoromethylbenzenesulfonyl peroxide in the absence of solvent and in the presence of ethylbenzene and cumene. *J. Org. Chem.* 40, 2274–2278.
- de Frémont, P., Marion, N., and Nolan, S.P. (2009). Carbenes: synthesis, properties, and organometallic chemistry. *Coordin. Chem. Rev.* 253, 862–892.
- Deng, Y., Jing, C., Arman, H., and Doyle, M.P. (2016). Reactivity and selectivity in catalytic reactions of enoldiazoacetamides. assessment of metal carbenes as intermediates. *Organometallics* 35, 3413–3420.
- Denmark, S.E., Edwards, J.P., and Wilson, S.R. (1991). Solution and solid-state structure of the “Wittig-Furukawa” cyclopropanation reagent. *J. Am. Chem. Soc.* 113, 723–725.
- Denmark, S.E., Edwards, J.P., and Wilson, S.R. (1992). Solution- and solid-state structural studies of (halomethyl)zinc reagents. *J. Am. Chem. Soc.* 114, 2592–2602.
- Dorwald, F.Z. (1999). Metal Carbenes in Organic Synthesis (Wiley-VCH).
- Dötz, K.H., and Stendel, J., Jr. (2009). Fischer carbene complexes in organic synthesis: metal-assisted and metal-templated reactions. *Chem. Rev.* 109, 3227–3274.
- Doyle, M.P., McKervey, M., and Ye, T. (1998). Modern Catalytic Methods for Organic Synthesis with Diazo Compounds: From Cyclopropanes to Ylides (Wiley).
- Gessner, V.H. (2016). Stability and reactivity control of carbenoids: recent advances and perspectives. *Chem. Commun. (Camb.)* 52, 12011–12023.
- Goh, S.H., Closs, L.E., and Closs, G.L. (1969). Carbenoid decomposition of aryl diazomethanes with lithium and zinc halides. A convenient method for the synthesis of arylcyclopropanes. *J. Org. Chem.* 34, 25–31.
- González, M.J., González, J., López, L.A., and Vicente, R. (2015). Zinc-catalyzed alkene cyclopropanation through zinc vinyl carbenoids generated from cyclopropenes. *Angew. Chem. Int. Ed.* 54, 12139–12143.
- Greb, A., Poh, J.-S., Greed, S., Battilocchio, C., Pasau, P., Blakemore, D.C., and Ley, S.V. (2017). A versatile route to unstable diazo compounds via oxadiazolines and their use in aryl–alkyl cross-coupling reactions. *Angew. Chem. Int. Ed.* 56, 16602–16605.
- Grubbs, R.H., Trnka, T.M., and Sanford, M.S. (2003). Transition metal–carbene complexes in olefin metathesis and related reactions. In *Current Methods in Inorganic Chemistry*, vol. 3, H. Kuroawa and A. Yamamoto, eds. (Elsevier Science B.V), pp. 187–231.
- Guo, X., and Hu, W. (2013). Novel multicomponent reactions via trapping of protic onium ylides with electrophiles. *Acc. Chem. Res.* 46, 2427–2440.
- Jia, M., and Ma, S. (2016). New approaches to the synthesis of metal carbenes. *Angew. Chem. Int. Ed.* 55, 9134–9166.
- Johnson, L.K., Grubbs, R.H., and Ziller, J.W. (1993). Synthesis of tungsten vinyl alkylidene complexes via the reactions of $WCl_2(NAr)(PX_3)_3$ ($X = R, OMe$) precursors with 3,3-disubstituted cyclopropenes. *J. Am. Chem. Soc.* 115, 8130–8145.
- Knochel, P., Chou, T.-S., Chen, H.G., Yeh, M.C.P., and Rozema, M.J. (1989). Nucleophilic reactivity of zinc and copper carbenoids. 2. *J. Org. Chem.* 54, 5202–5204.
- Lévesque, É., Goudreau, S.R., and Charette, A.B. (2014). Improved zinc-catalyzed Simmons-Smith reaction: access to various 1,2,3-trisubstituted cyclopropanes. *Org. Lett.* 16, 1490–1493.
- Ma, J., Zhang, L., and Zhu, S. (2016). Enynal/enynone: a safe and practical carbenoid precursor. *Curr. Org. Chem.* 20, 102–118.
- Mindiola, D.J., and Scott, J. (2011). Spot the difference. *Nat. Chem.* 3, 15–17.
- Moss, R.A., and Doyle, M.P. (2014). *Contemporary Carbene Chemistry* (John Wiley & Sons).
- Nishimura, R.H.V., Murie, V.E., Soldi, R.A., Lopes, J.L.C., and Clososki, G.C. (2015). Zinc, lithium and magnesium carbenoids: chemical properties and relevant applications in organic synthesis. *J. Braz. Chem. Soc.* 26, 2175–2188.
- Obradors, C., and Echavarren, A.M. (2014). Gold-catalyzed rearrangements and beyond. *Acc. Chem. Res.* 47, 902–912.
- Pasco, M., Gilboa, N., Mejuch, T., and Marek, I. (2013). The Renaissance of zinc carbenoid in stereoselective synthesis in acyclic systems. *Organometallics* 32, 942–950.
- Rutherford, C., Yeh, M.C.P., Schipor, I., Chen, H.G., and Knochel, P. (1989). The addition of the highly functionalized zinc, copper reagents $RCu(CN)ZnI$ to nitro olefins. *J. Org. Chem.* 54, 5200–5202.
- Rubin, M., Rubina, M., and Gevorgyan, V. (2007). Transition metal chemistry of cyclopropenes and cyclopropanes. *Chem. Rev.* 107, 3117–3179.
- Rubina, M., Rubin, M., and Gevorgyan, V. (2004). Catalytic enantioselective hydrostannation of cyclopropenes. *J. Am. Chem. Soc.* 126, 3688–3689.
- Schrock, R.R. (2002). High oxidation state multiple metal–carbon bonds. *Chem. Rev.* 102, 145–179.
- Selvaraj, R., Chintala, S.R., Taylor, M.T., and Fox, J.M. (2014). 3-Hydroxymethyl-3-phenylcyclopropene. *Org. Synth.* 91, 322–337.
- Vabre, R., Island, B., Diehl, C.J., Schreiner, P.R., and Marek, I. (2015). Forming stereogenic centers in acyclic systems from alkynes. *Angew. Chem. Int. Ed.* 54, 9996–9999.
- Vicente, R. (2016). Recent progresses towards the strengthening of cyclopropene chemistry. *Synthesis* 48, 2343–2360.
- Wang, K., and Wang, J. (2019). Transition-metal-catalyzed cross-coupling with non-diazo carbene precursors. *Synlett* 30, 542–551.
- Wittig, G., and Schwarzenbach, K. (1959). Diazomethan und zinkjodid. *Angew. Chem.* 20, 652.
- Xia, Y., Qiu, D., and Wang, J. (2017). Transition-metal-catalyzed cross-couplings through carbene migratory insertion. *Chem. Rev.* 117, 13810–13889.
- Zhang, D., Zhou, J., Xia, F., and Hu, W. (2015a). Bond cleavage, fragment modification and reassembly in enantioselective three-component reactions. *Nat. Commun.* 6, 5801.
- Zhang, H., Wang, B., Yi, H., Zhang, Y., and Wang, J. (2015b). Rh(II)-catalyzed [2,3]-sigmatropic rearrangement of sulfur ylides derived from cyclopropenes and sulfides. *Org. Lett.* 17, 3322–3325.
- Zollinger, H. (1995). *Diazo Chemistry I and II* (Wiley-WCH).

Supplemental Information

**Metal-Dependent Umpolung Reactivity
of Carbenes Derived from Cyclopropenes**

Dan Zhang, Zhenghui Kang, Junwen Liu, and Wenhao Hu

Supplementary Figures

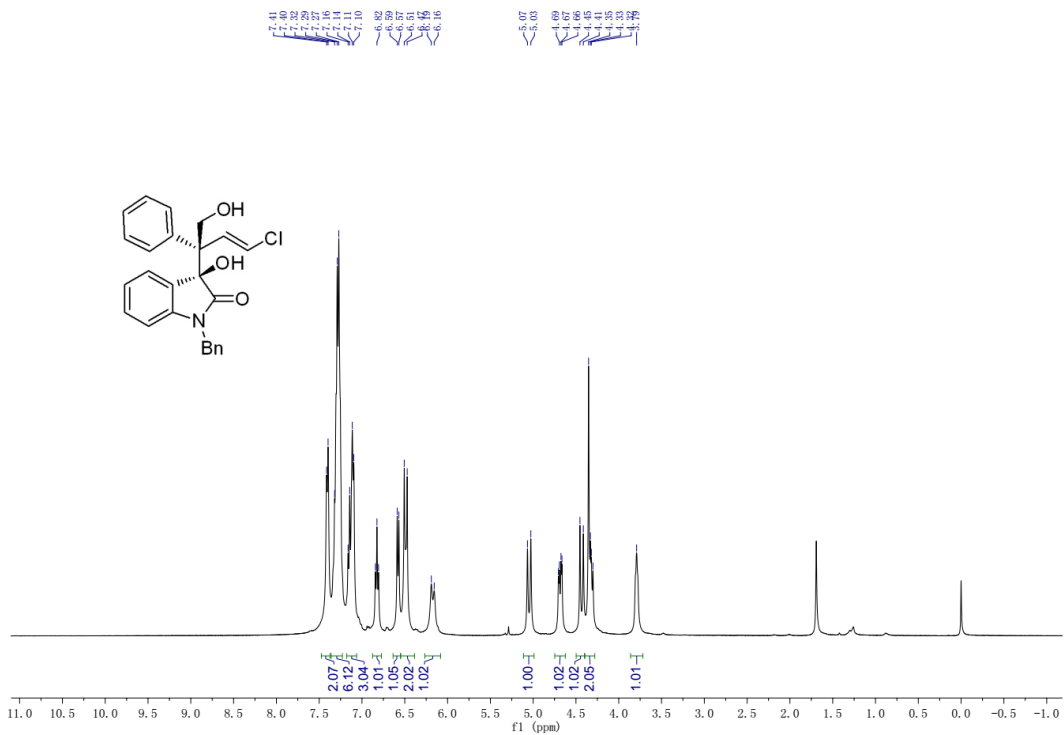


Figure S1. ^1H NMR (400 MHz, CDCl_3) spectrum for **3a**, related to **Figure 2**.

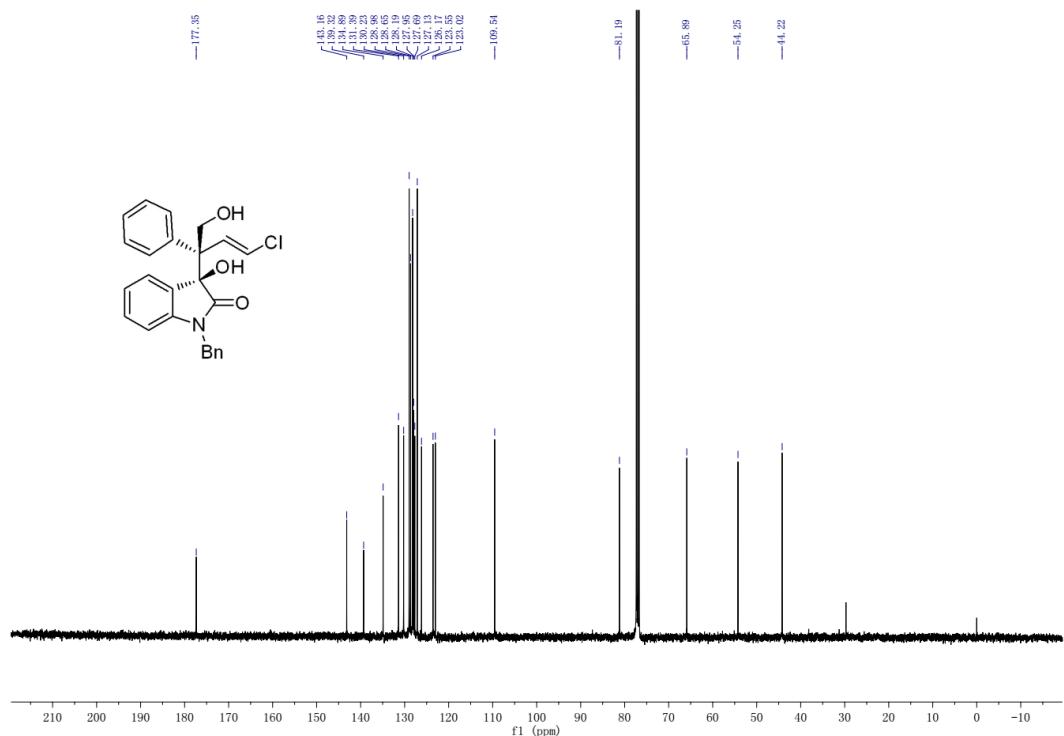


Figure S2. ^{13}C NMR (100 MHz, CDCl_3) spectrum for **3a**, related to Figure 2.

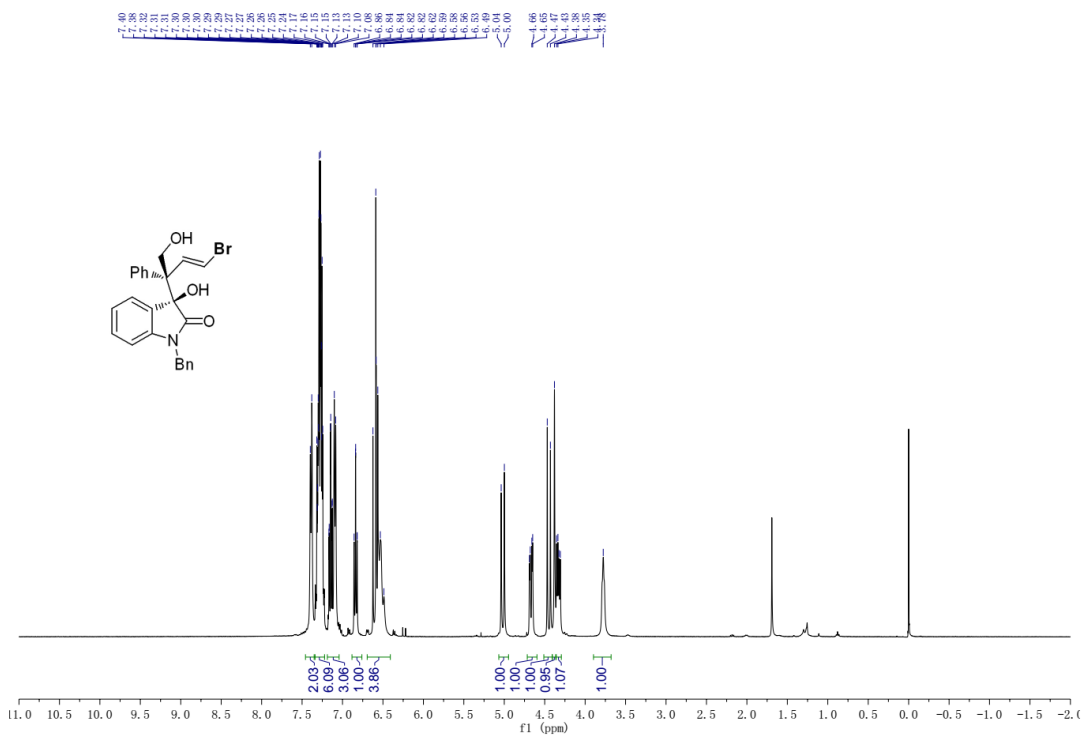


Figure S3. ^1H NMR (400 MHz, CDCl_3) spectrum for **3b**, related to **Figure 2**.

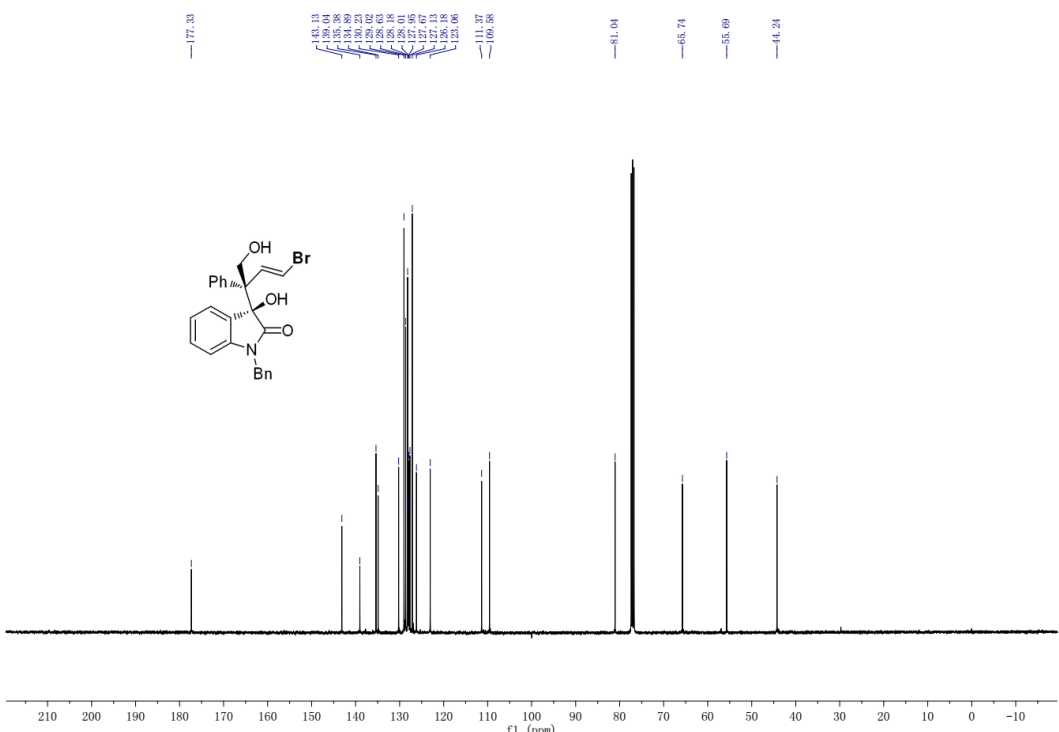


Figure S4. ^{13}C NMR (100 MHz, CDCl_3) spectrum for **3b**, related to **Figure 2**.

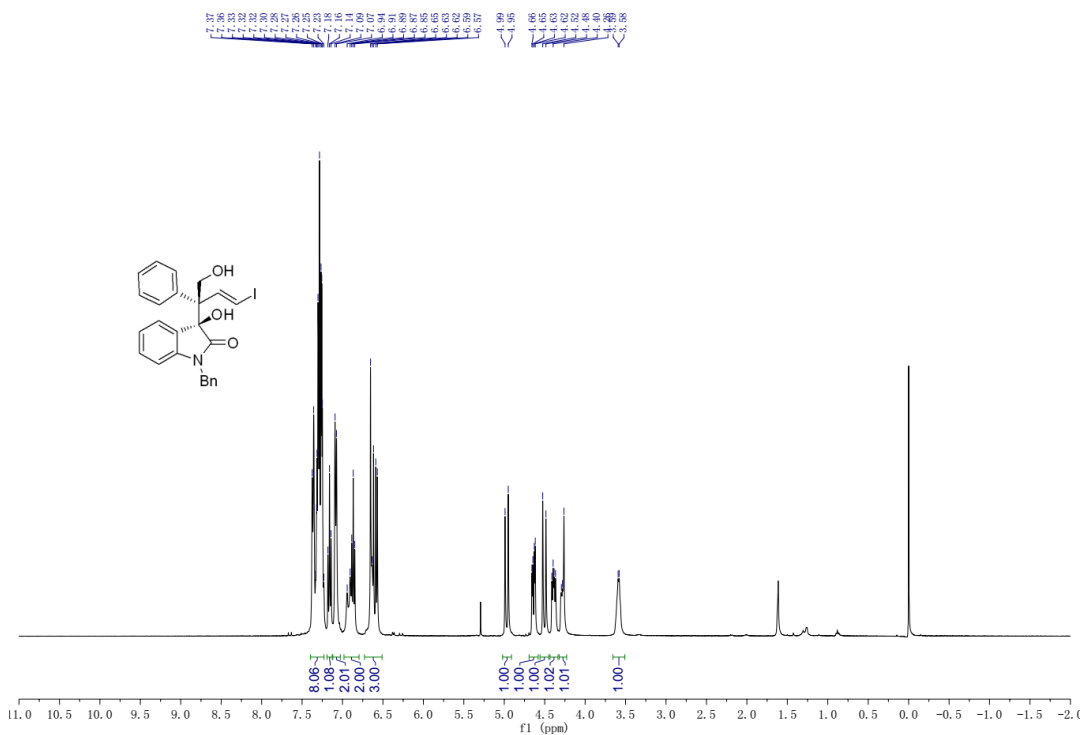


Figure S5. ^1H NMR (400 MHz, CDCl_3) spectrum for **3c**, related to **Figure 2**.

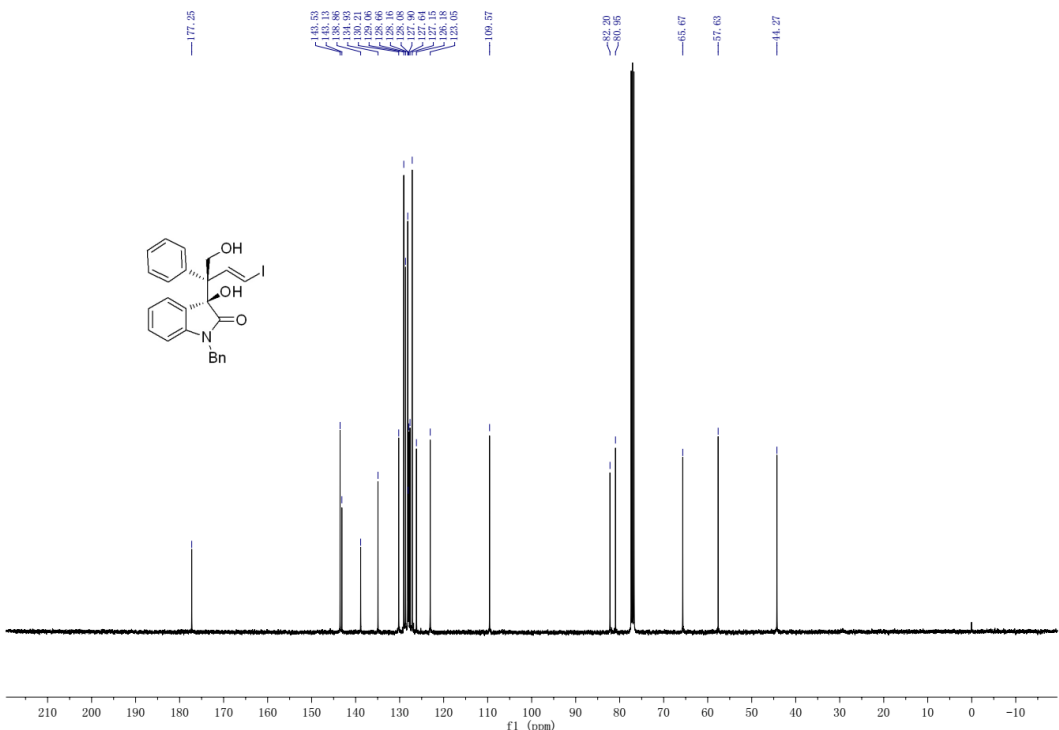


Figure S6. ^{13}C NMR (100 MHz, CDCl_3) spectrum for **3c**, related to **Figure 2**.

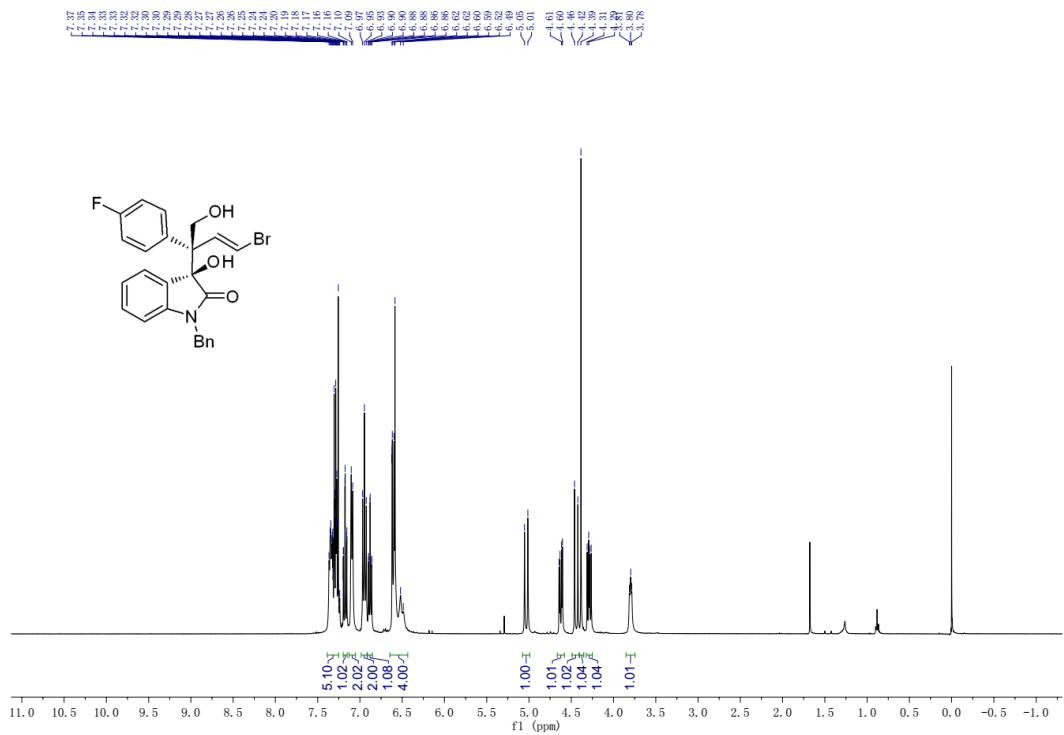


Figure S7. ^1H NMR (400 MHz, CDCl_3) spectrum for **3d**, related to **Figure 2**.

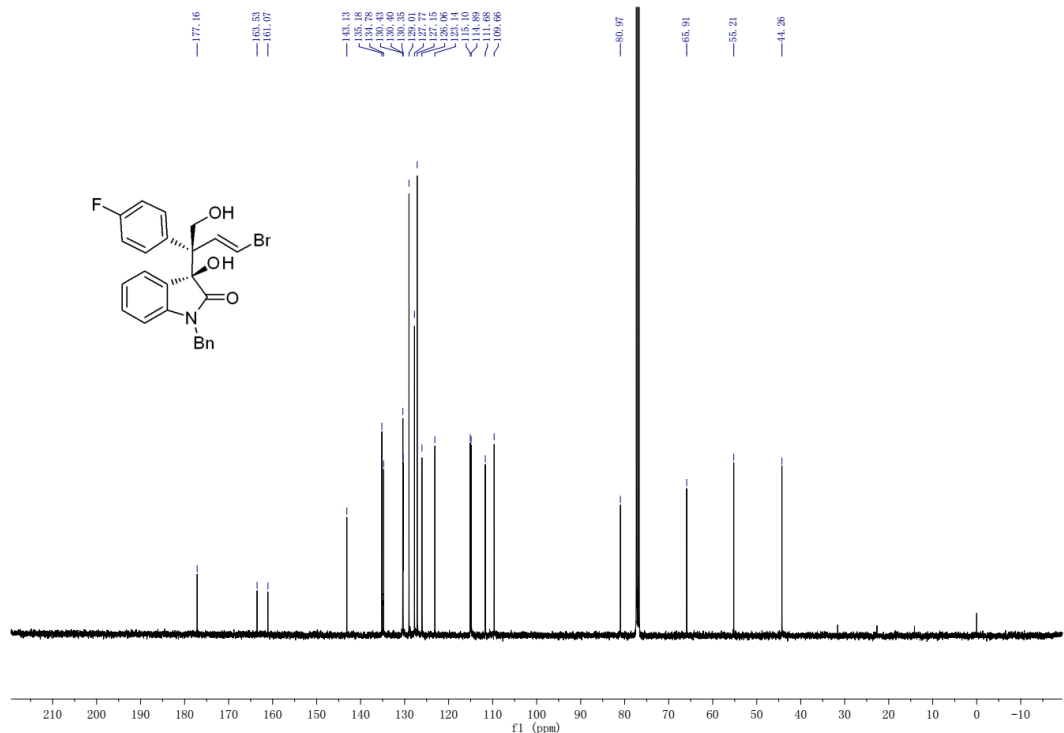


Figure S8. ^{13}C NMR (100 MHz, CDCl_3) spectrum for **3d**, related to **Figure 2**.

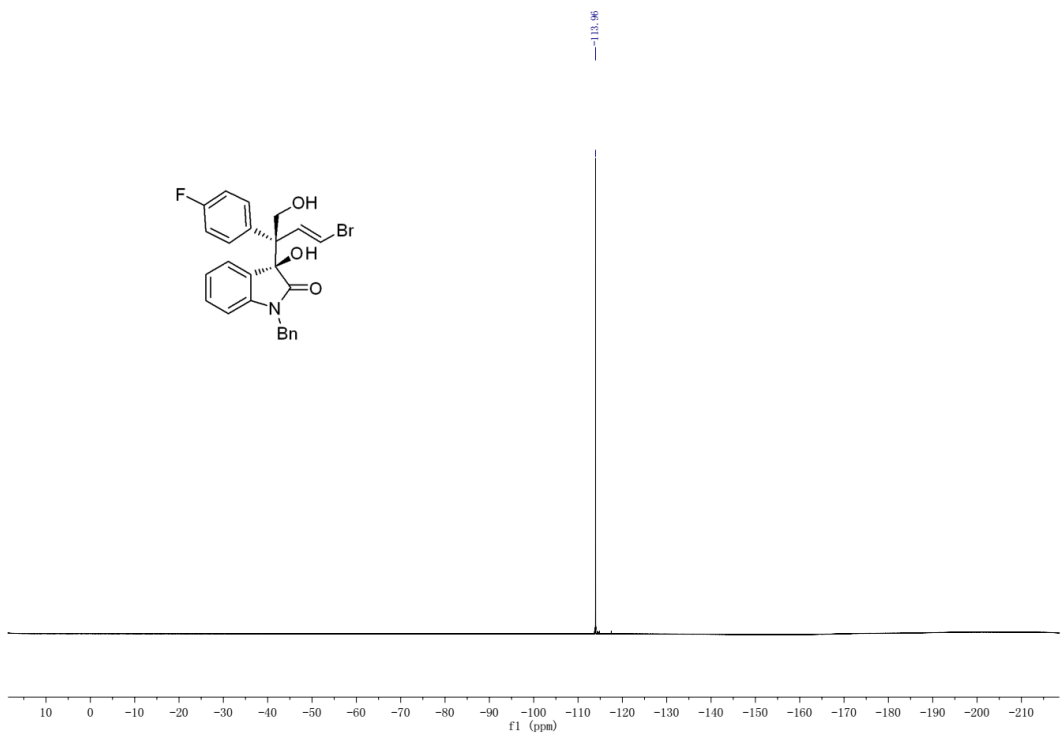


Figure S9. ^{19}F NMR (376 MHz, CDCl_3) spectrum for **3d**, related to **Figure 2**.

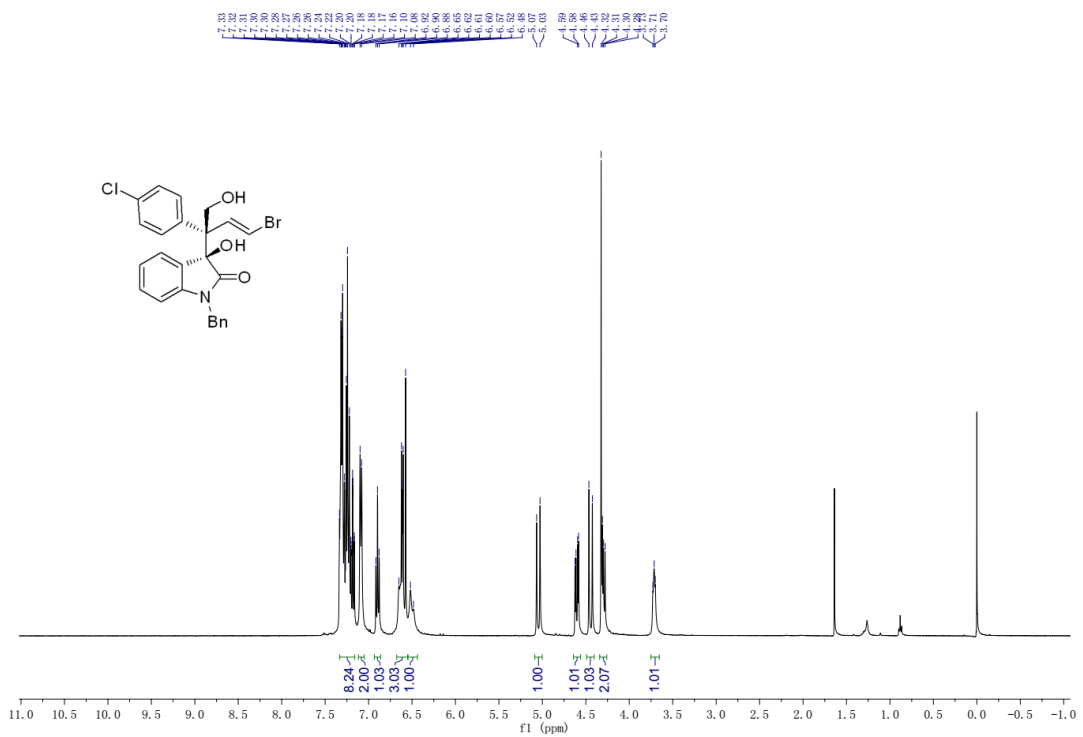


Figure S10. ^1H NMR (400 MHz, CDCl_3) spectrum for **3e**, related to Figure 2.

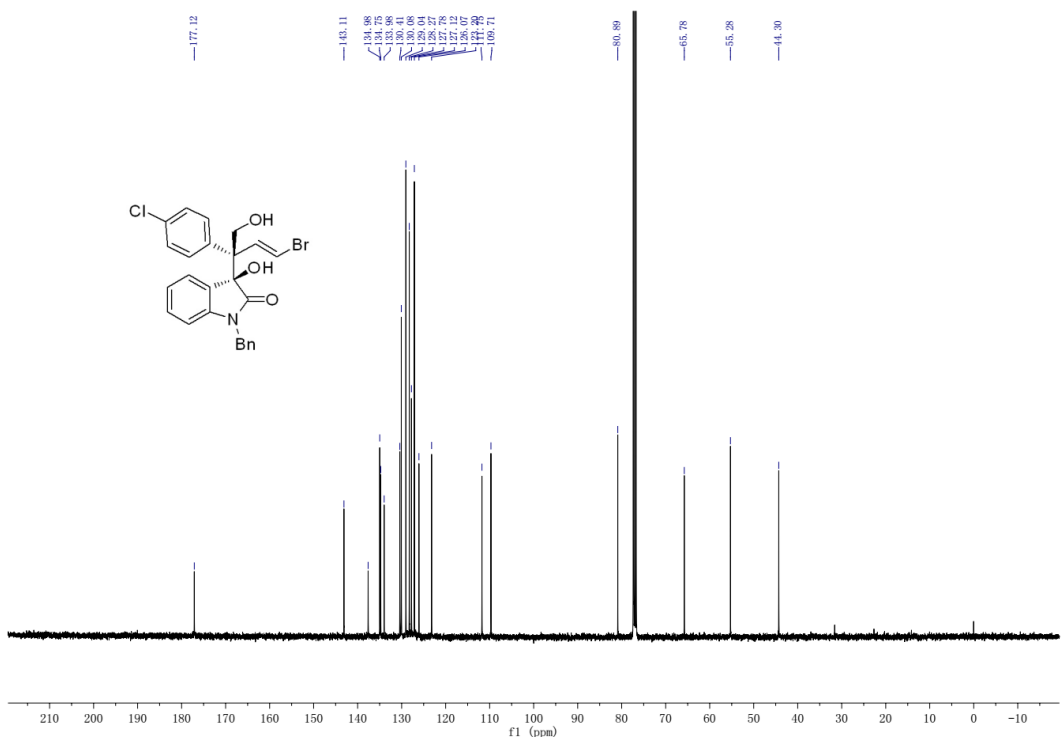


Figure S11. ^{13}C NMR (100 MHz, CDCl_3) spectrum for **3e**, related to Figure 2.

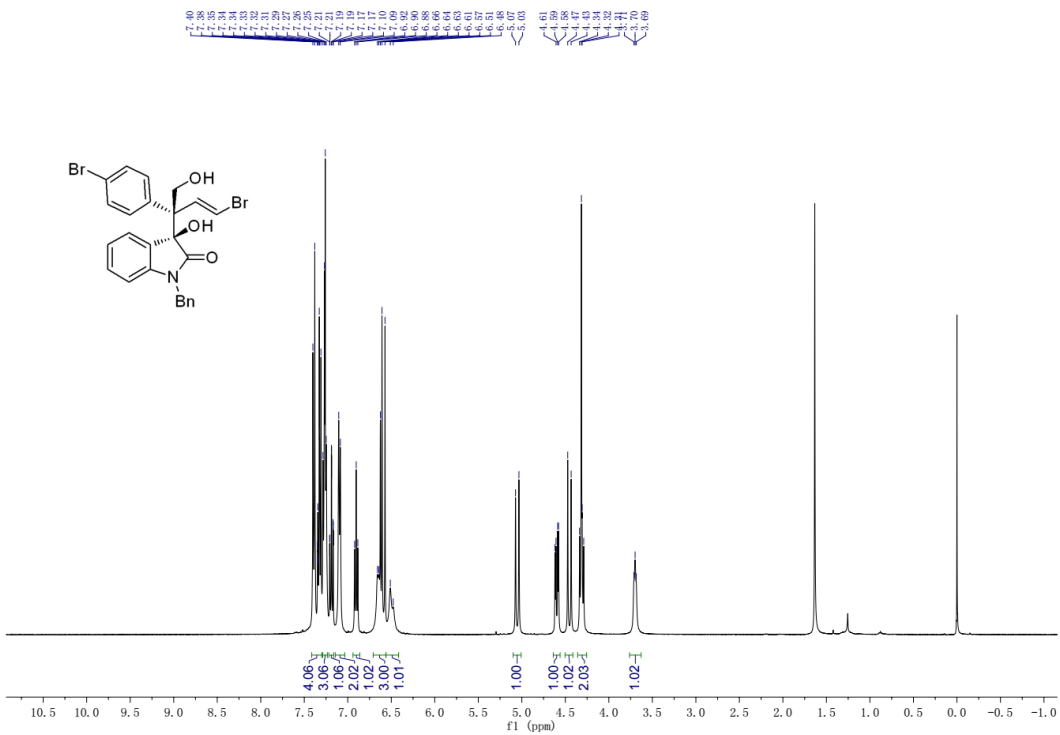


Figure S12. ^1H NMR (400 MHz, CDCl_3) spectrum for **3f**, related to **Figure 2**.

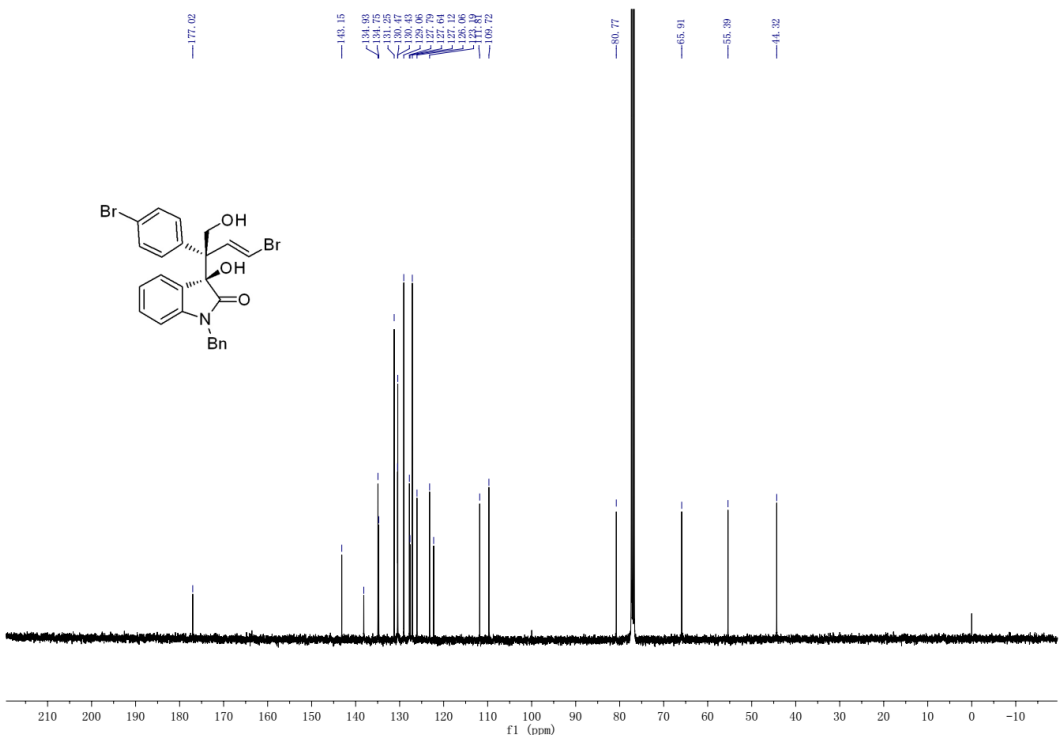


Figure S13. ^{13}C NMR (100 MHz, CDCl_3) spectrum for **3f**, related to **Figure 2**.

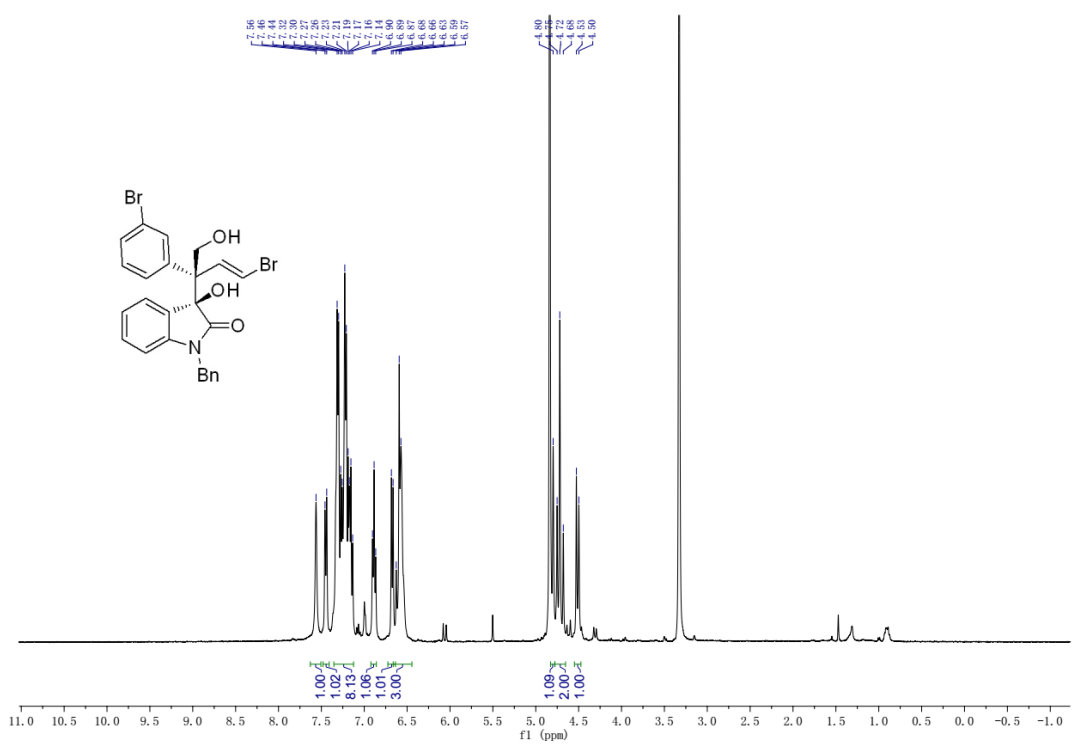


Figure S14. ^1H NMR (400 MHz, MeOD) spectrum for **3g**, related to **Figure 2**.

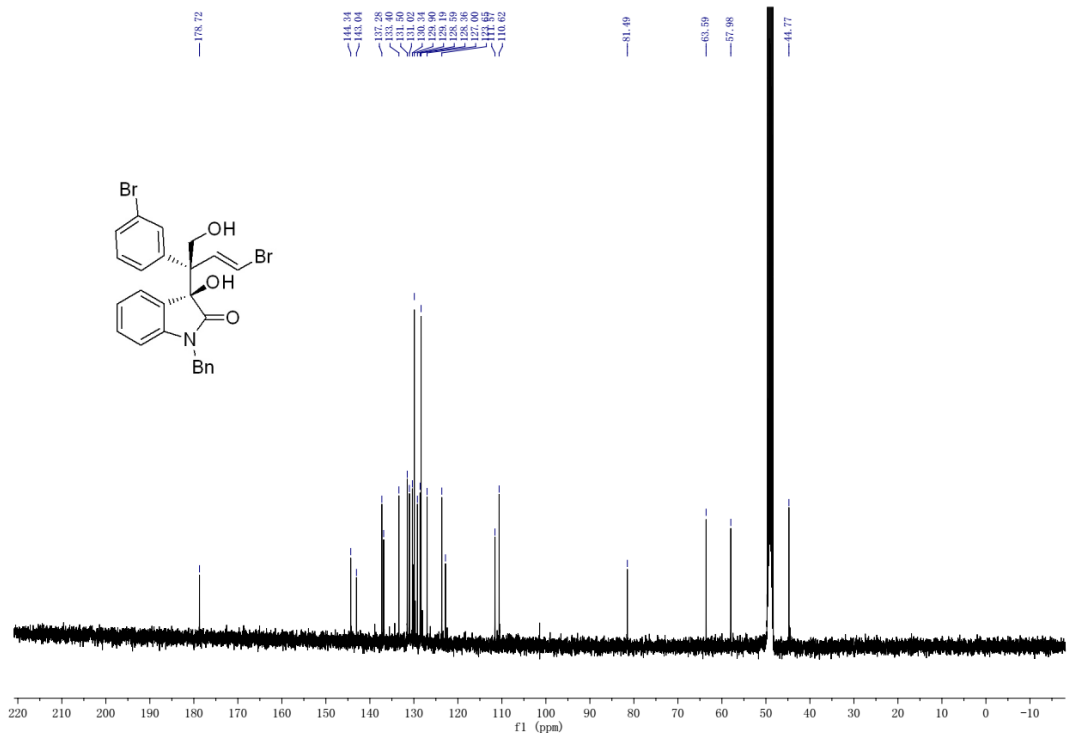


Figure S15. ^{13}C NMR (100 MHz, MeOD) spectrum for **3g**, related to **Figure 2**.

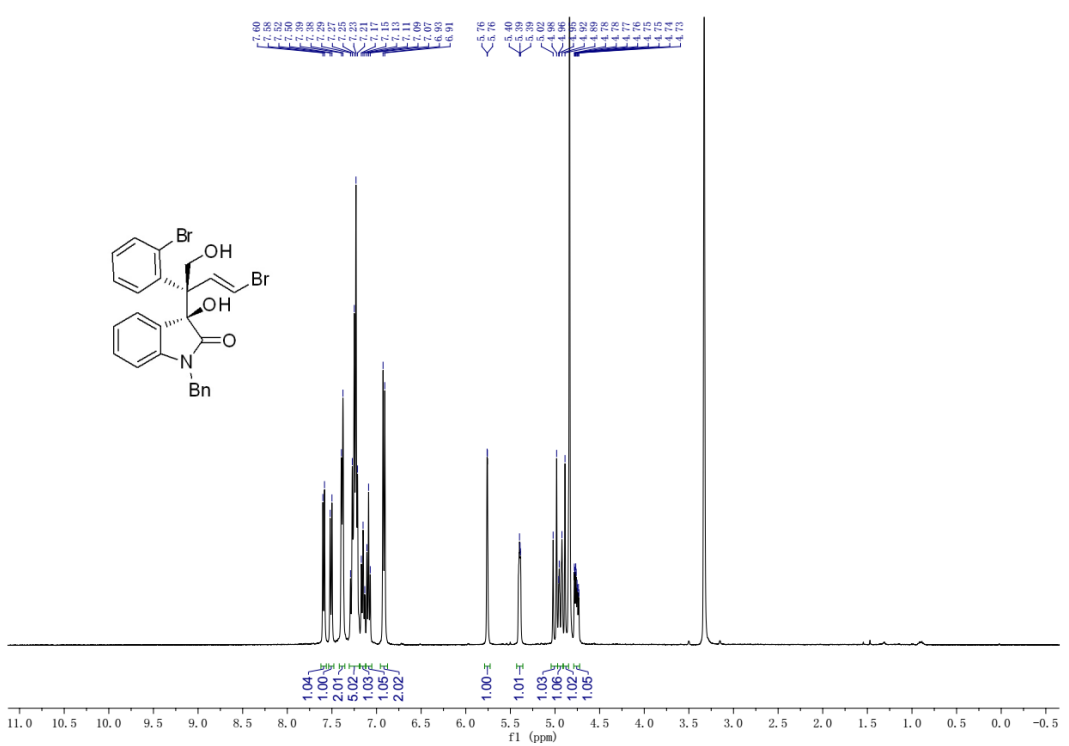


Figure S16. ^1H NMR (400 MHz, MeOD) spectrum for **3h**, related to **Figure 2**.

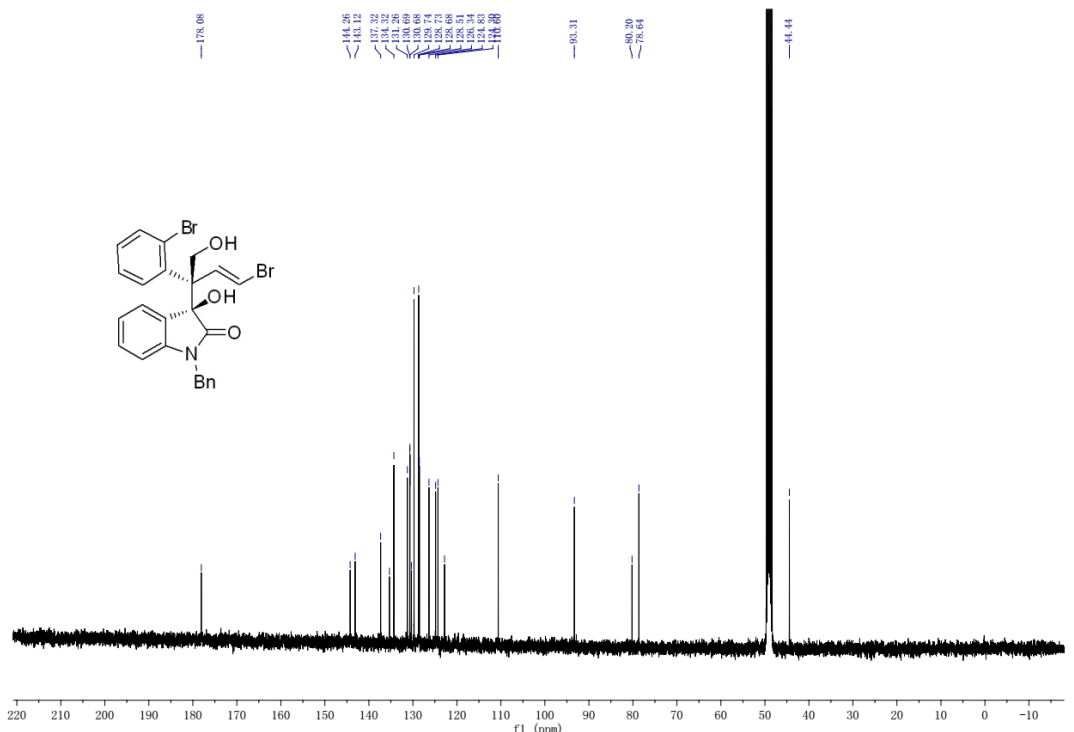


Figure S17. ^{13}C NMR (100 MHz, MeOD) spectrum for **3h**, related to **Figure 2**.

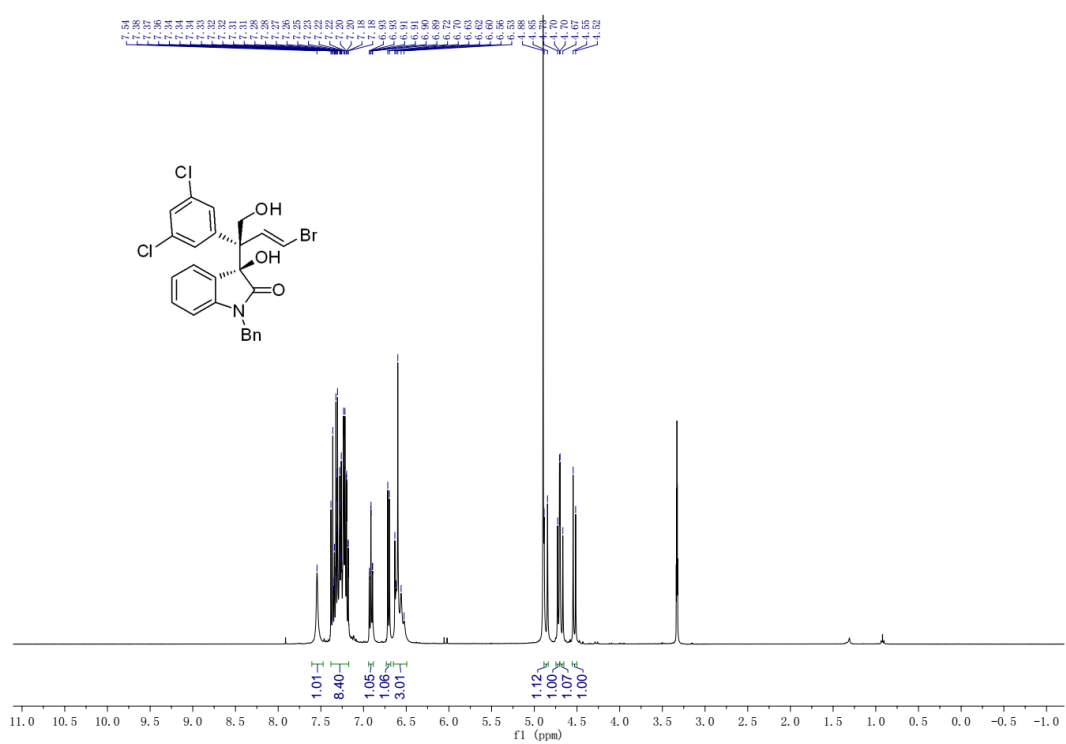


Figure S18. ¹H NMR (400 MHz, MeOD) spectrum for 3i, related to **Figure 2**.

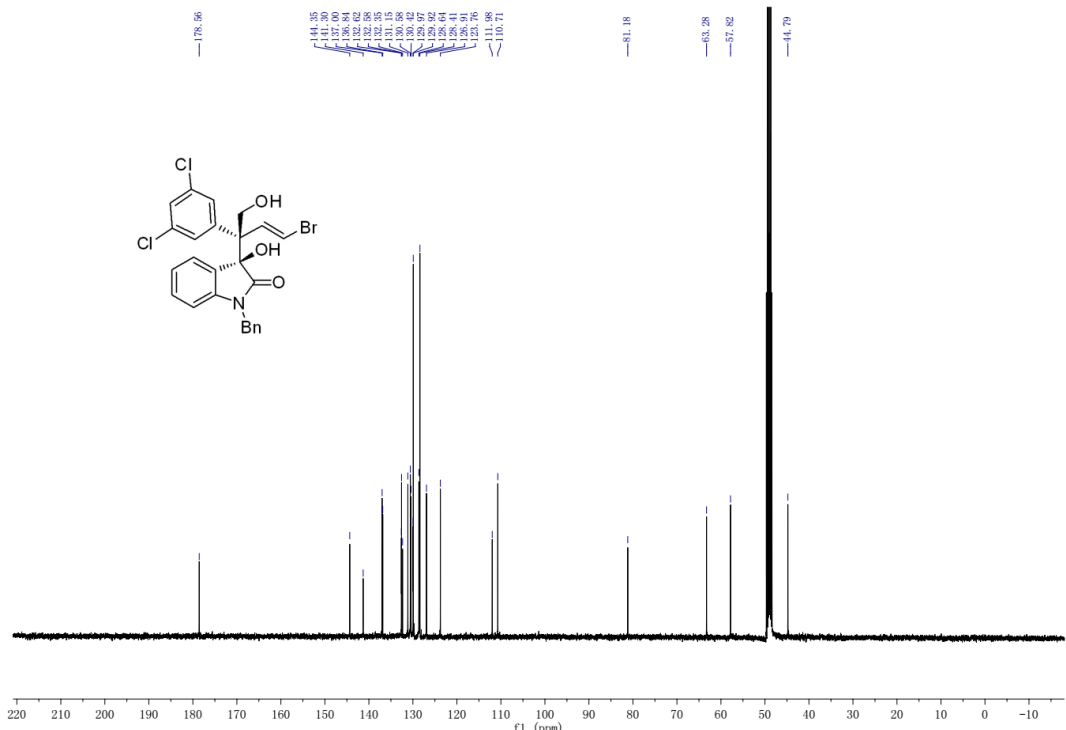


Figure S19. ¹³C NMR (100 MHz, MeOD) spectrum for 3i, related to **Figure 2**.

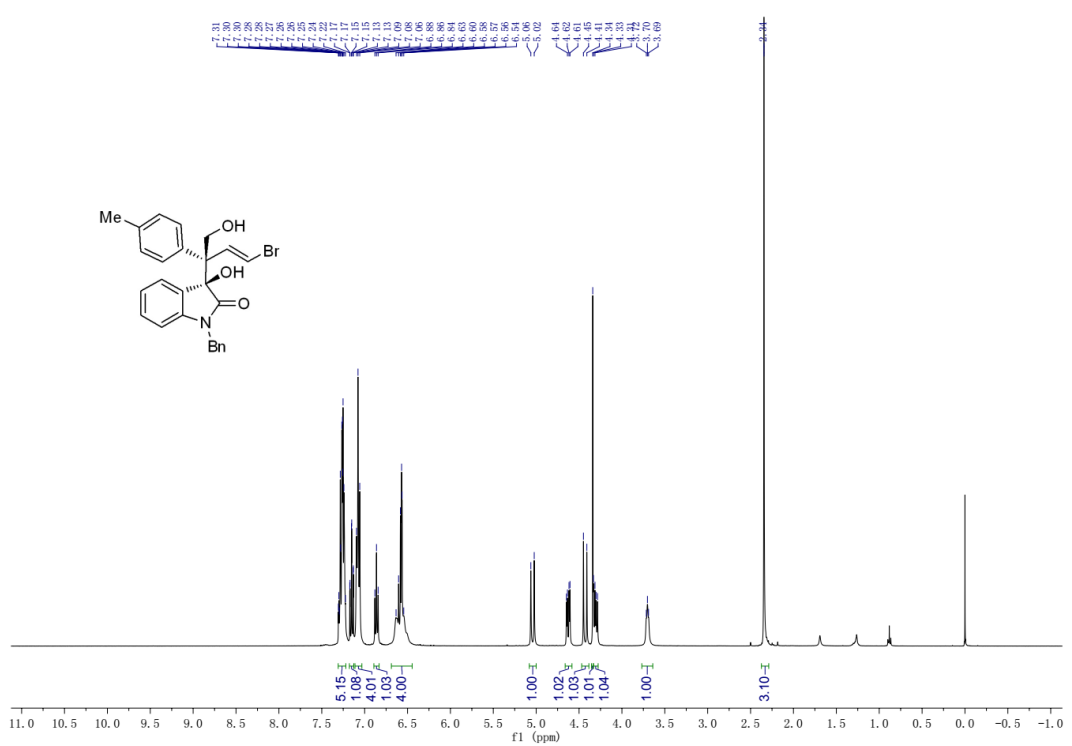


Figure S20. ^1H NMR (400 MHz, CDCl_3) spectrum for **3j**, related to **Figure 2**.

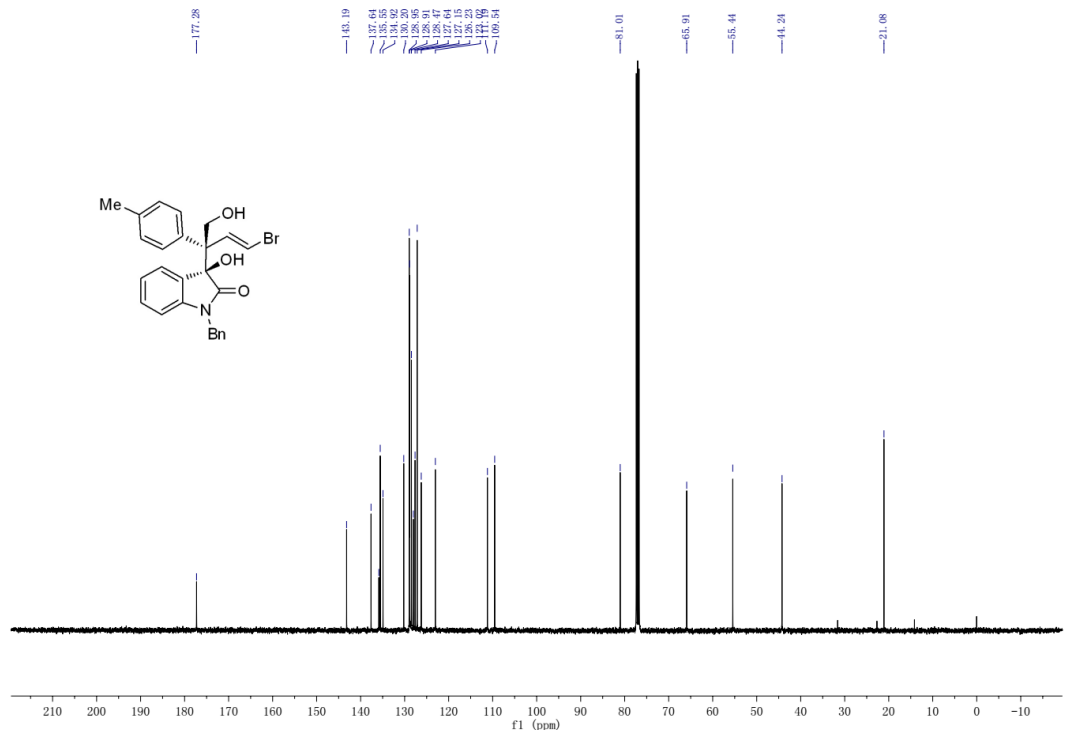


Figure S21. ^{13}C NMR (100 MHz, CDCl_3) spectrum for **3j**, related to **Figure 2**.

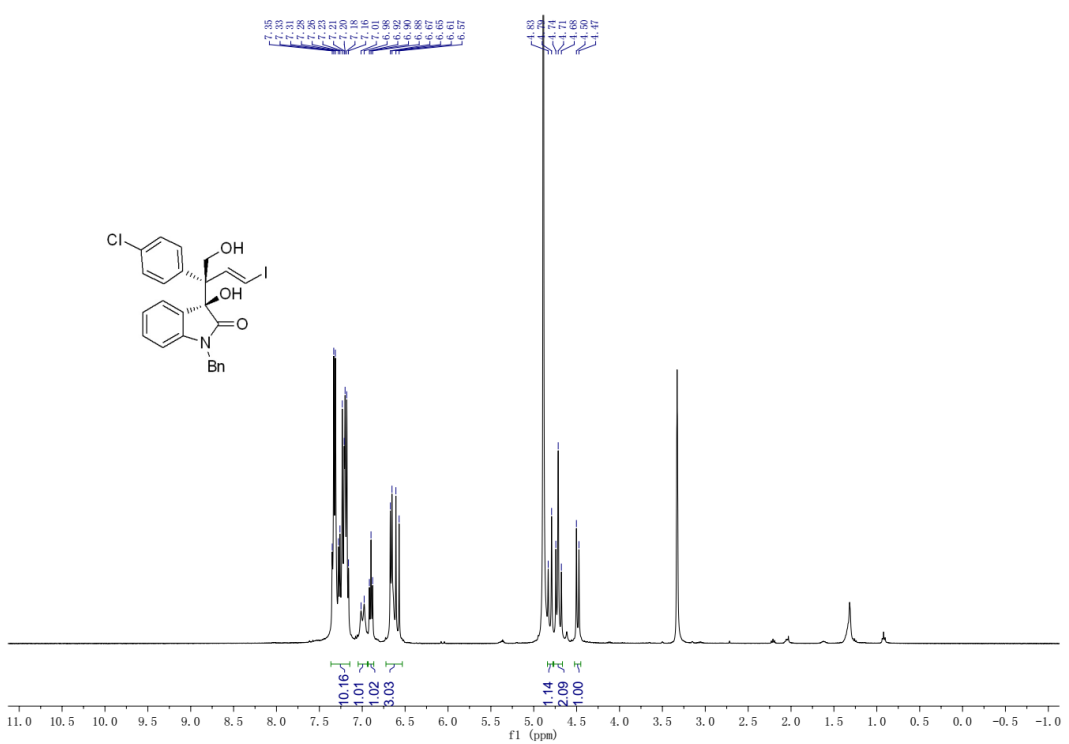


Figure S22. ^1H NMR (400 MHz, MeOD) spectrum for **3k**, related to **Figure 2**.

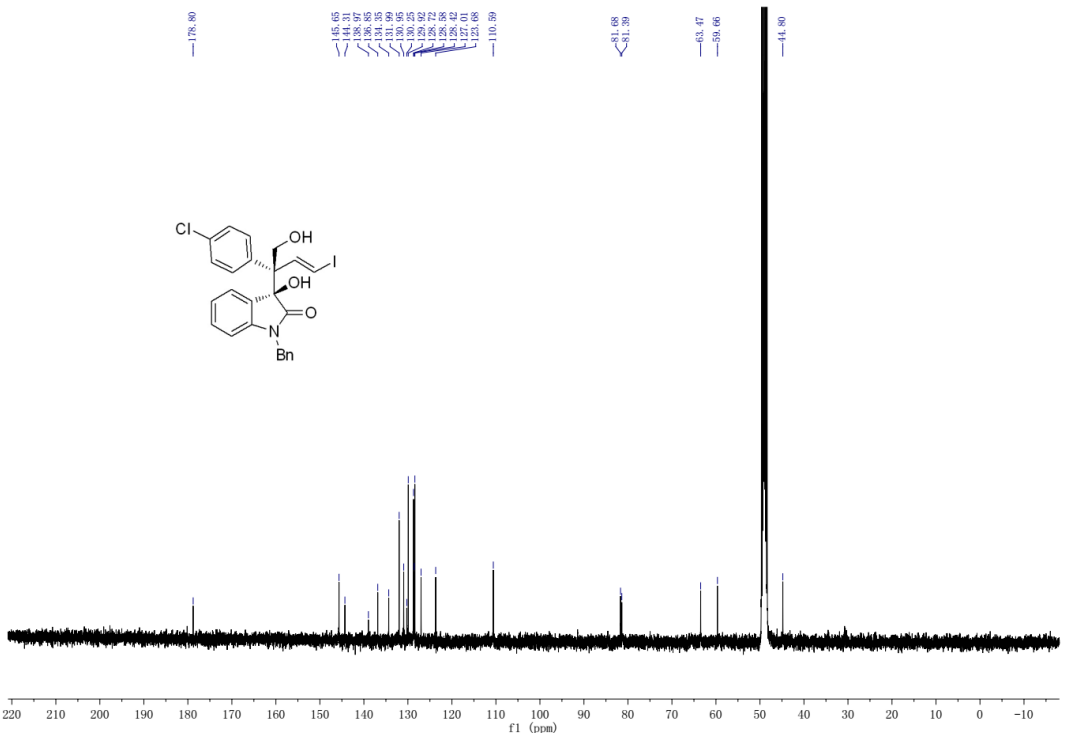


Figure S23. ^{13}C NMR (100 MHz, MeOD) spectrum for **3k**, related to **Figure 2**.

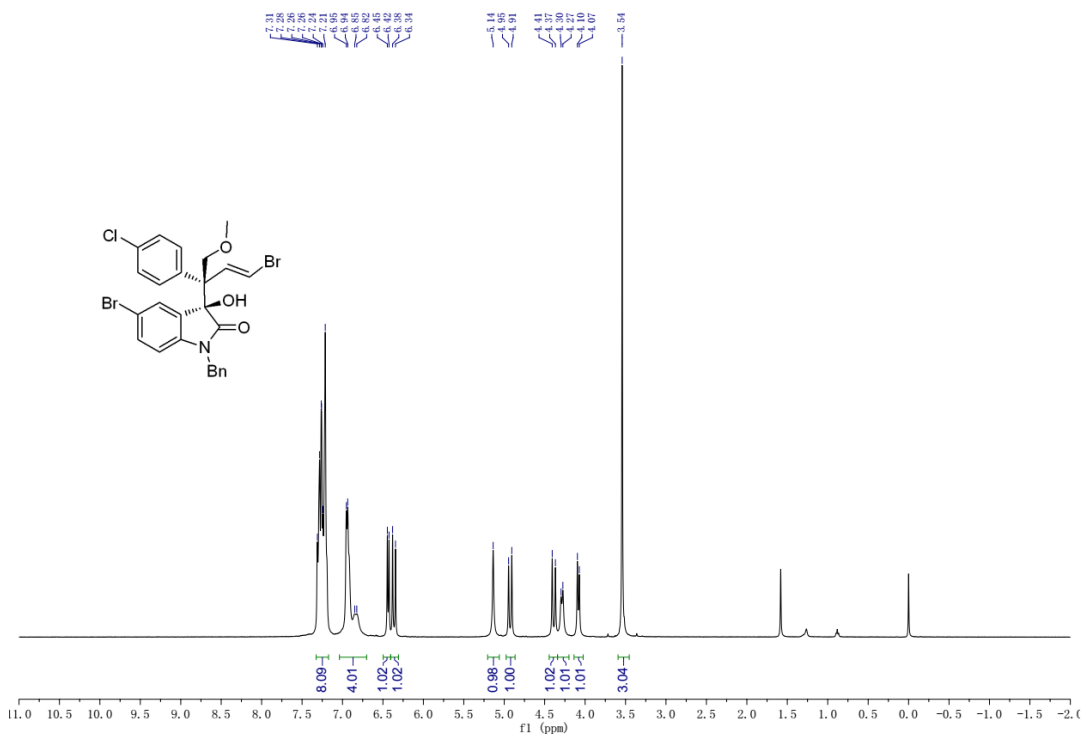


Figure S24. ^1H NMR (400 MHz, CDCl_3) spectrum for **3l**, related to **Figure 2**.

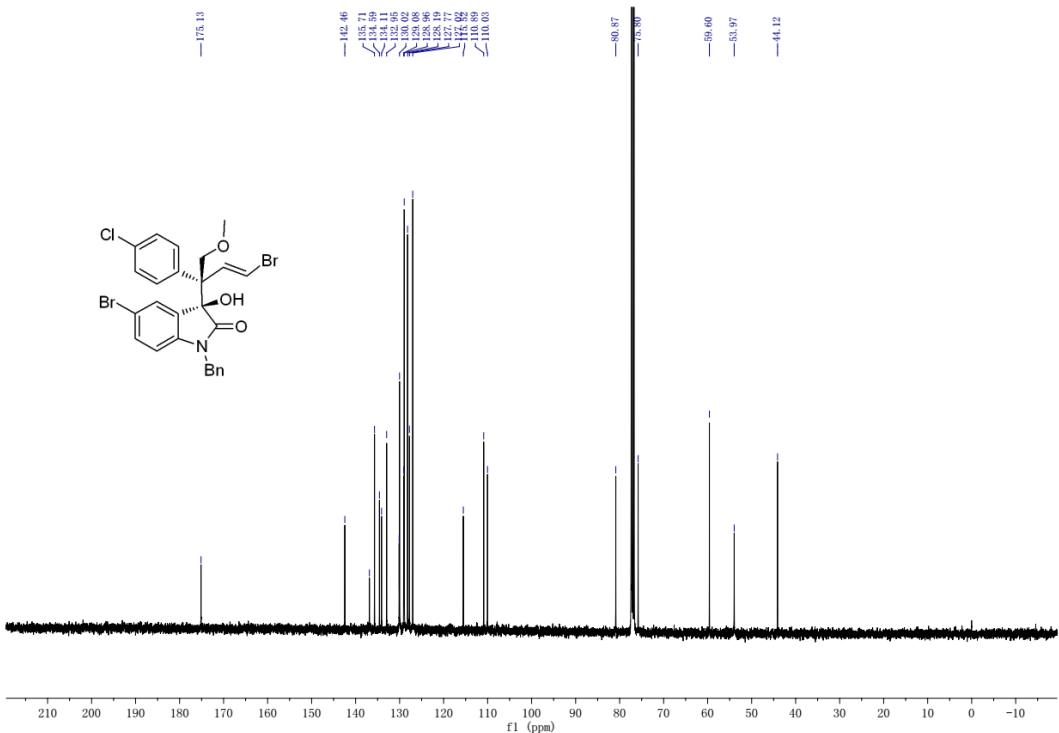


Figure S25. ^{13}C NMR (100 MHz, CDCl_3) spectrum for **3l**, related to **Figure 2**.

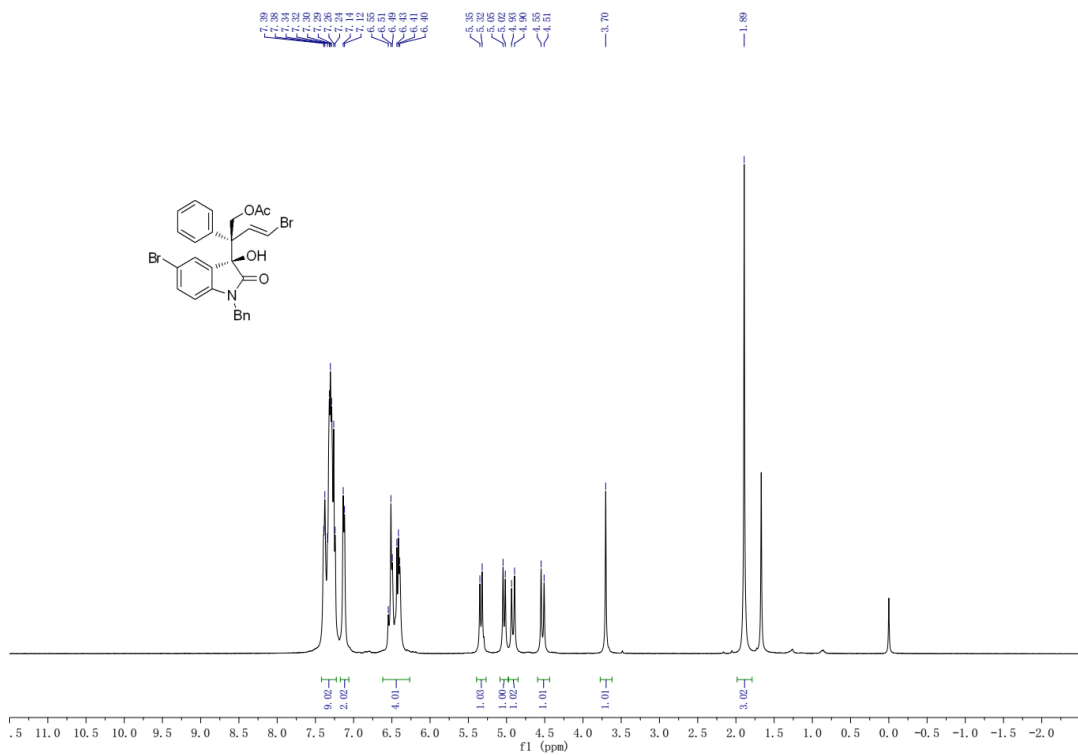


Figure S26. ^1H NMR (400 MHz, CDCl_3) spectrum for **3m**, related to **Figure 2**.

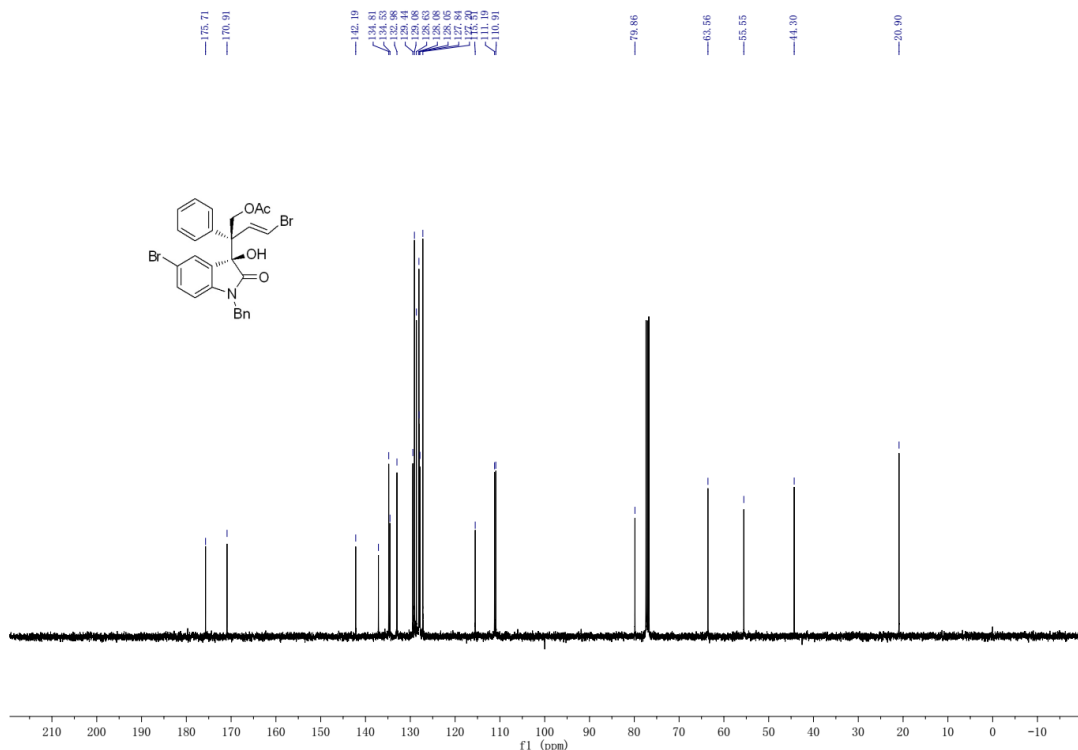


Figure S27. ^{13}C NMR (100 MHz, CDCl_3) spectrum for **3m**, related to **Figure 2**.

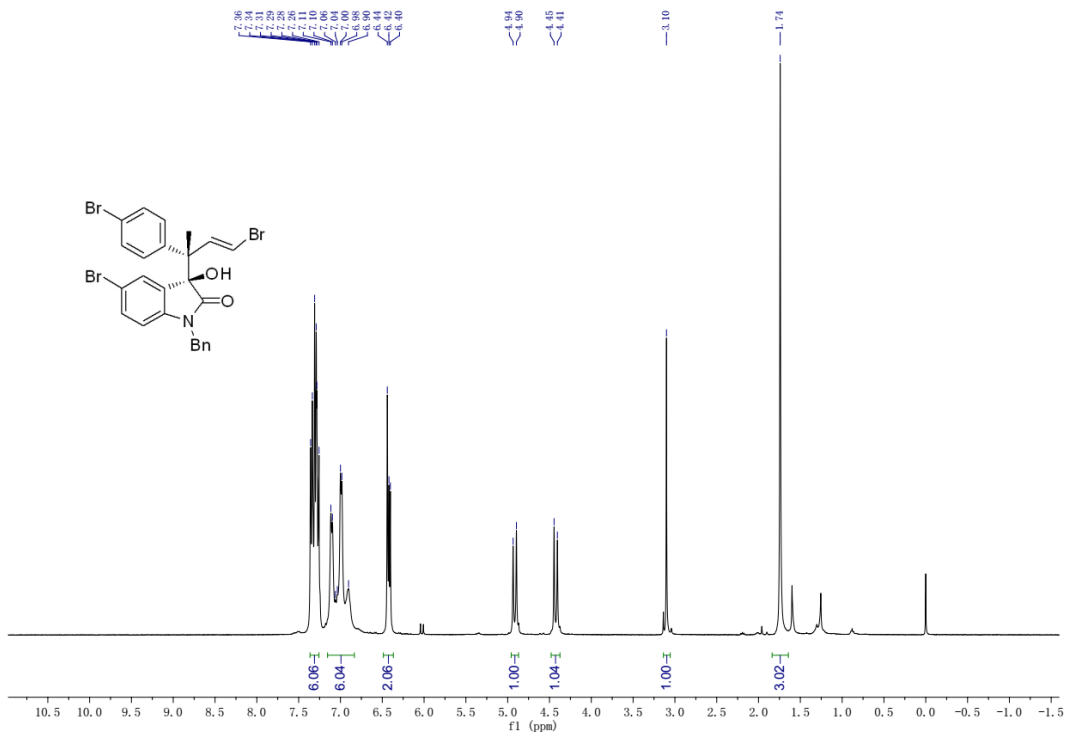


Figure S28. ^1H NMR (400 MHz, CDCl_3) spectrum for **3n**, related to Figure 2.

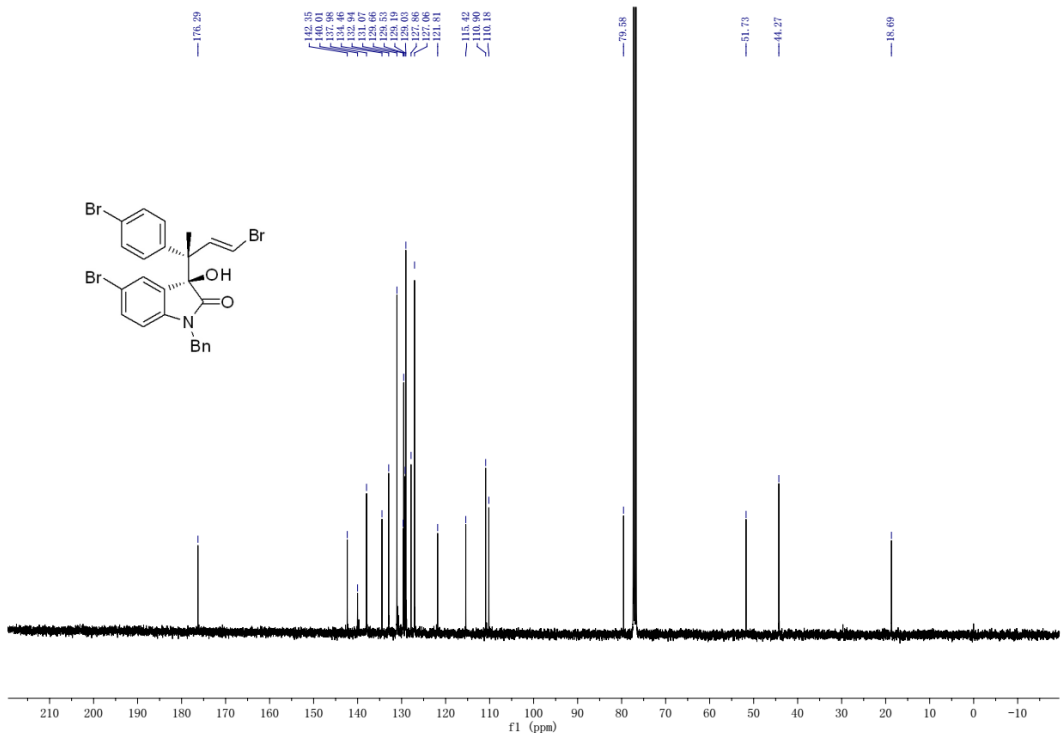


Figure S29. ^{13}C NMR (100 MHz, CDCl_3) spectrum for **3n**, related to Figure 2.

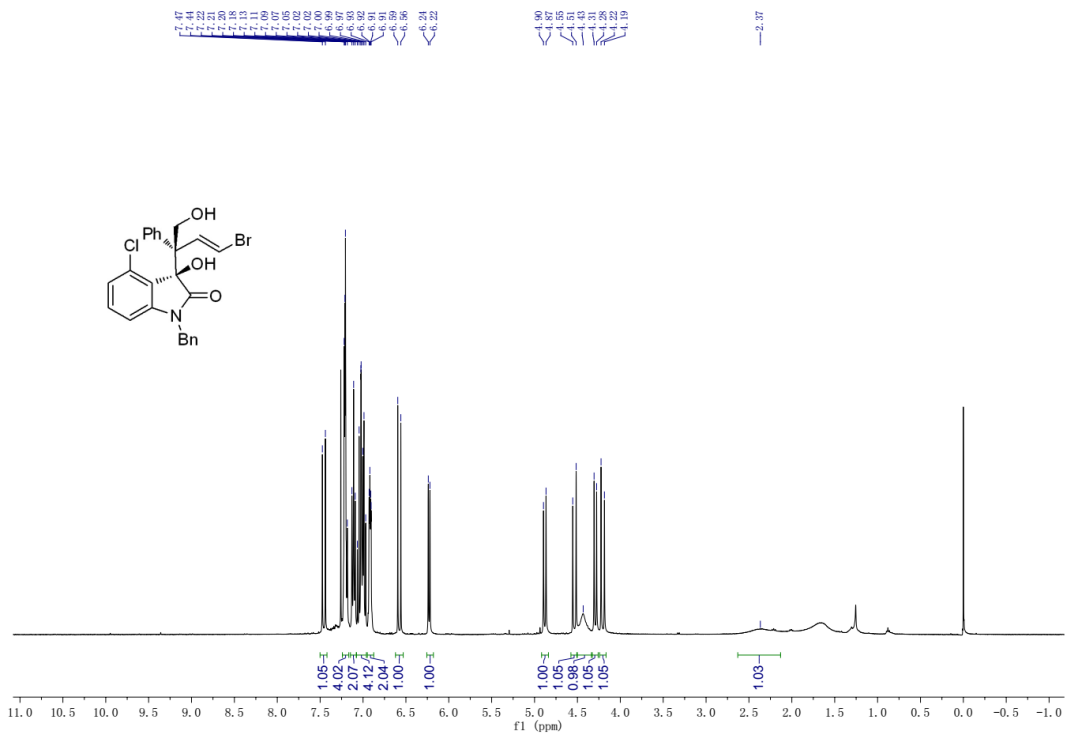


Figure S30. ¹H NMR (400 MHz, CDCl₃) spectrum for **3o**, related to **Figure 2**.

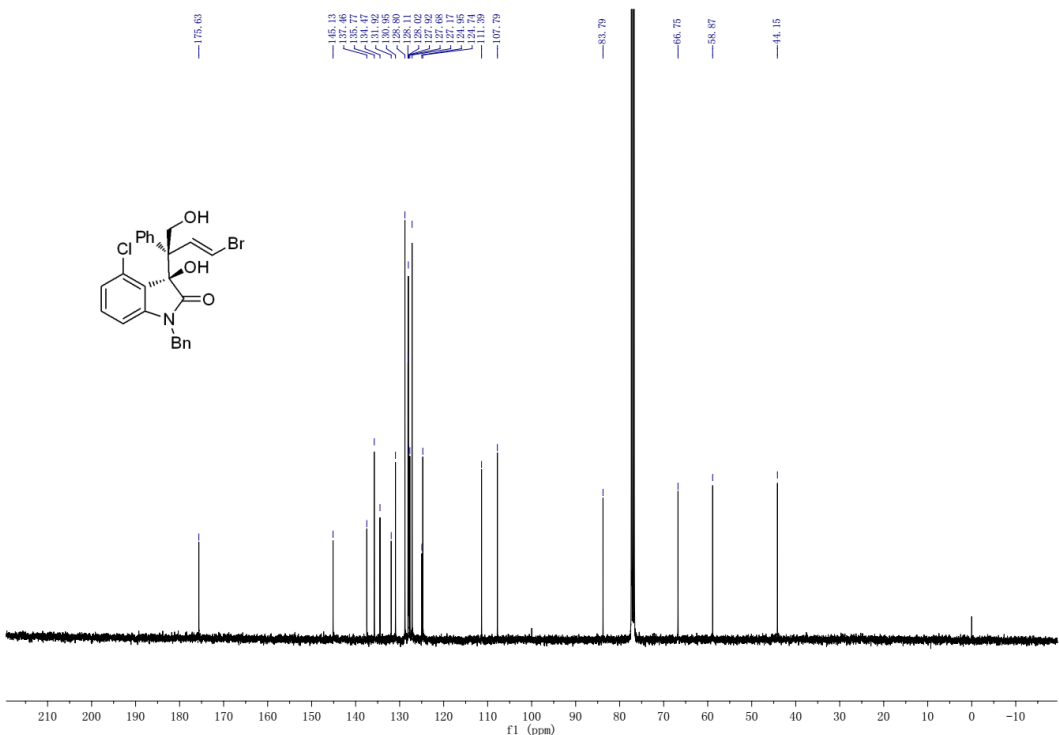


Figure S31. ¹³C NMR (100 MHz, CDCl₃) spectrum for **3o**, related to **Figure 2**.

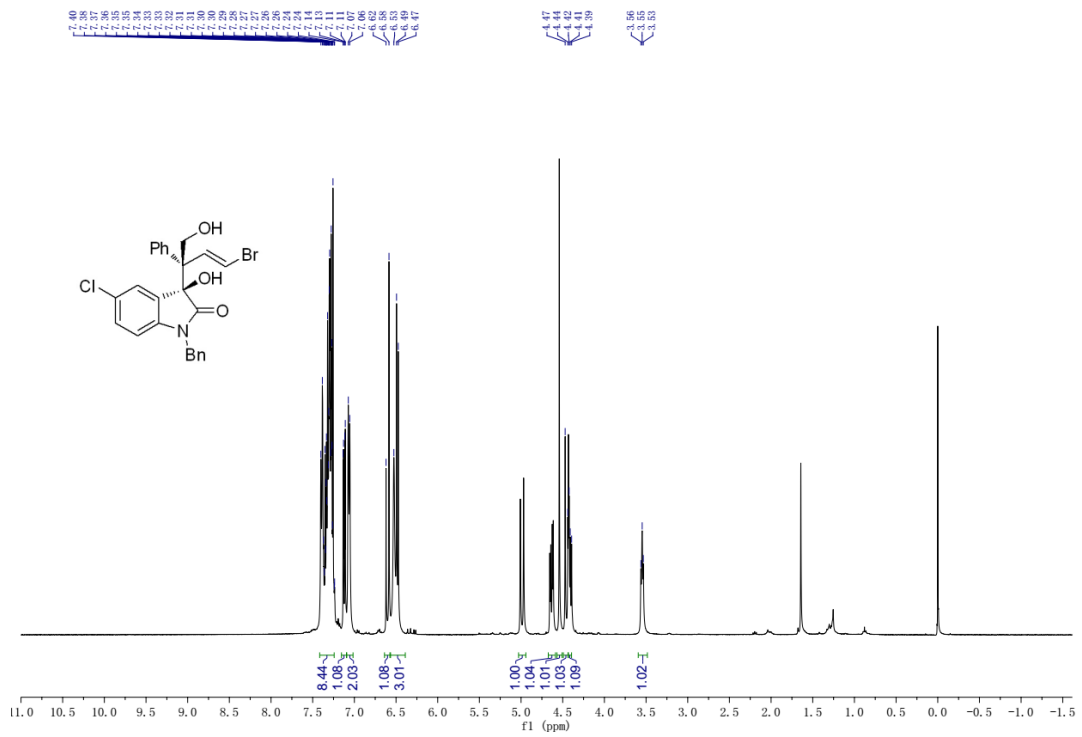


Figure S32. ^1H NMR (400 MHz, CDCl_3) spectrum for **3p**, related to Figure 2.

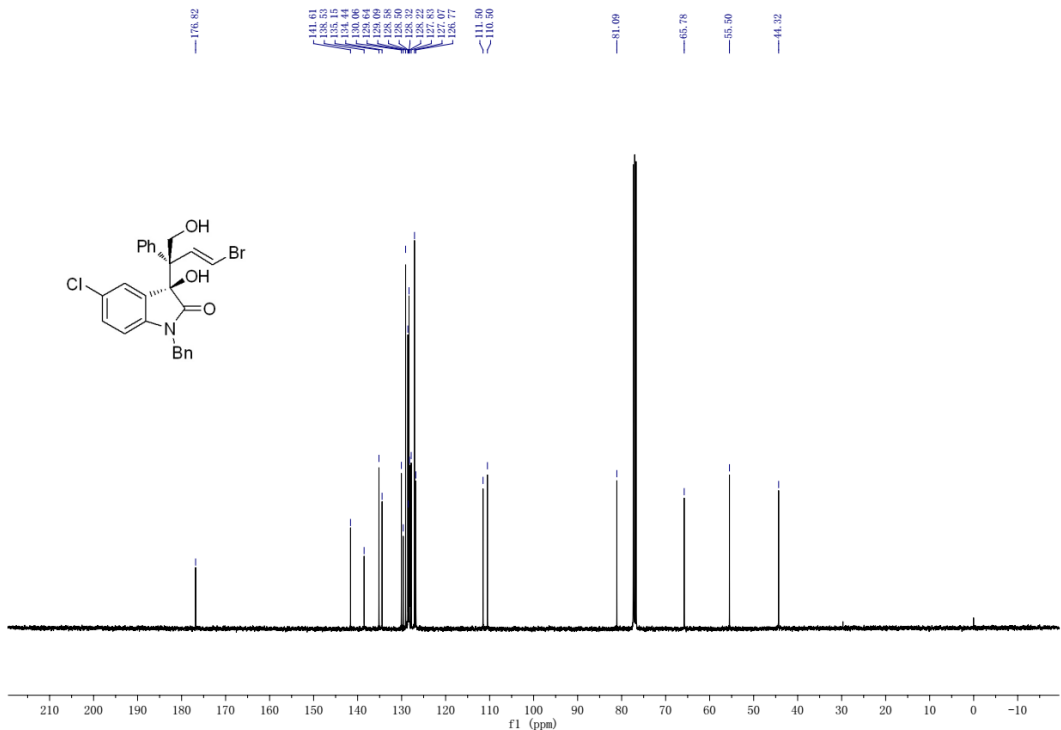


Figure S33. ^{13}C NMR (100 MHz, CDCl_3) spectrum for **3p**, related to **Figure 2**.

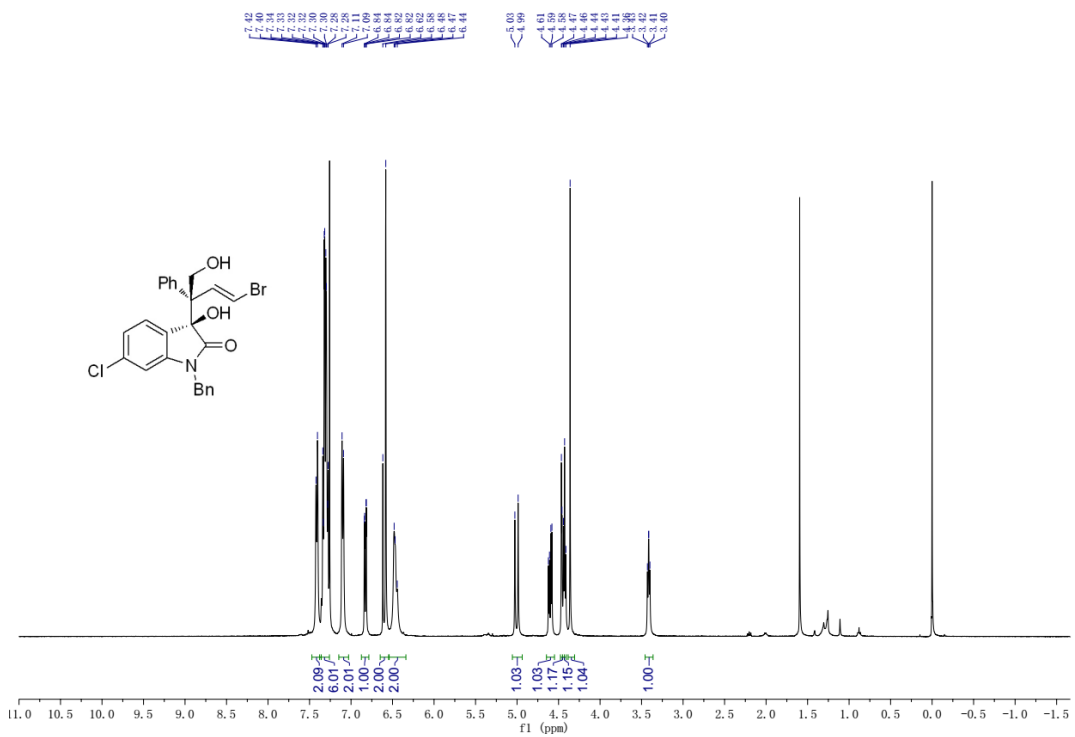


Figure S34. ^1H NMR (400 MHz, CDCl_3) spectrum for **3q**, related to **Figure 2**.

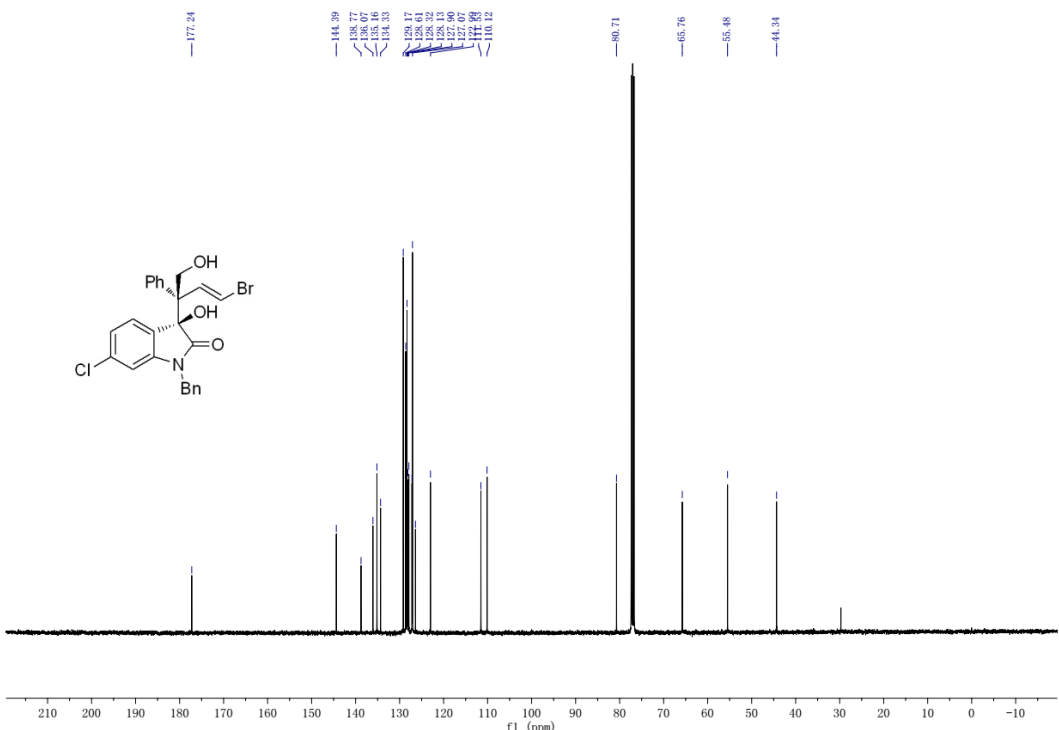


Figure S35. ^{13}C NMR (100 MHz, CDCl_3) spectrum for **3q**, related to **Figure 2**.

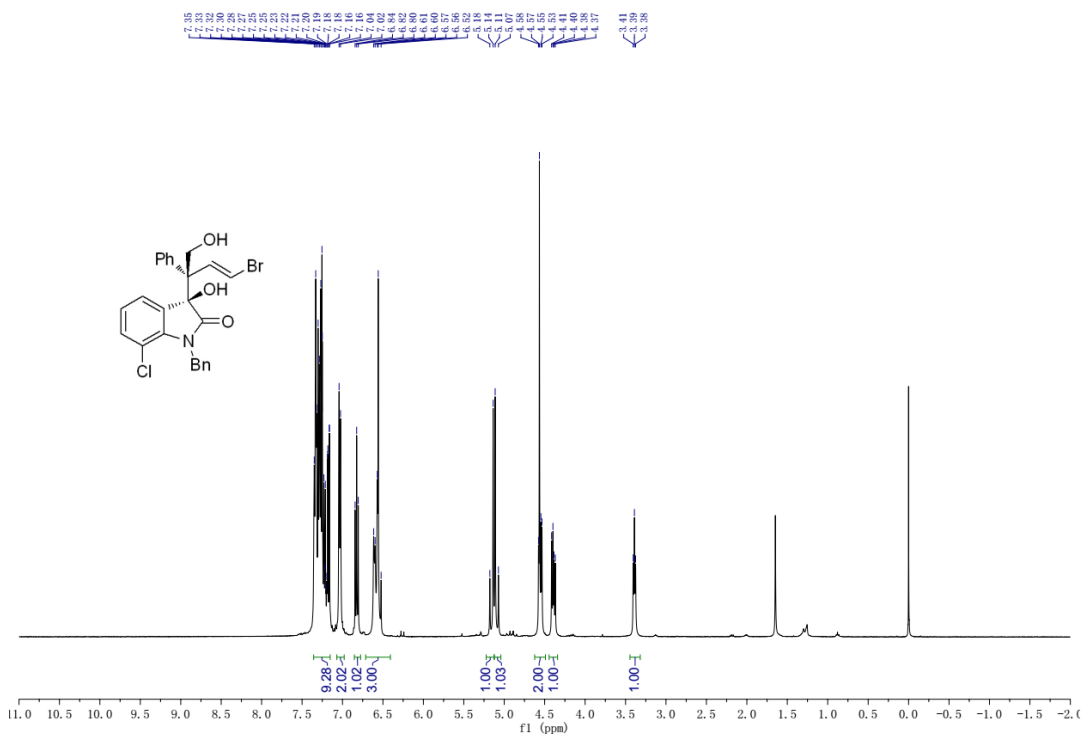


Figure S36. ^1H NMR (400 MHz, CDCl_3) spectrum for **3r**, related to **Figure 2**.

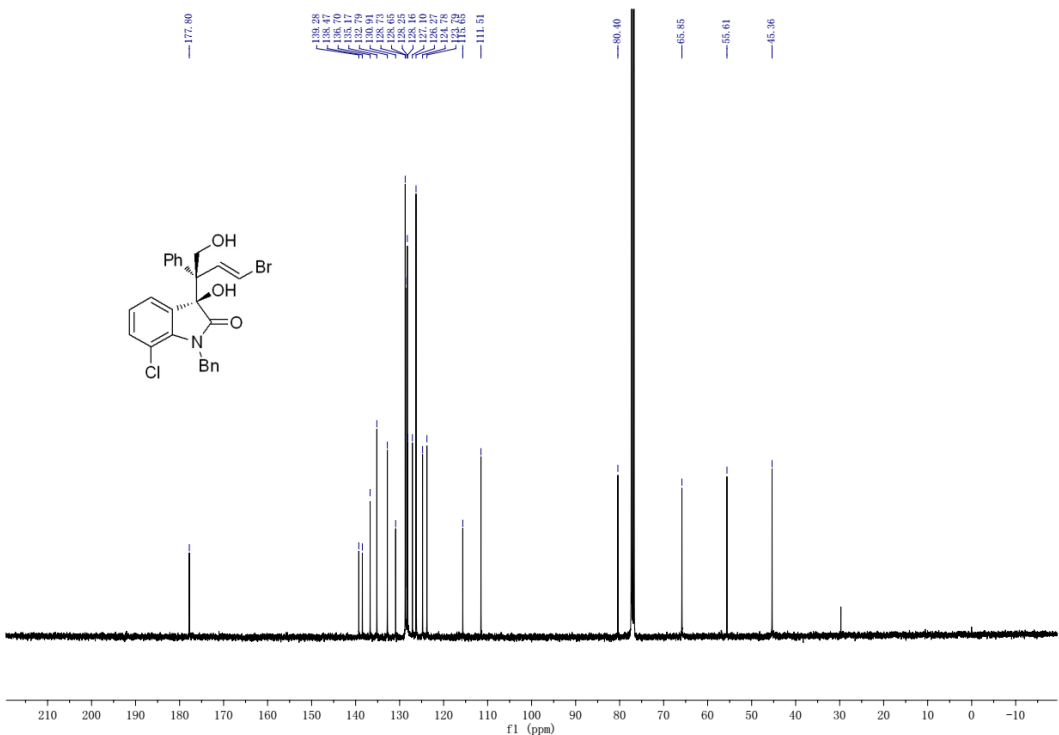


Figure S37. ^{13}C NMR (100 MHz, CDCl_3) spectrum for **3r**, related to **Figure 2**.

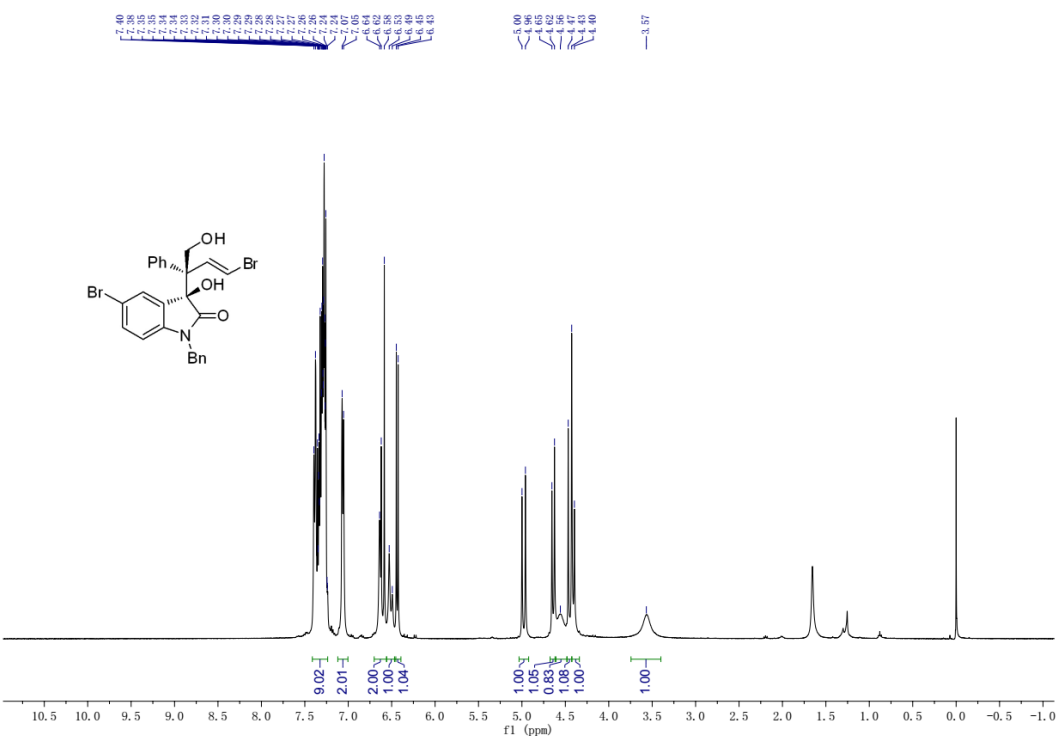


Figure S38. ^1H NMR (400 MHz, CDCl_3) spectrum for **3s**, related to **Figure 2**.

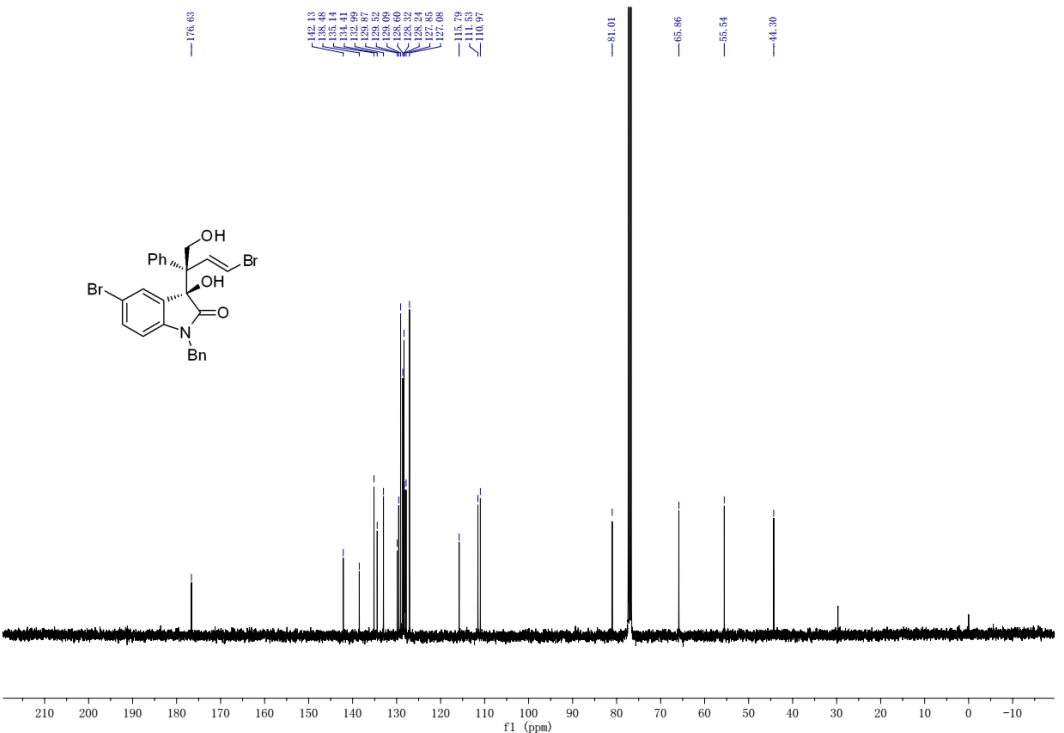


Figure S39. ^{13}C NMR (100 MHz, CDCl_3) spectrum for **3s**, related to **Figure 2**.

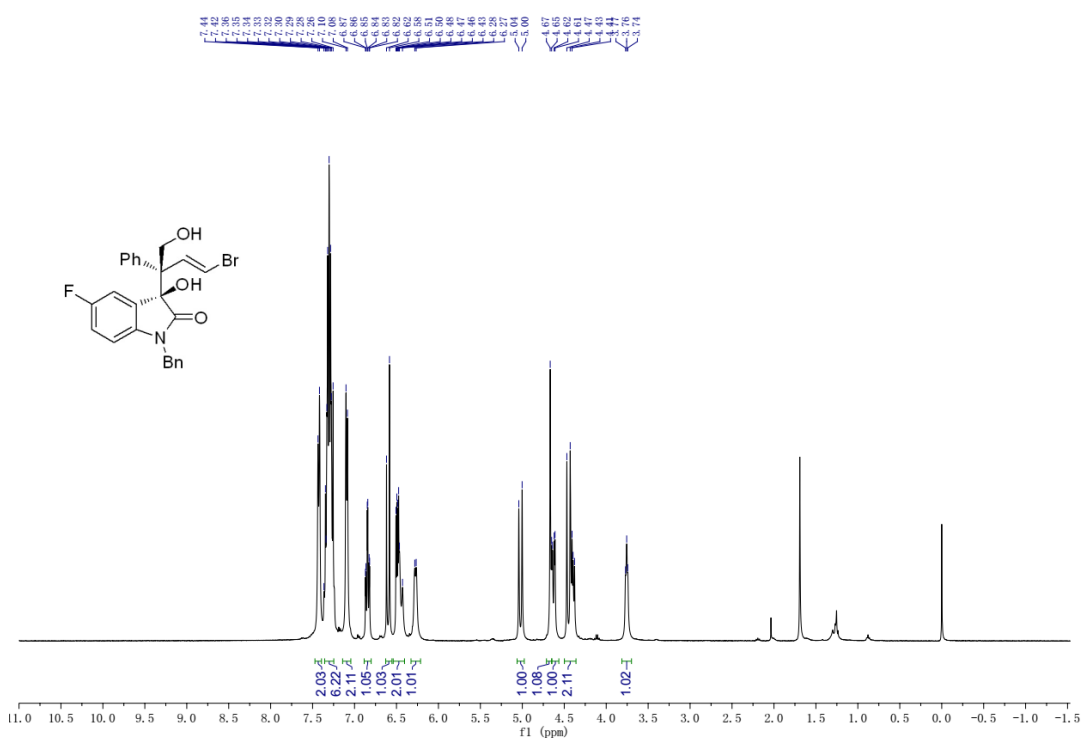


Figure S42. ^1H NMR (400 MHz, CDCl_3) spectrum for **3u**, related to **Figure 2**.

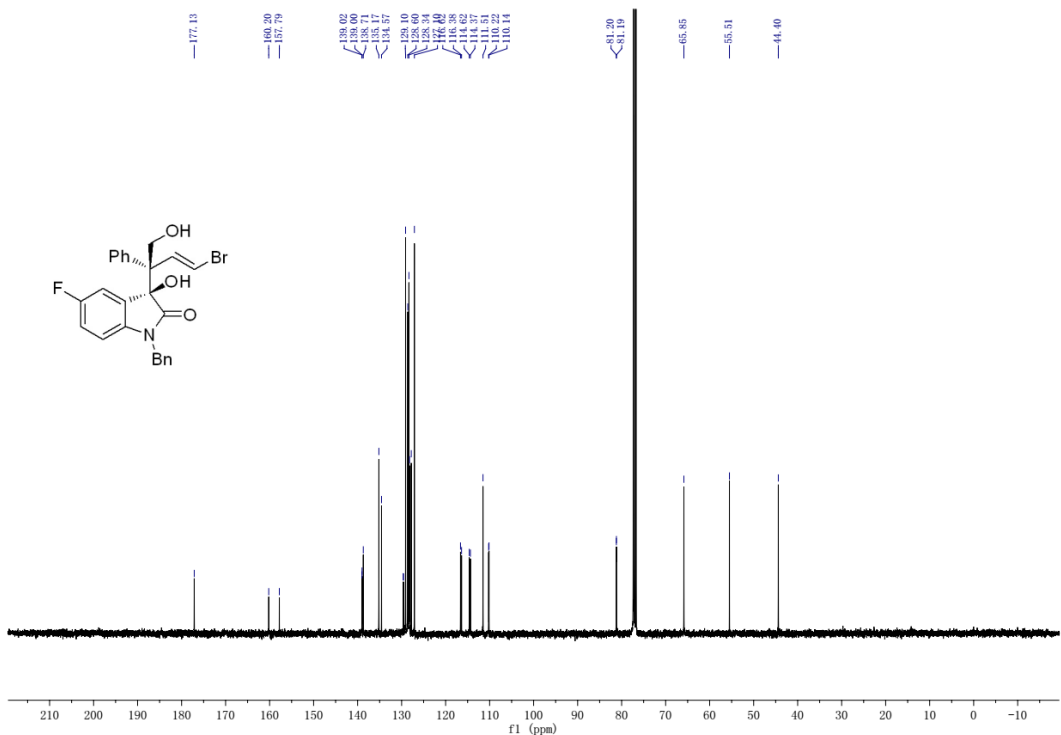


Figure S43. ^{13}C NMR (100 MHz, CDCl_3) spectrum for **3u**, related to **Figure 2**.

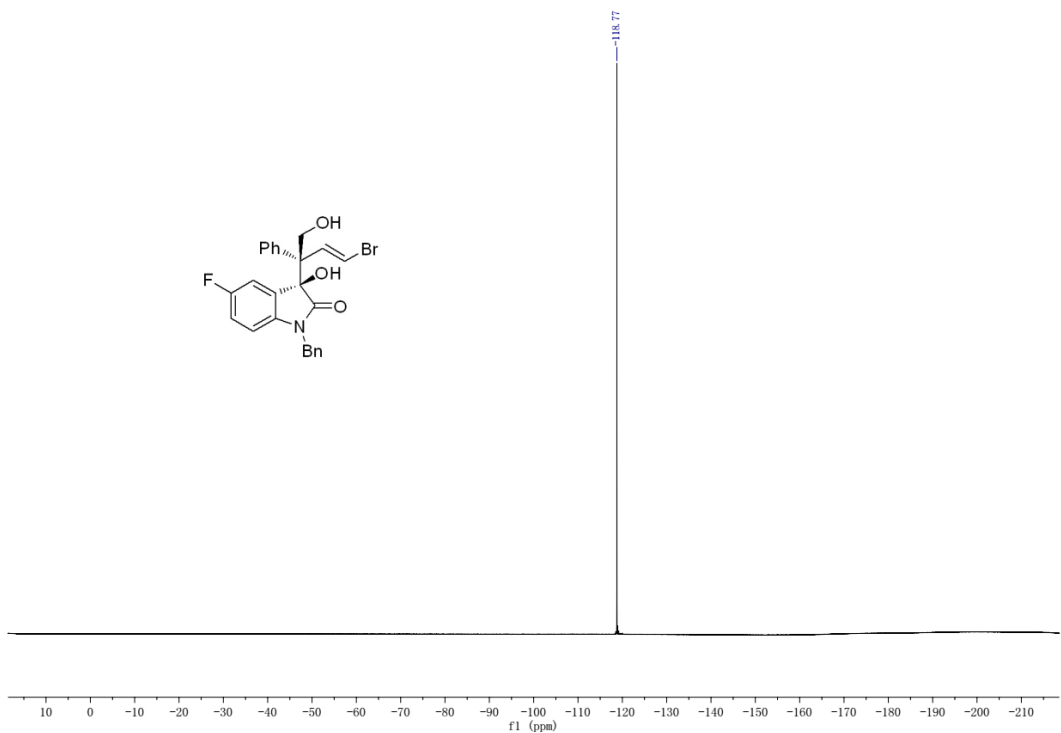


Figure S44. ^{19}F NMR (376 MHz, CDCl_3) spectrum for **3u**, related to **Figure 2**.

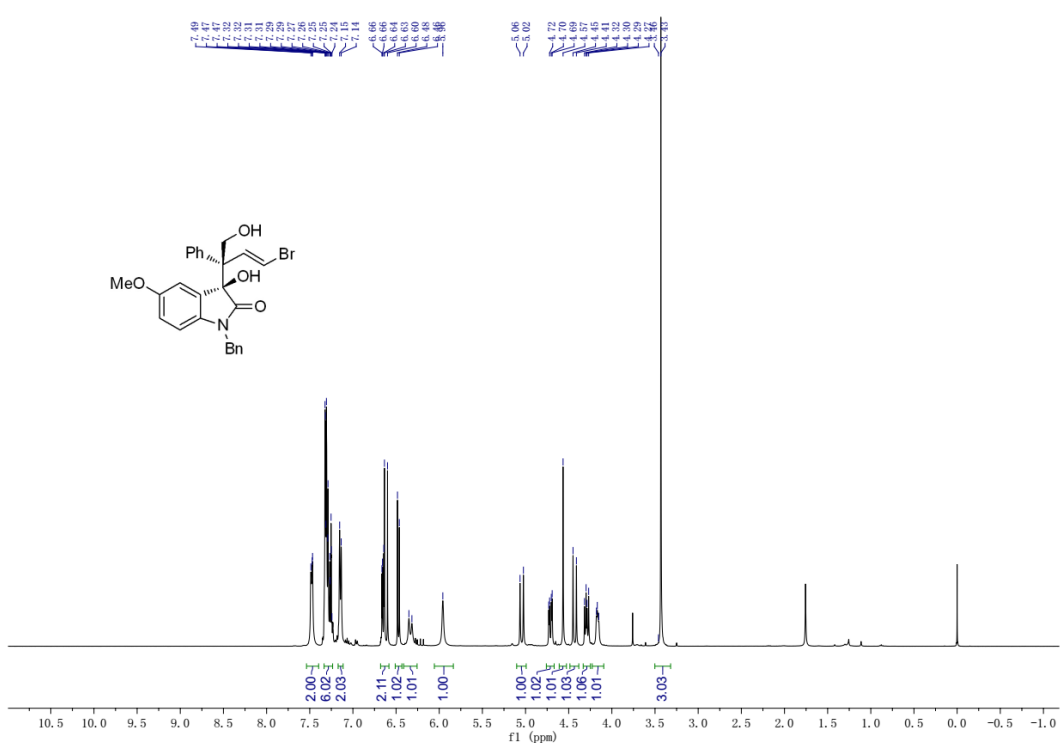


Figure S45. ^1H NMR (400 MHz, CDCl_3) spectrum for **3v**, related to Figure 2.

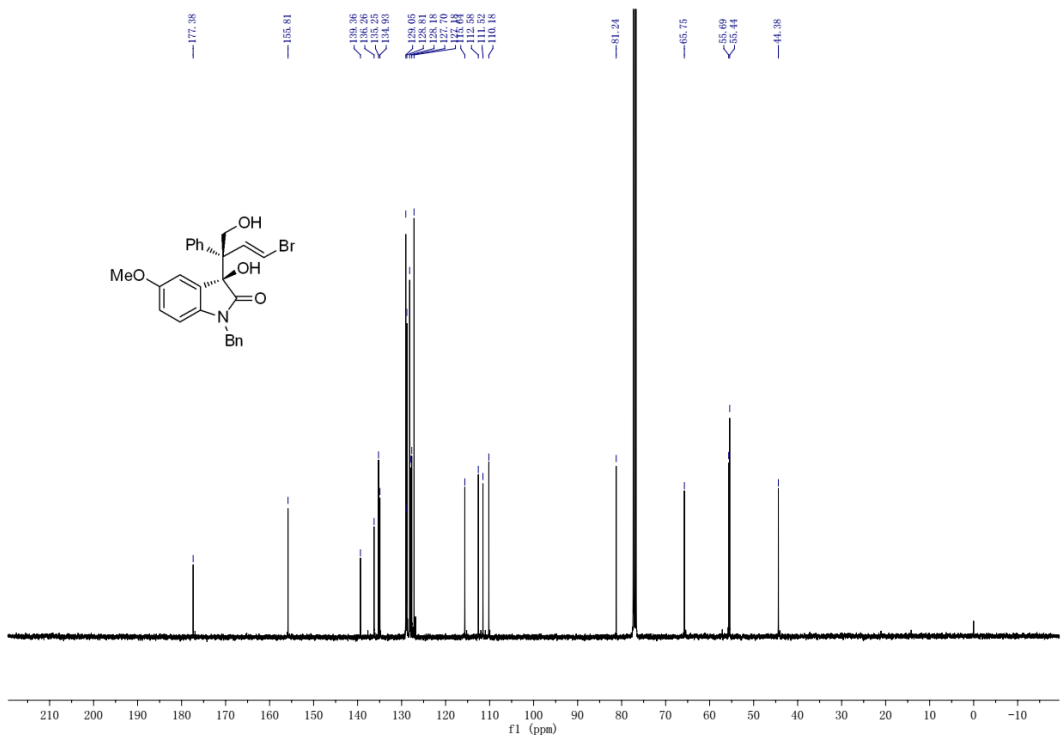


Figure S46. ^{13}C NMR (100 MHz, CDCl_3) spectrum for **3v**, related to **Figure 2**.

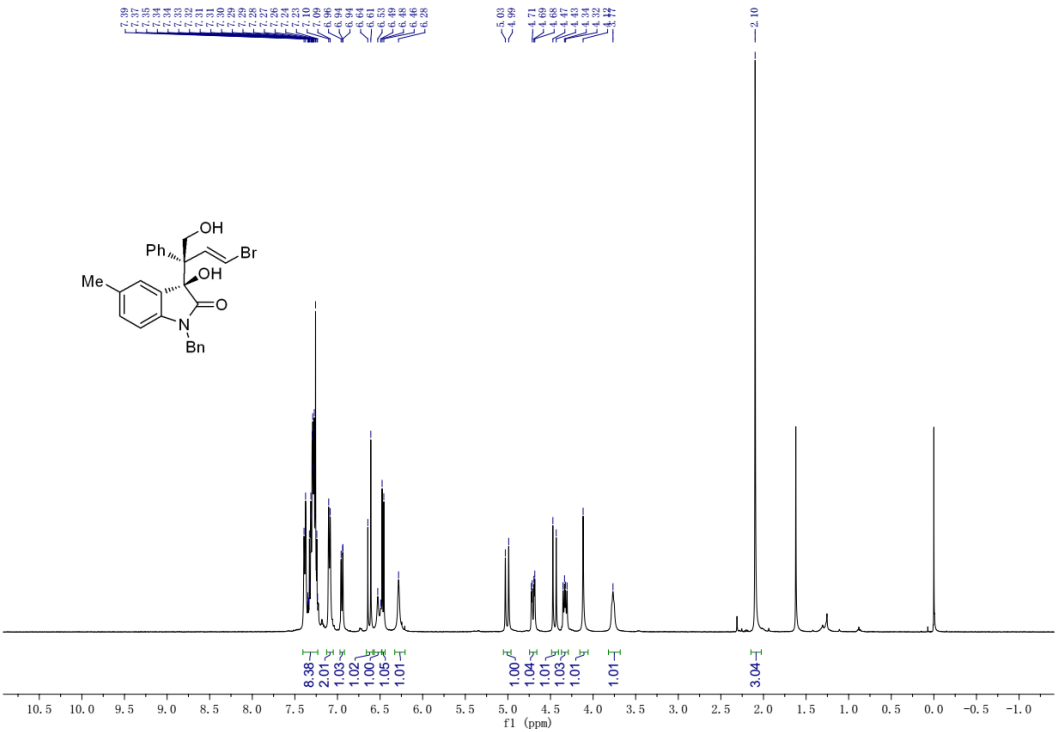


Figure S47. ¹H NMR (400 MHz, CDCl₃) spectrum for 3w, related to **Figure 2**.

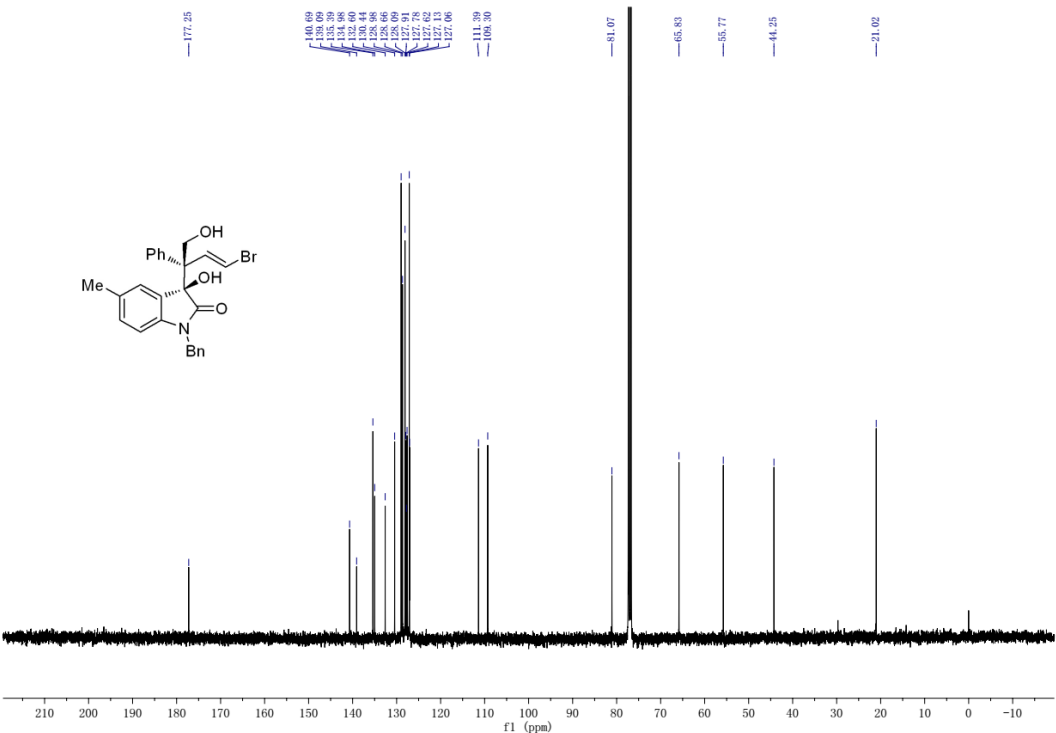


Figure S48. ¹³C NMR (100 MHz, CDCl₃) spectrum for 3w, related to **Figure 2**.

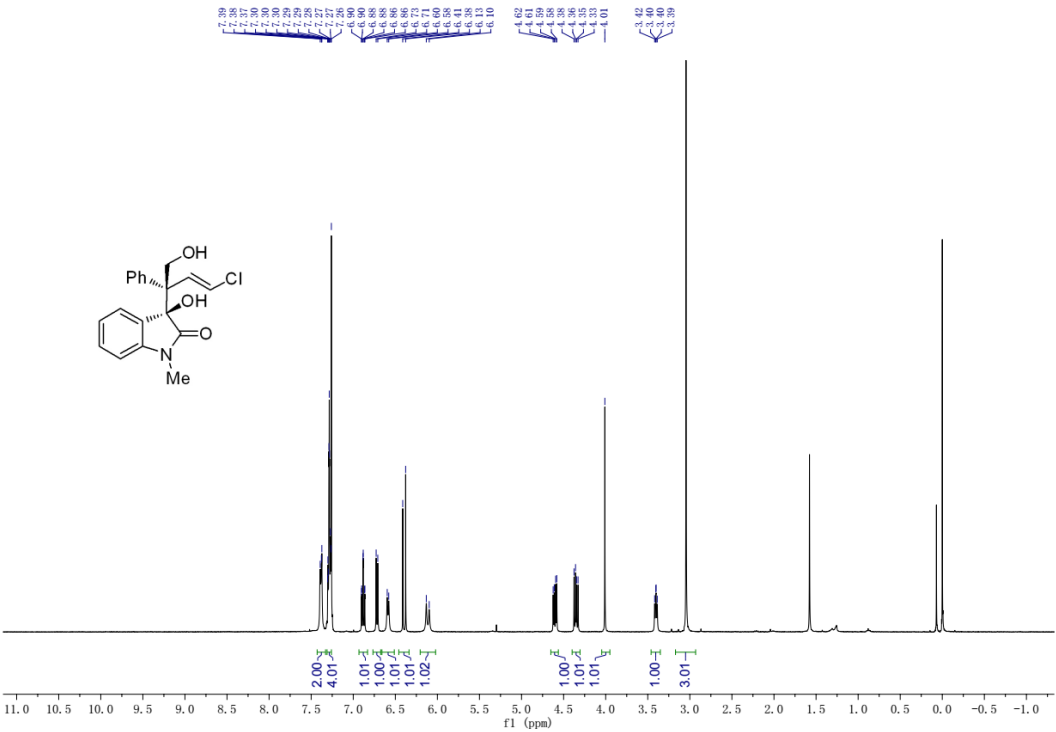


Figure S49. ^1H NMR (400 MHz, CDCl_3) spectrum for **3x**, related to **Figure 2**.

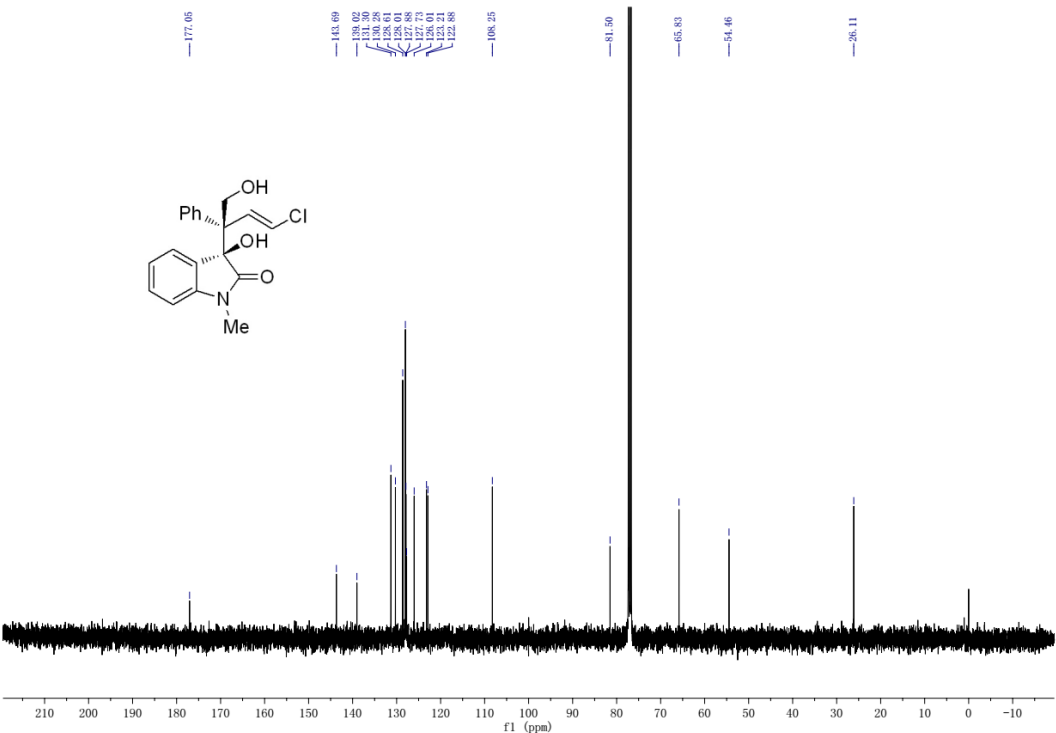


Figure S50. ^{13}C NMR (100 MHz, CDCl_3) spectrum for **3x**, related to **Figure 2**.

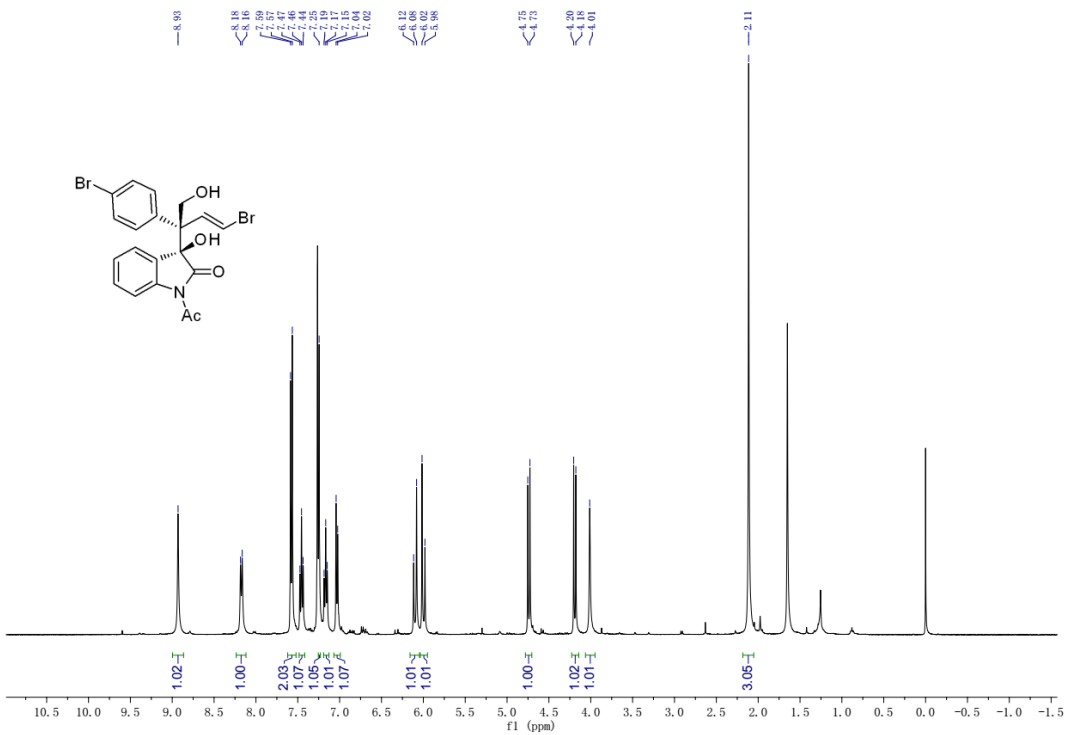


Figure S51. ¹H NMR (400 MHz, CDCl₃) spectrum for 3y, related to **Figure 2**.

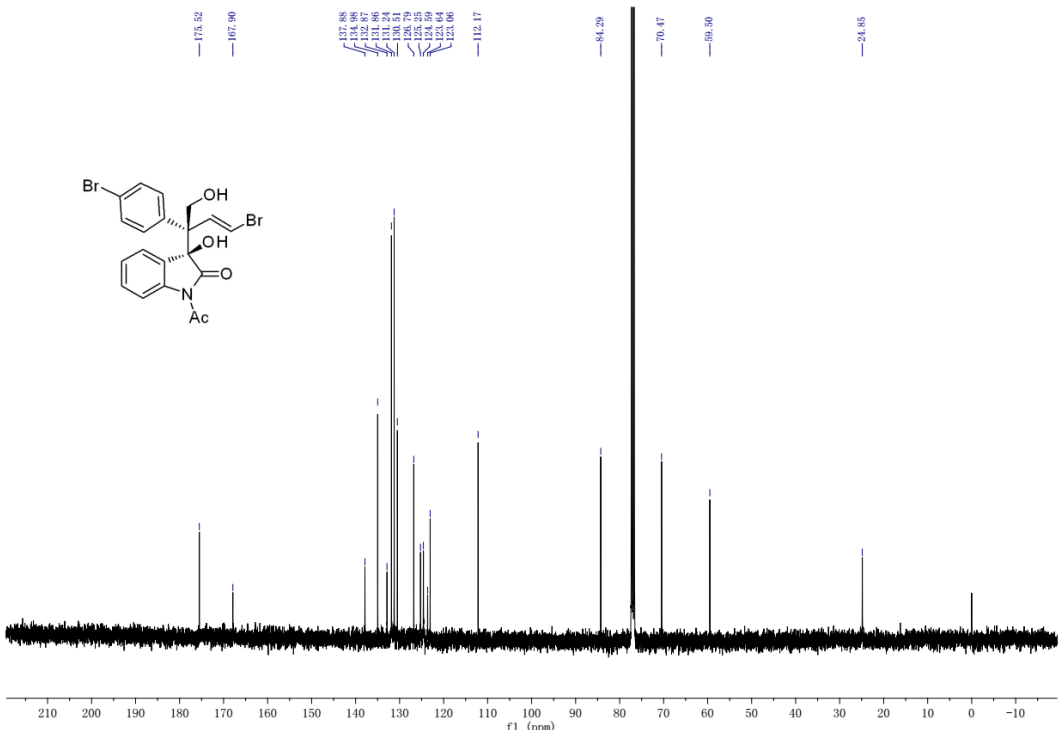


Figure S52. ¹³C NMR (100 MHz, CDCl₃) spectrum for 3y, related to **Figure 2**.

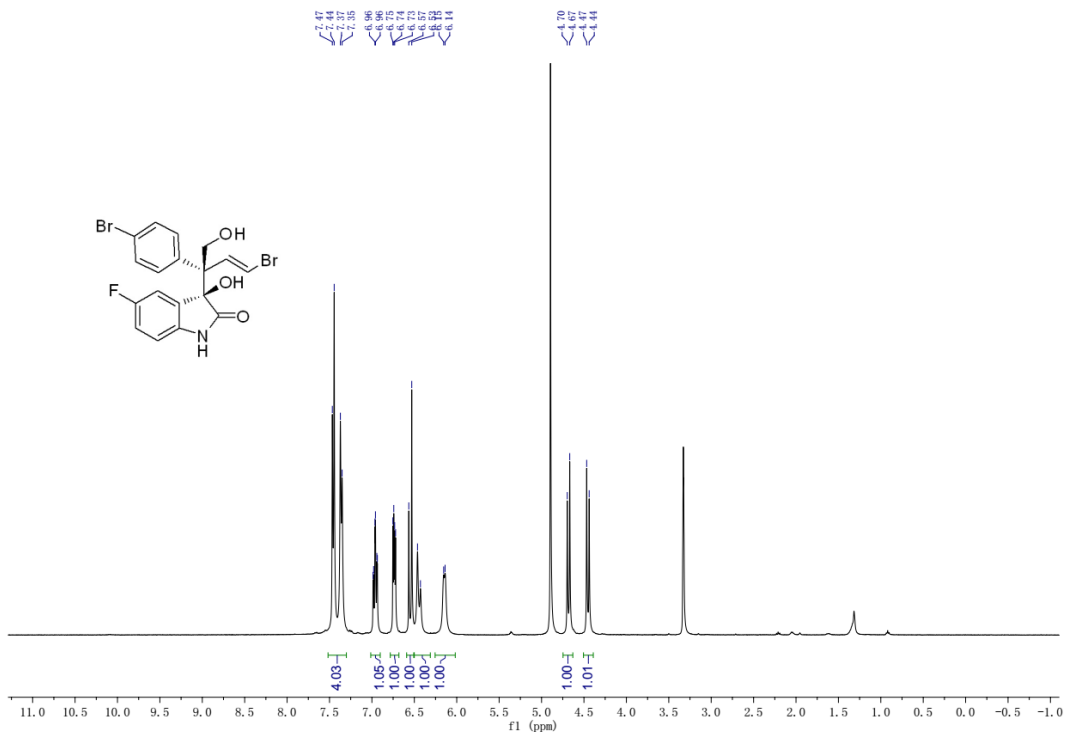


Figure S53. ^1H NMR (400 MHz, MeOD) spectrum for **3z**, related to **Figure 2**.

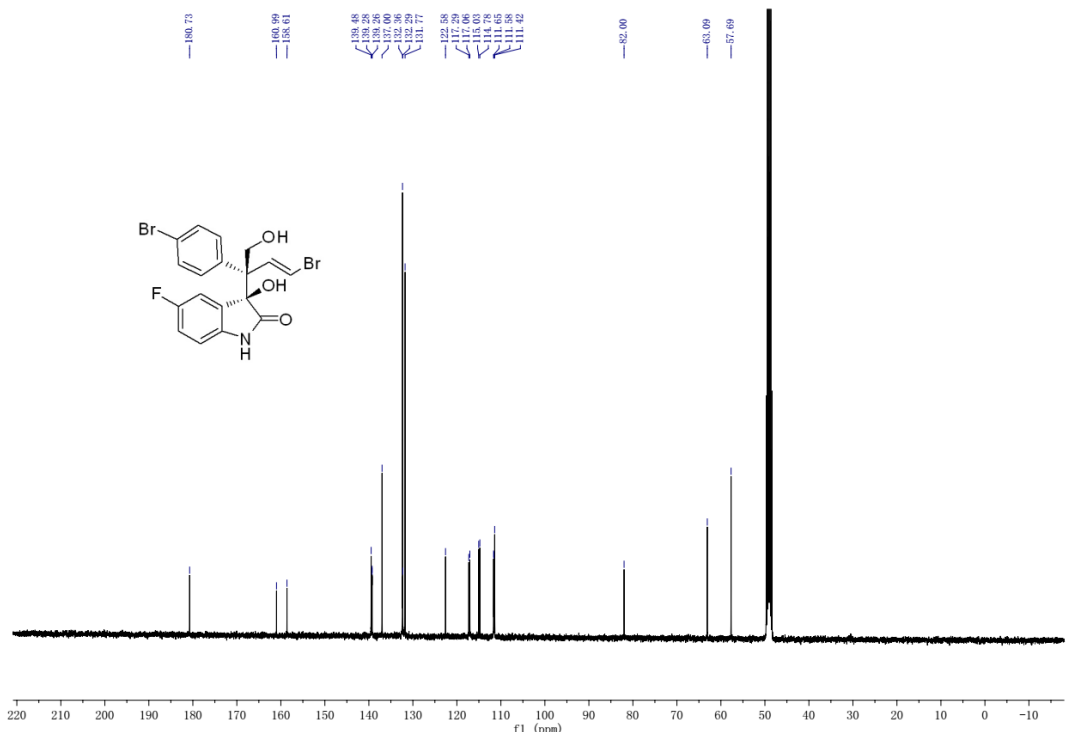


Figure S54. ^{13}C NMR (100 MHz, MeOD) spectrum for **3z**, related to **Figure 2**.

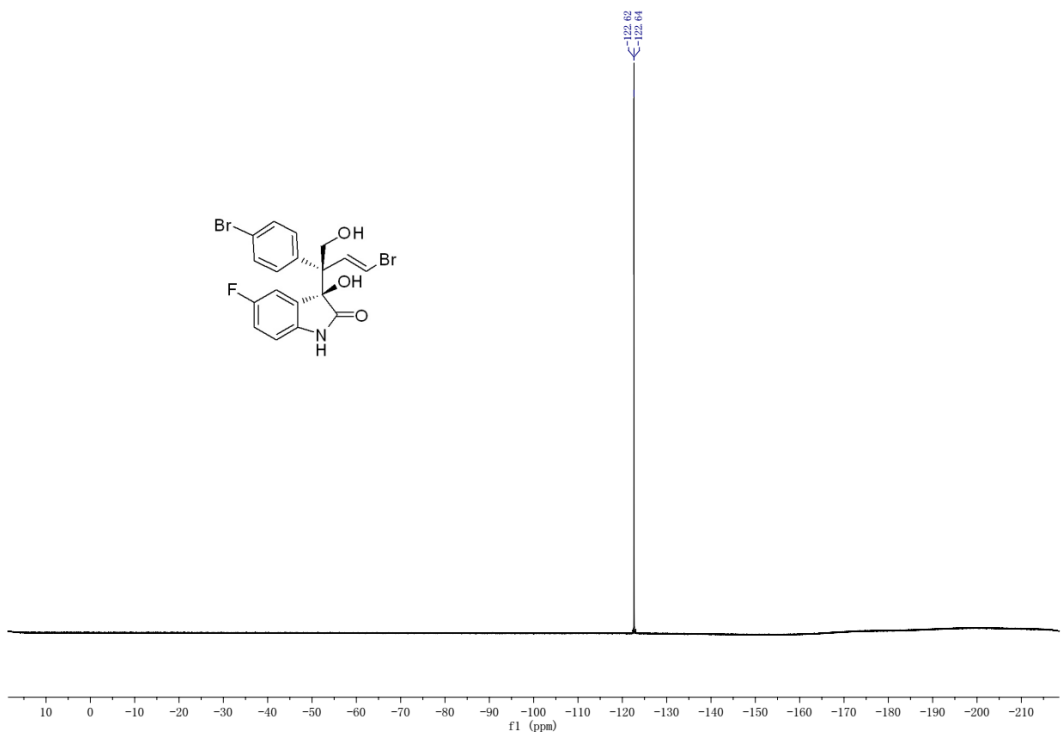


Figure S55. ^{19}F NMR (376 MHz, CDCl_3) spectrum for **3z**, related to **Figure 2**.

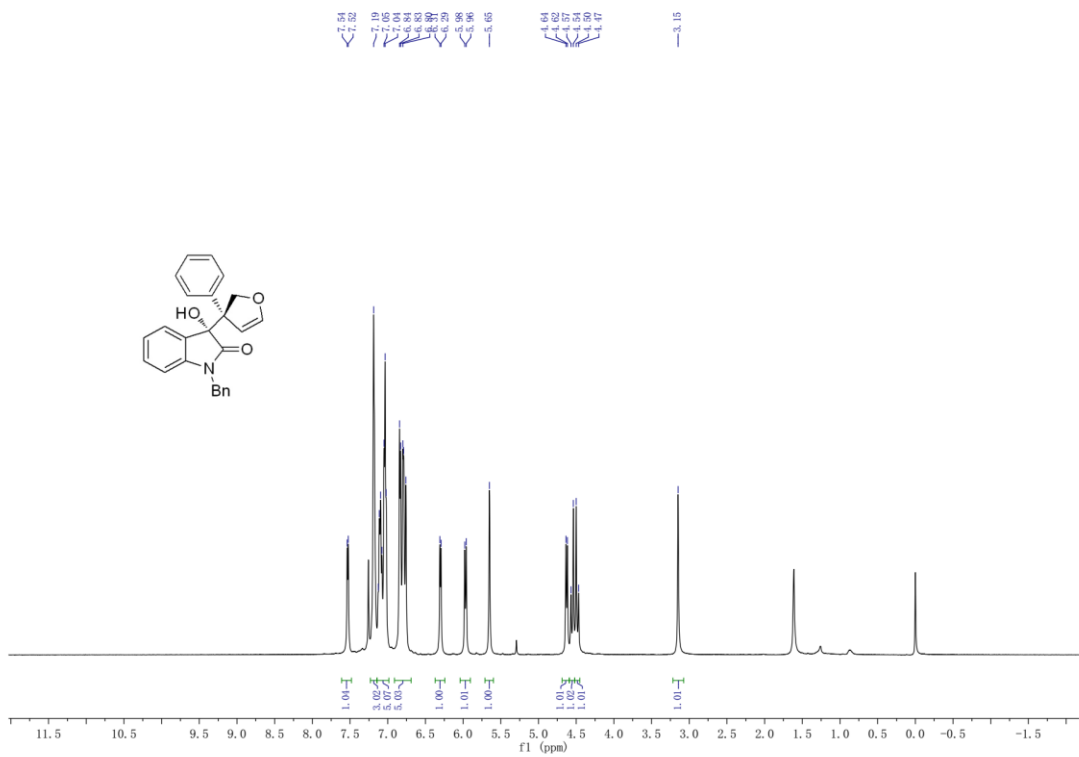


Figure S56. ¹H NMR (500 MHz, CDCl₃) spectrum for **4a**, related to **Figure 2**.

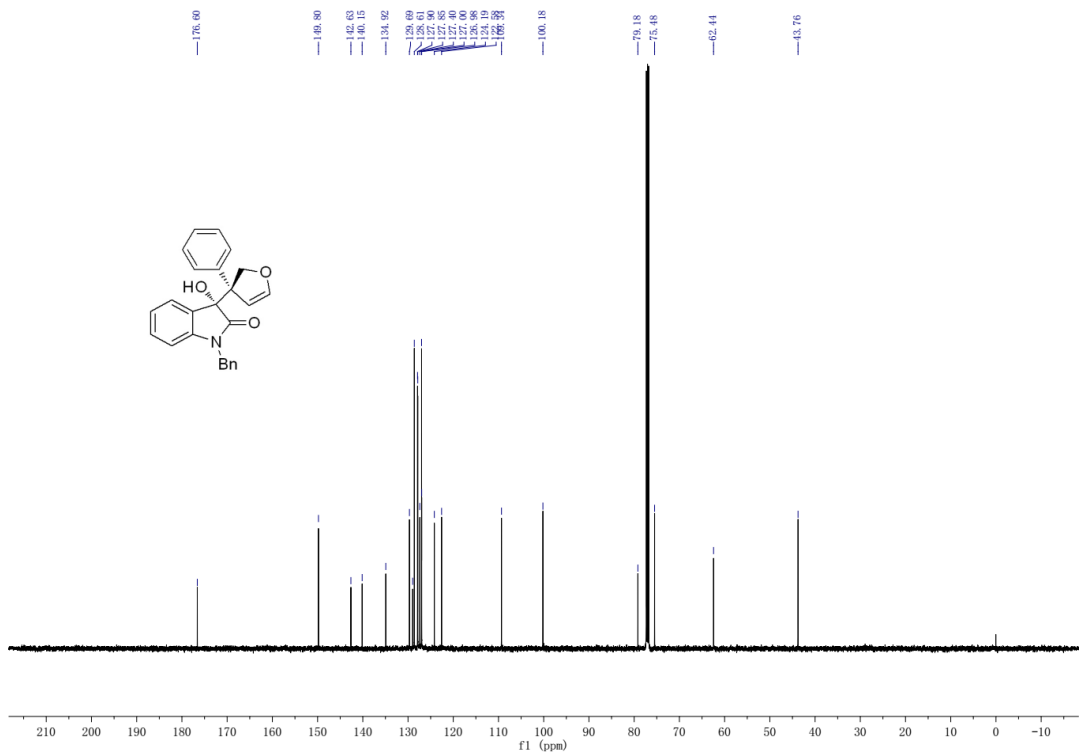


Figure S57. ¹³C NMR (125 MHz, CDCl₃) spectrum for **4a**, related to **Figure 2**.

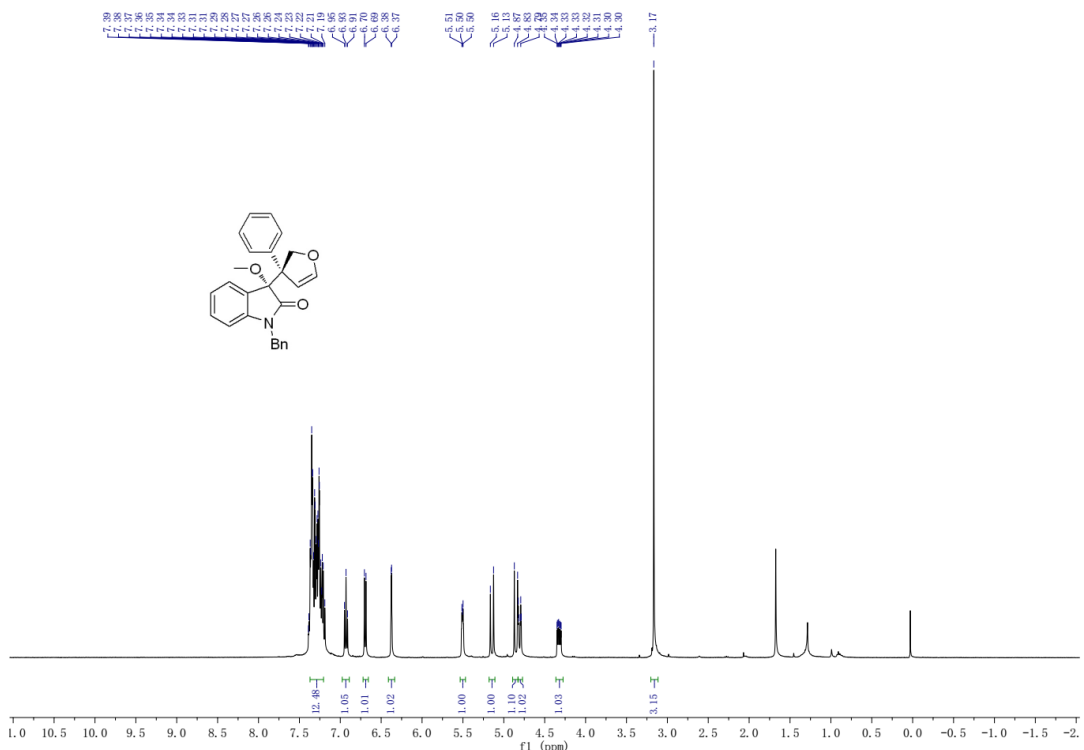


Figure S58. ¹H NMR (400 MHz, CDCl₃) spectrum for **4a'**, related to **Figure 2**.

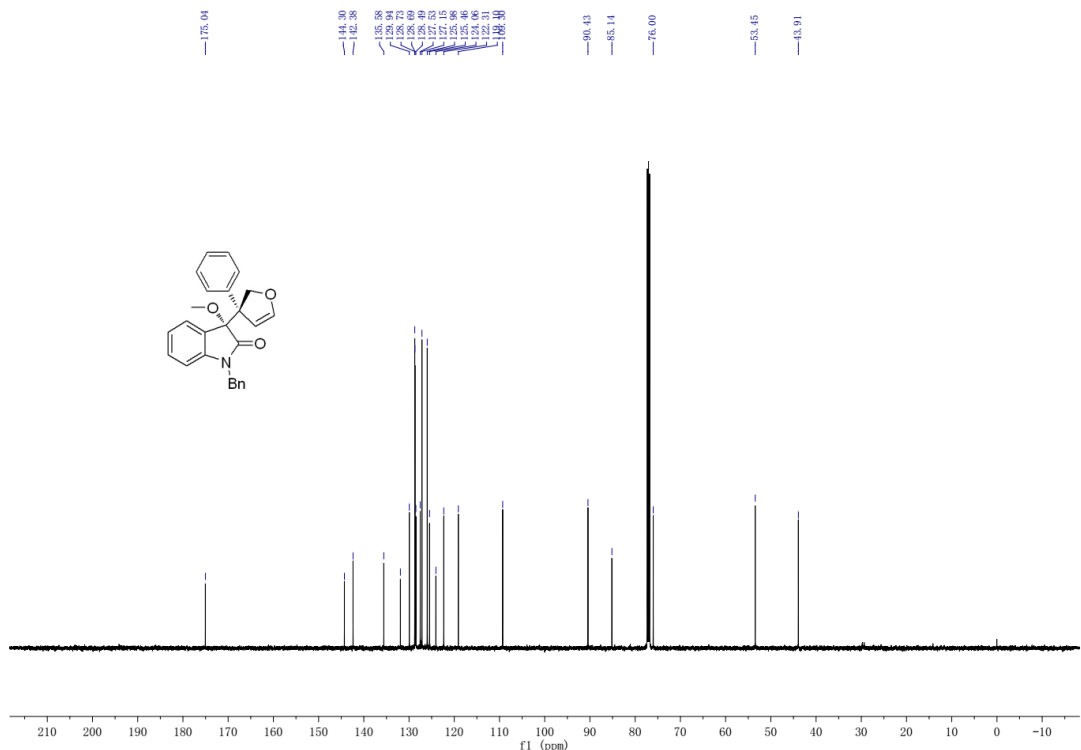


Figure S59. ¹³C NMR (100 MHz, CDCl₃) spectrum for **4a'**, related to **Figure 2**.

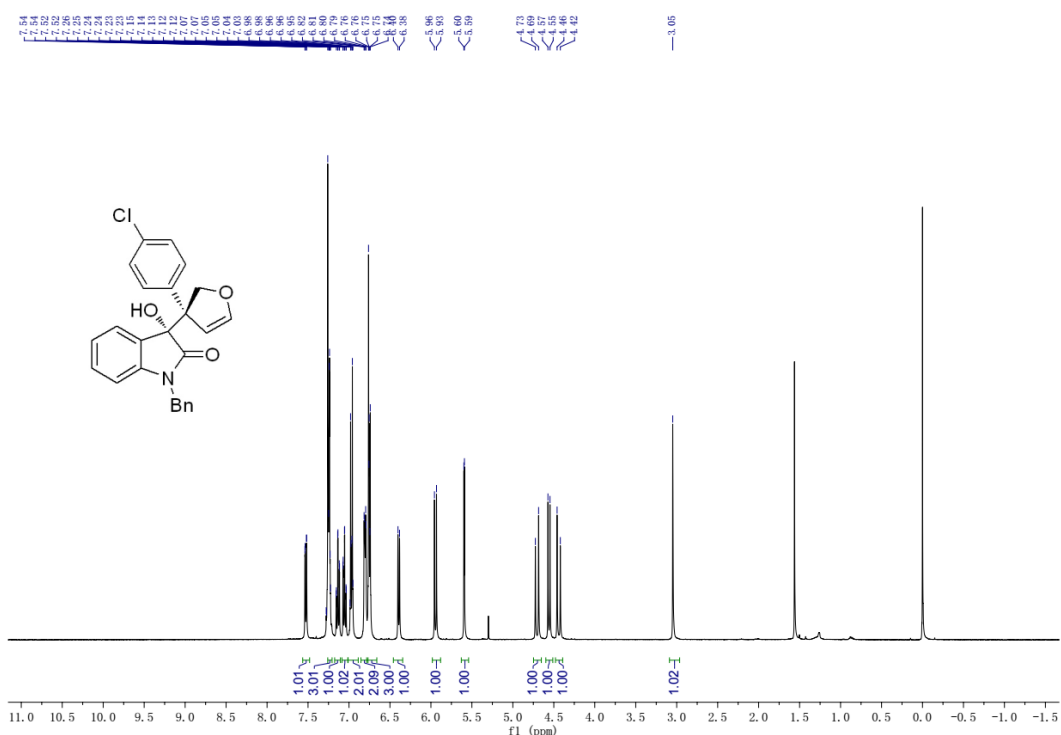


Figure S60. ^1H NMR (400 MHz, CDCl_3) spectrum for **4b**, related to Figure 2.

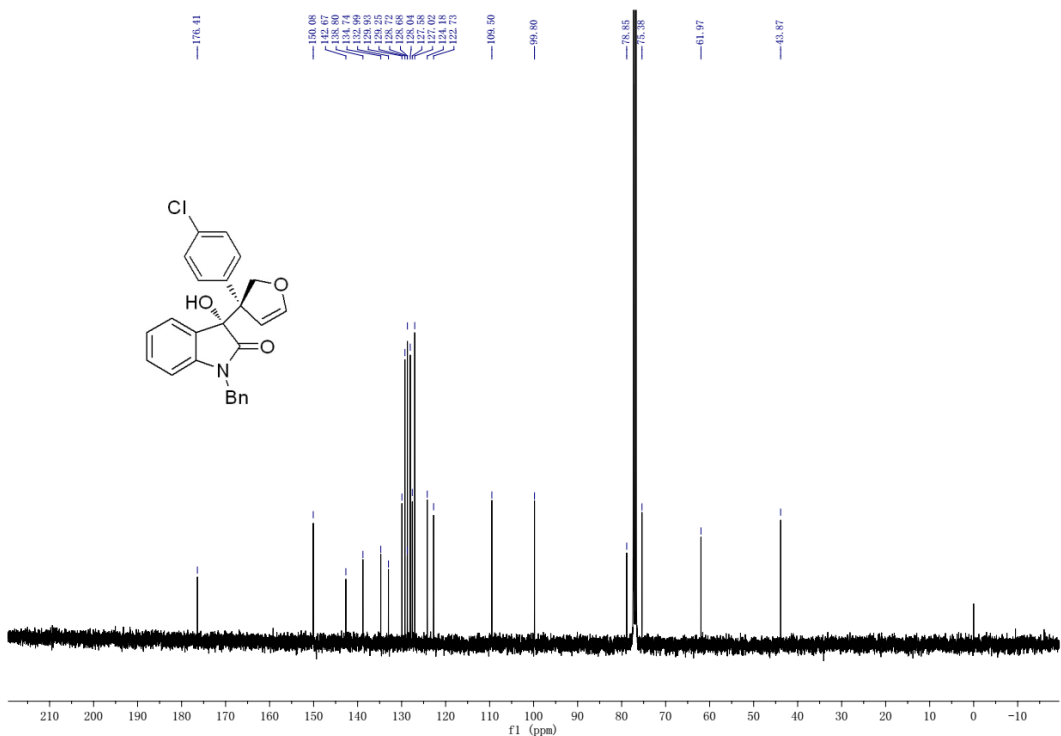


Figure S61. ^{13}C NMR (100 MHz, CDCl_3) spectrum for **4b**, related to Figure 2.

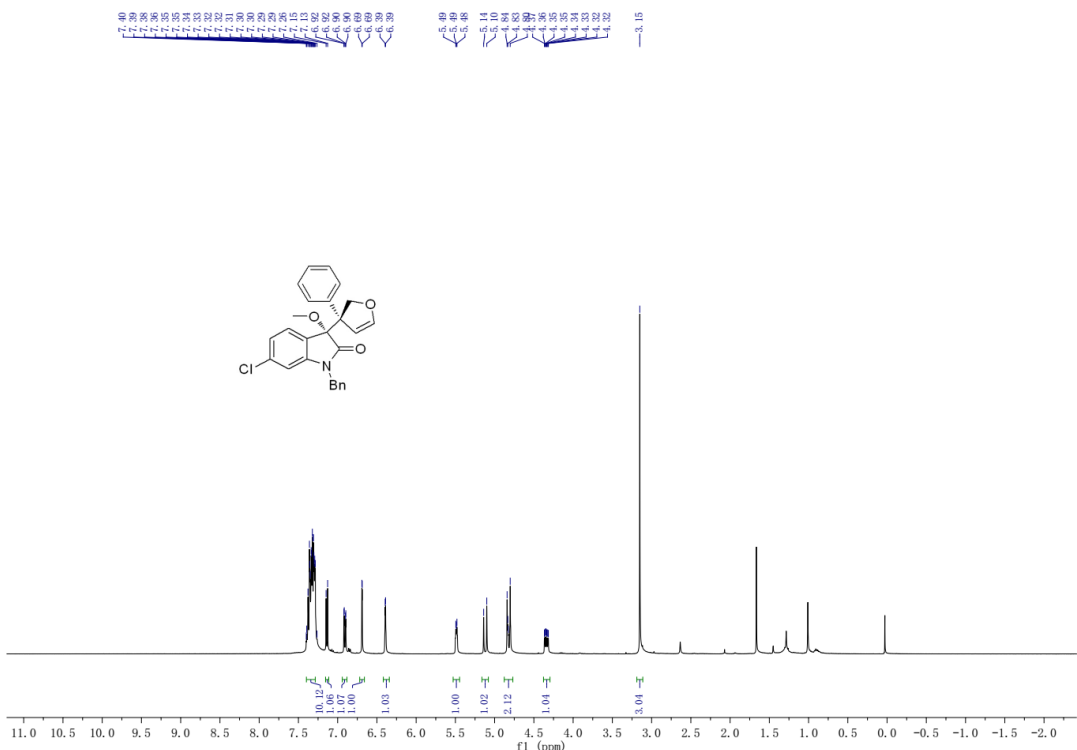


Figure S62. ¹H NMR (400 MHz, CDCl₃) spectrum for **4c'**, related to **Figure 2**.

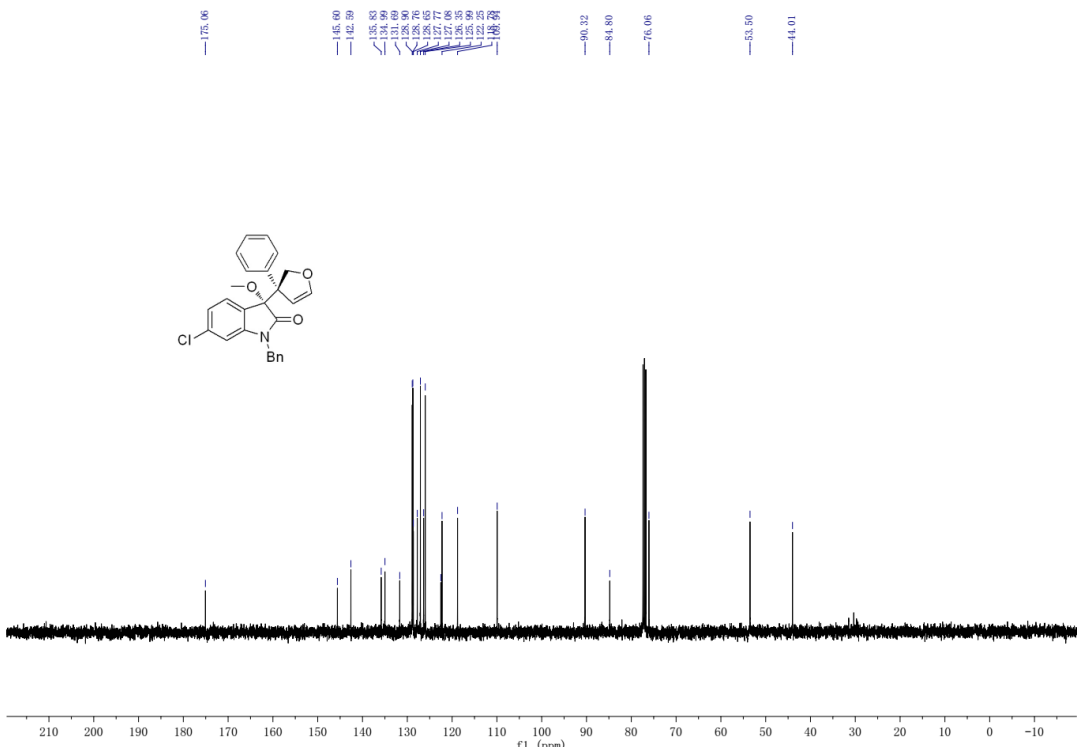


Figure S63. ¹³C NMR (100 MHz, CDCl₃) spectrum for **4c'**, related to **Figure 2**.

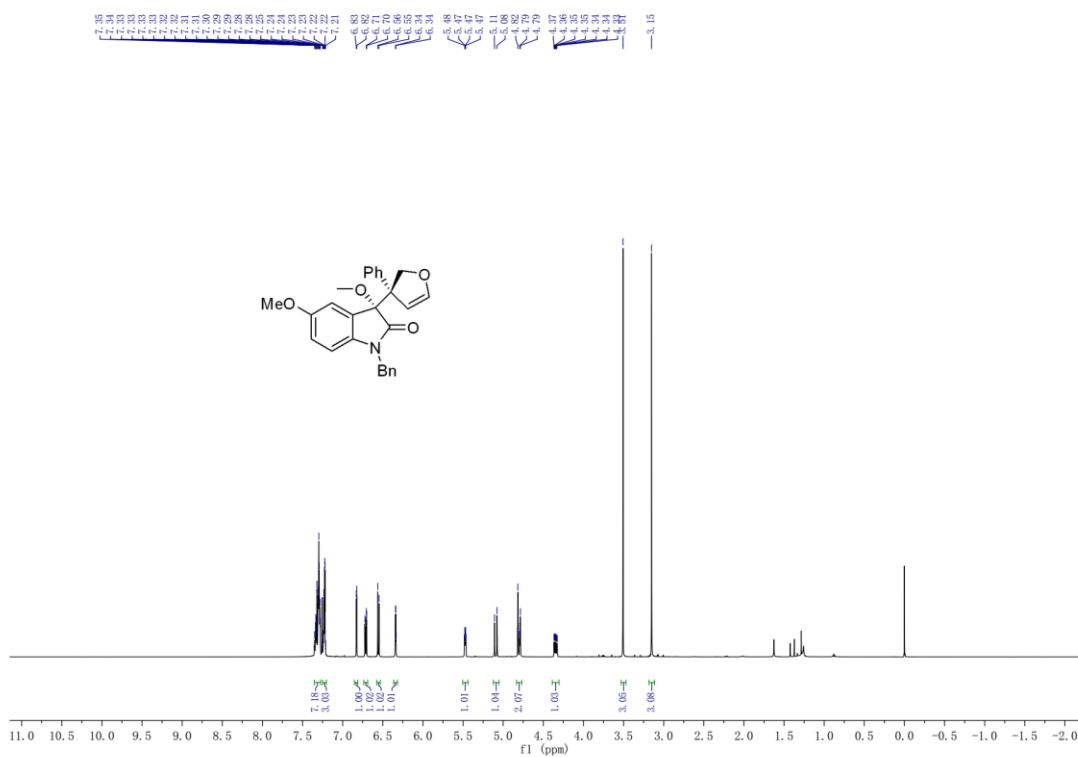


Figure S64. ¹H NMR (500 MHz, CDCl₃) spectrum for **4d'**, related to **Figure 2**.

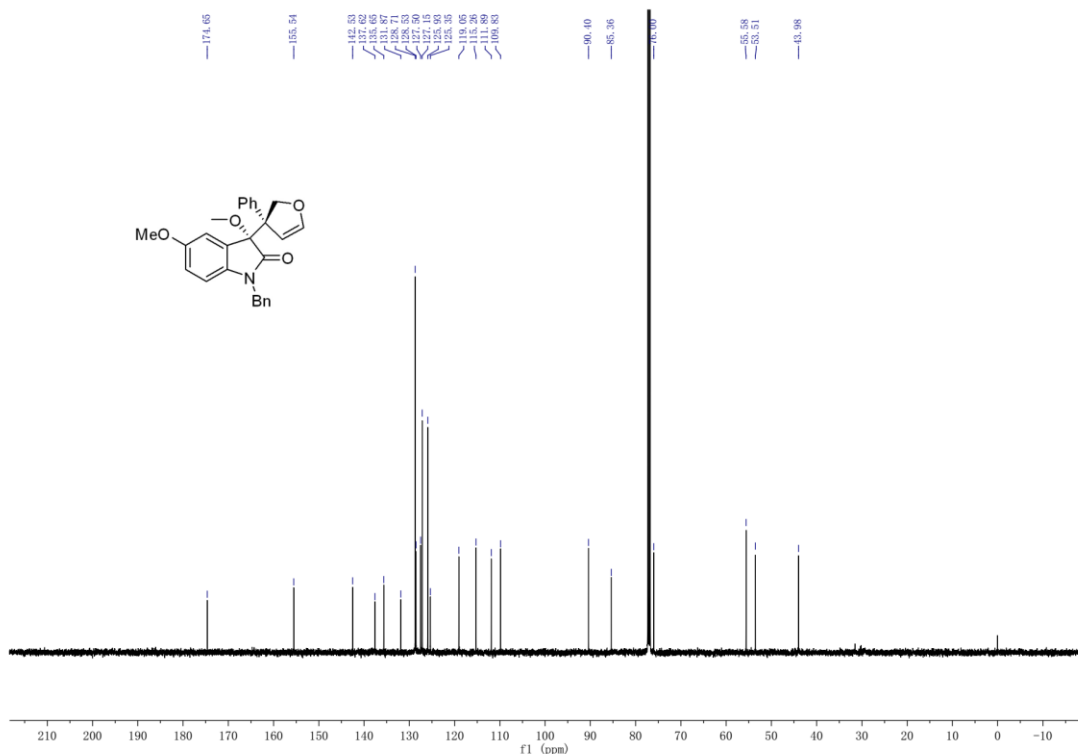


Figure S65. ¹³C NMR (125 MHz, CDCl₃) spectrum for **4d'**, related to **Figure 2**.

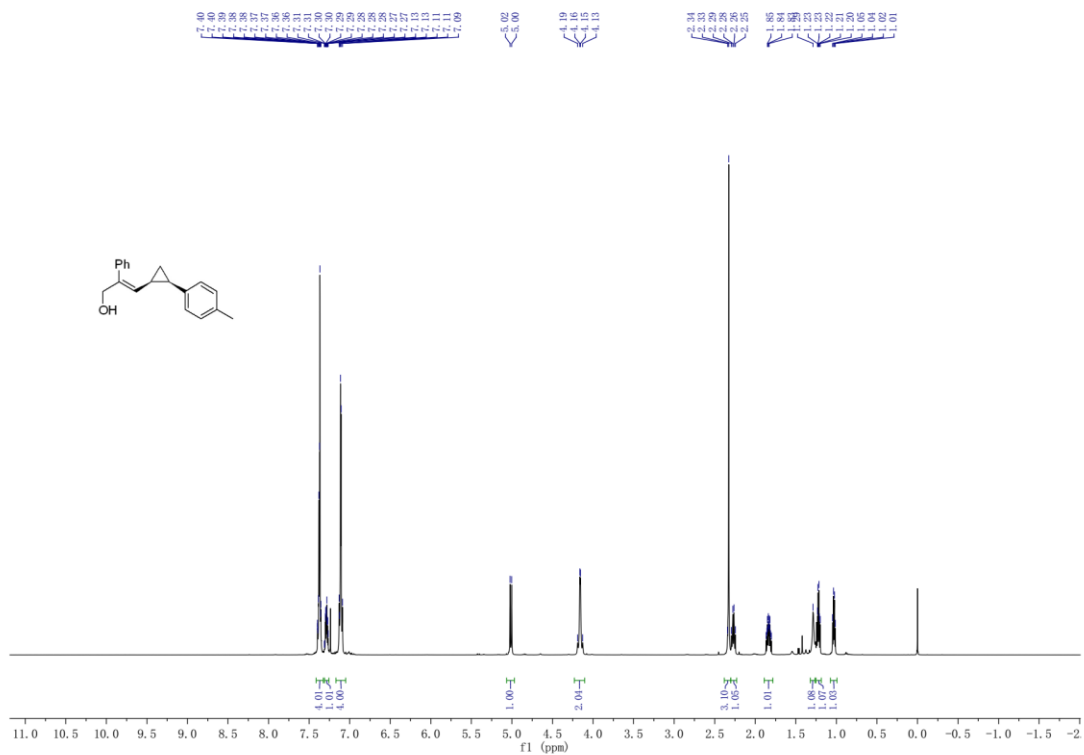


Figure S66. ^1H NMR (500 MHz, CDCl_3) spectrum for **5**, related to **Figure 2**.

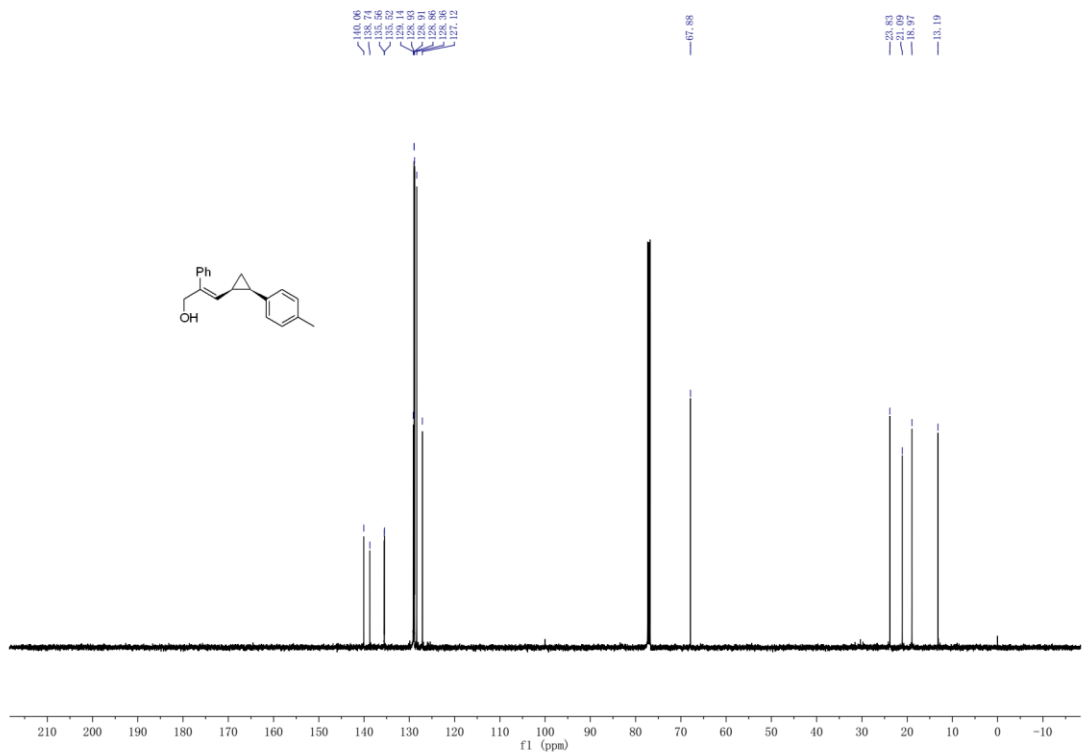


Figure S67. ^{13}C NMR (125 MHz, CDCl_3) spectrum for **5**, related to **Figure 2**.

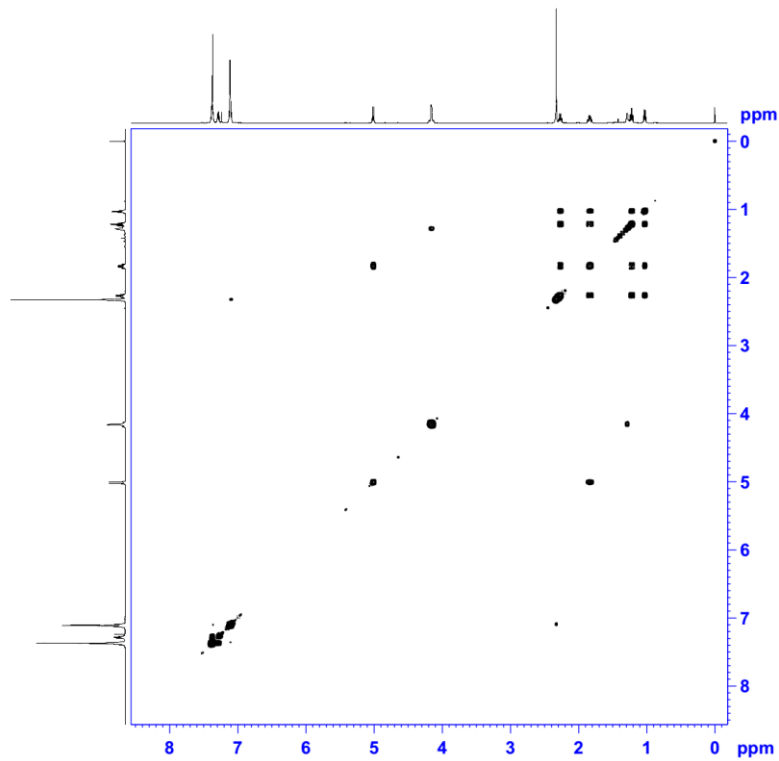


Figure S68. COSY spectrum for **5**, related to **Figure 2**.

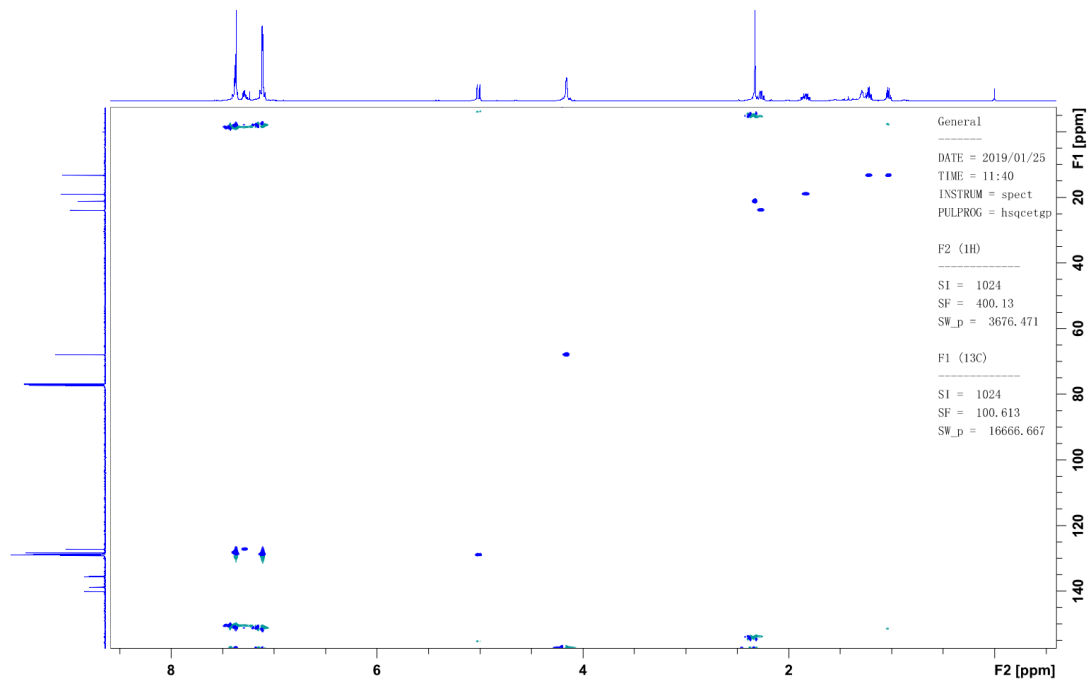


Figure S69. HSQC spectrum for **5**, related to **Figure 2**.

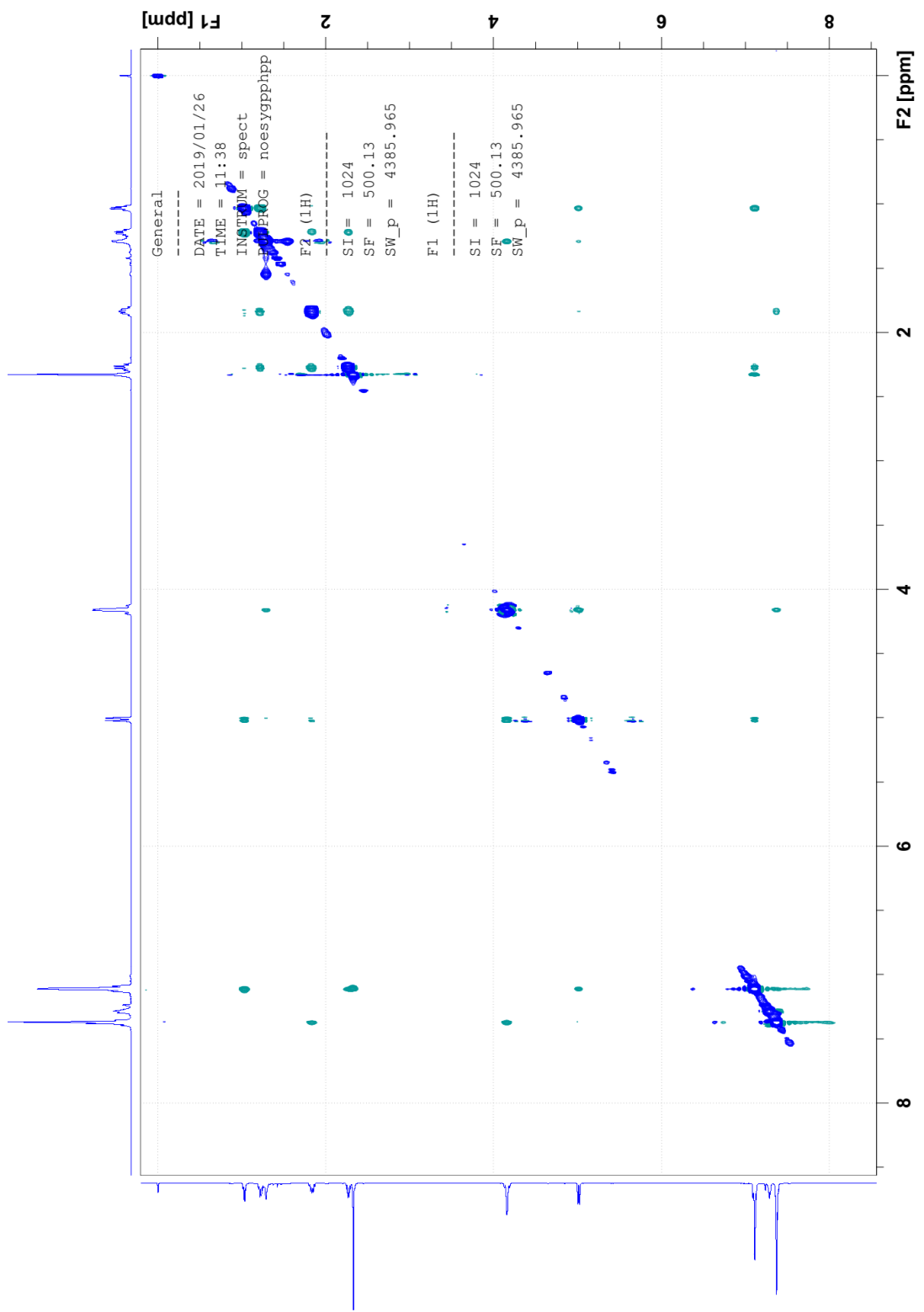


Figure S70. NOESY spectrum for **5**, related to **Figure 2**.

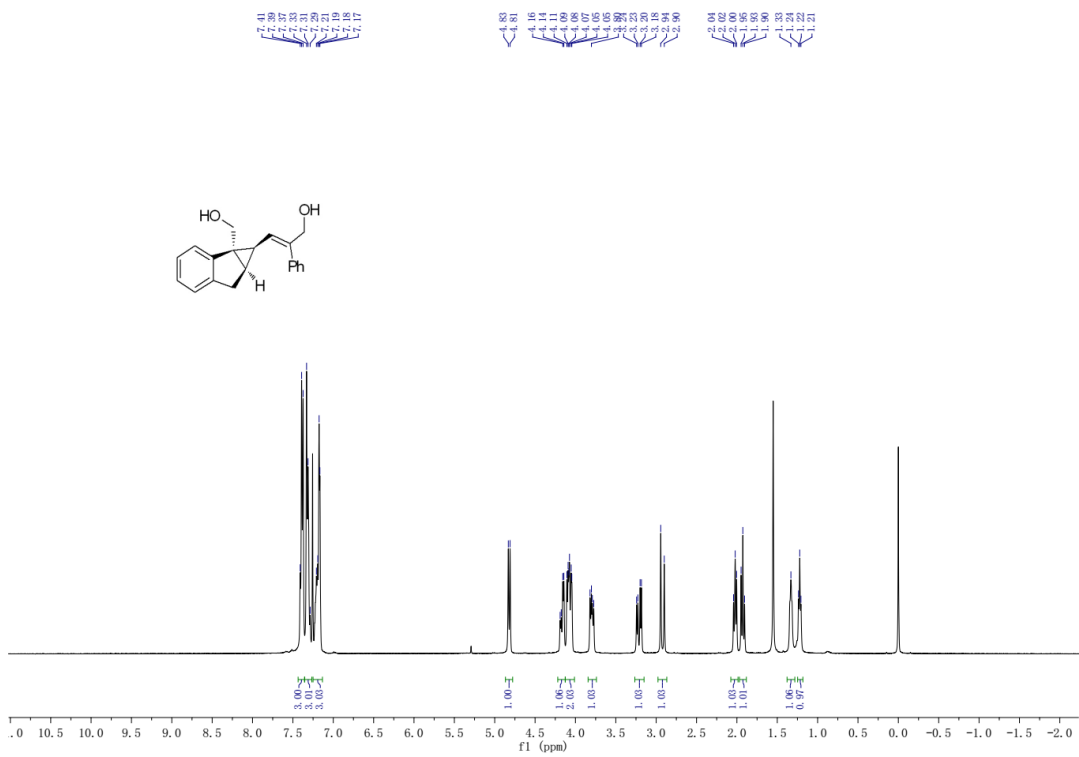


Figure S71. ^1H NMR (400 MHz, CDCl_3) spectrum for **6**, related to Figure 2.

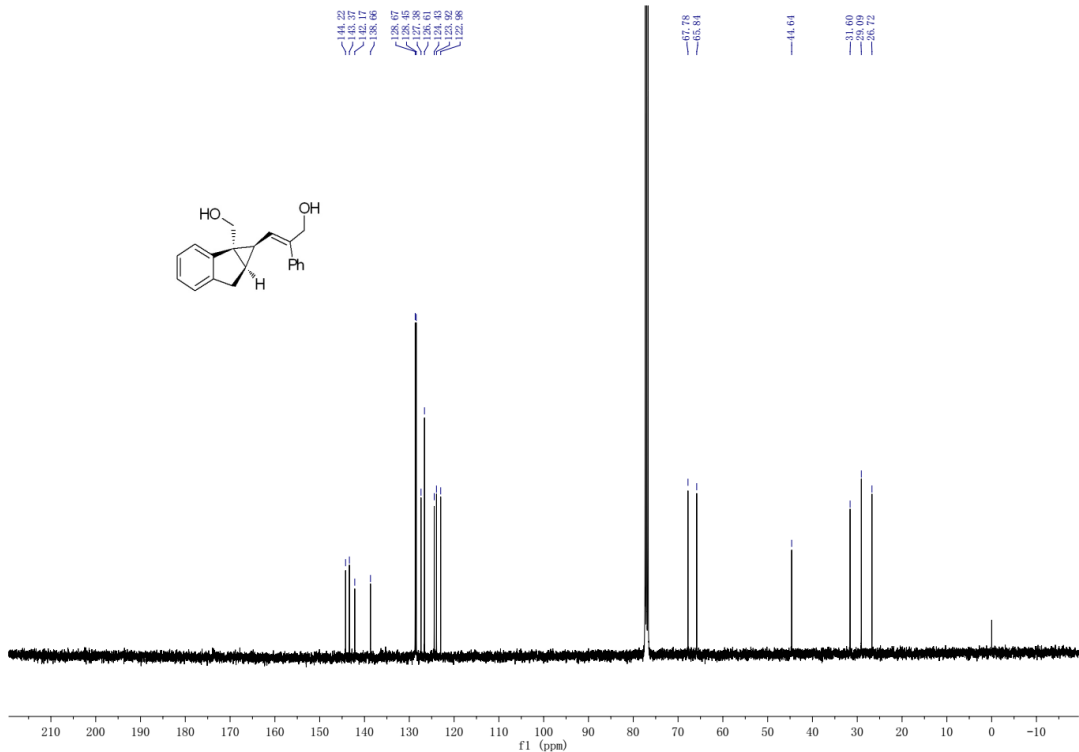


Figure S72. ^{13}C NMR (100 MHz, CDCl_3) spectrum for **6**, related to **Figure 2**.

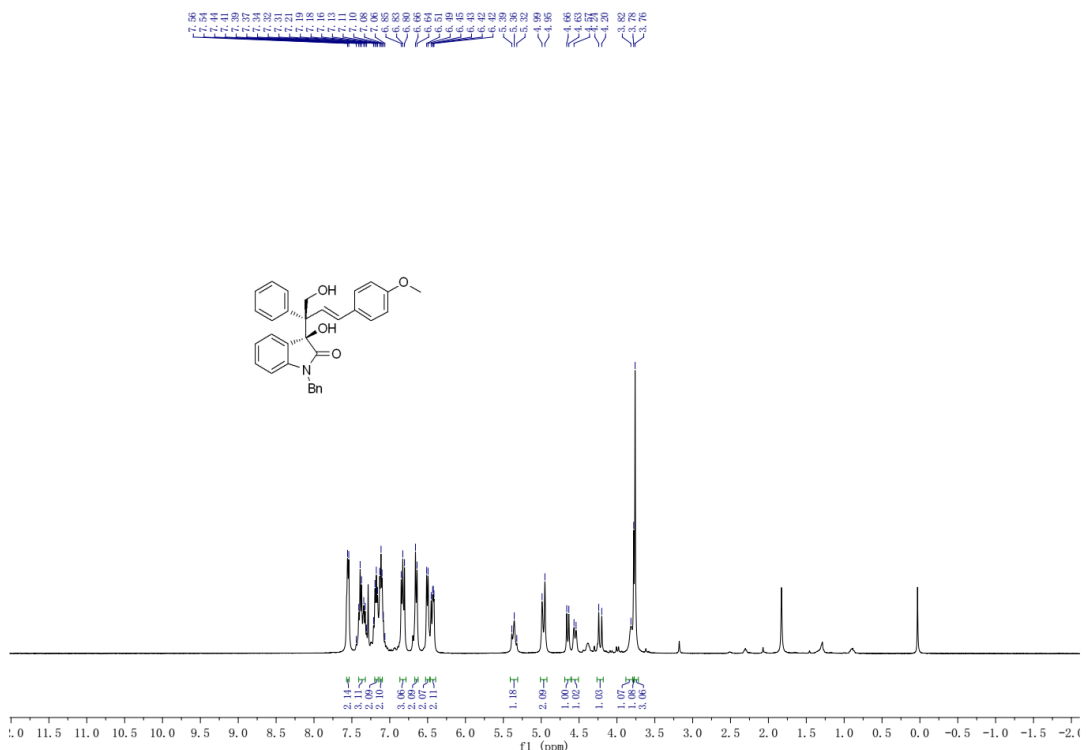


Figure S73. ^1H NMR (400 MHz, CDCl_3) spectrum for **7a**, related to Figure 3.

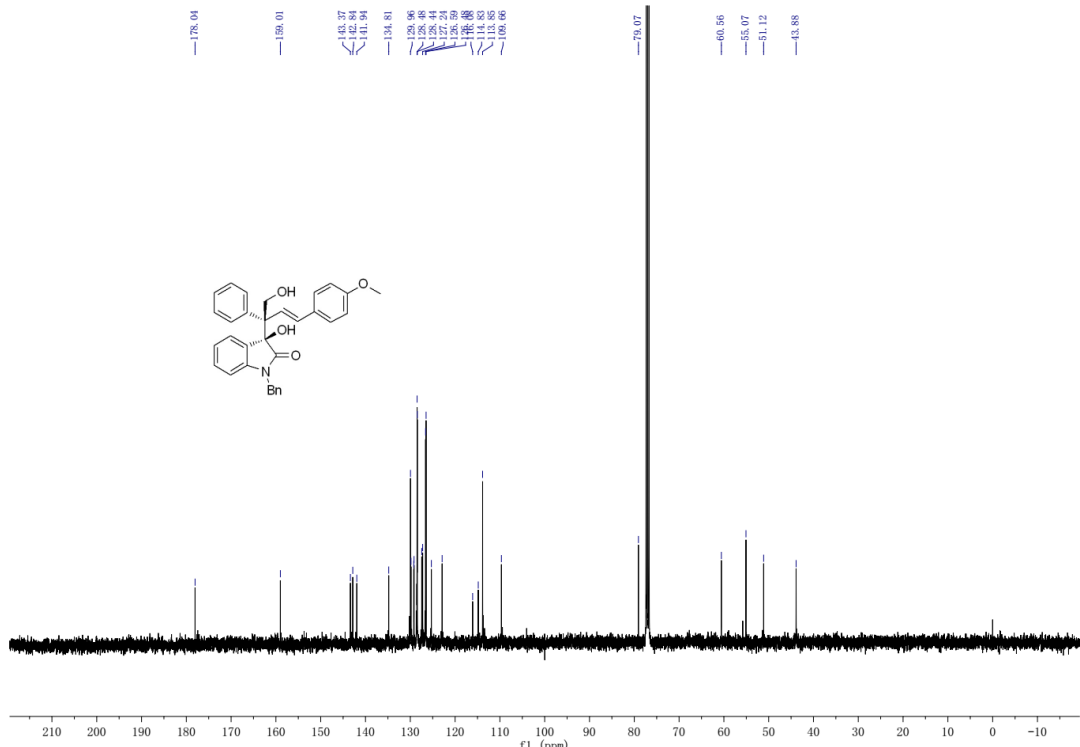


Figure S74. ^{13}C NMR (100 MHz, CDCl_3) spectrum for **7a**, related to Figure 3.

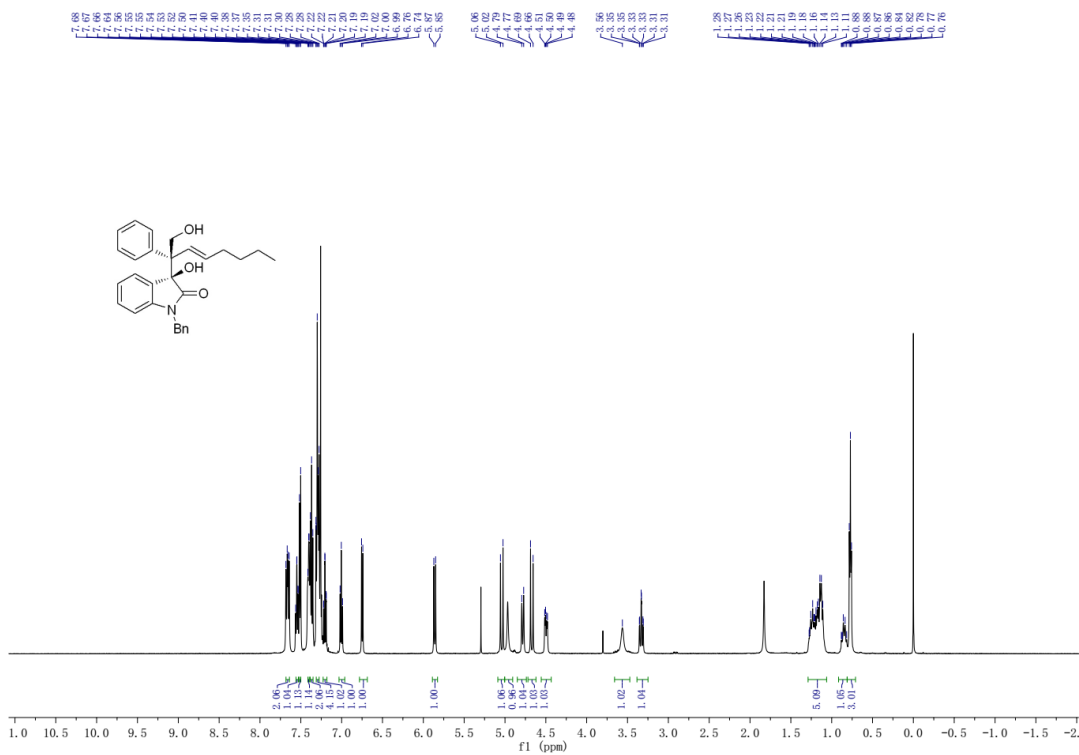


Figure S75. ^1H NMR (500 MHz, CDCl_3) spectrum for **7b**, related to Figure 3.

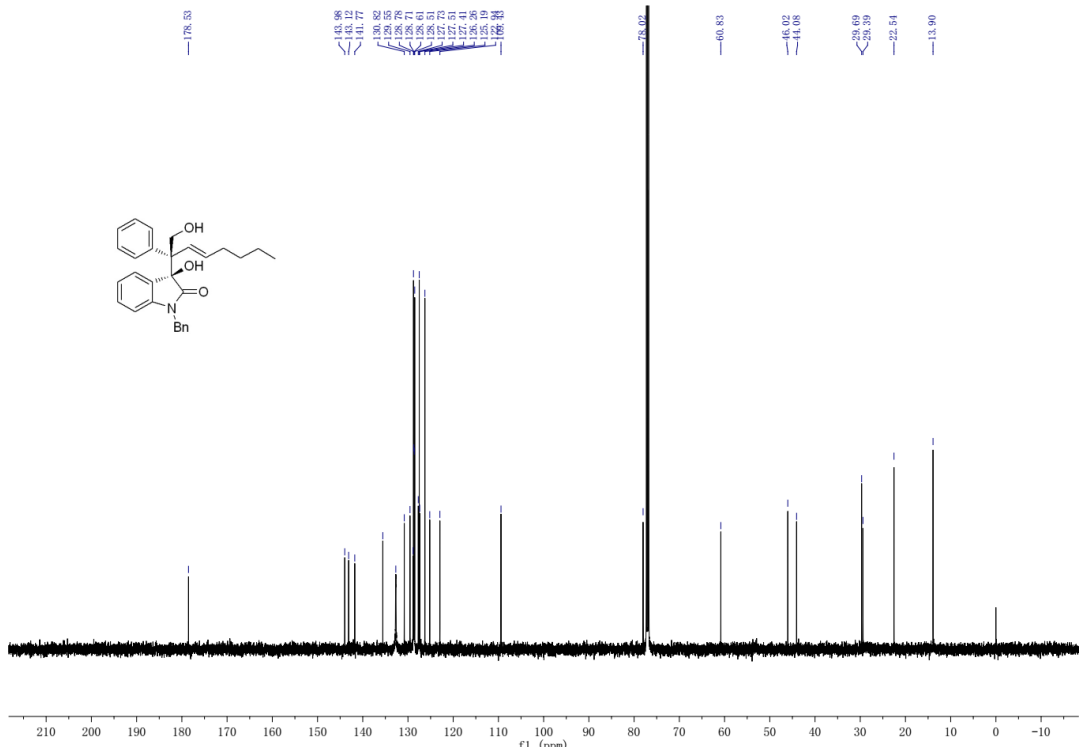


Figure S76. ^{13}C NMR (125 MHz, CDCl_3) spectrum for **7b**, related to Figure 3.

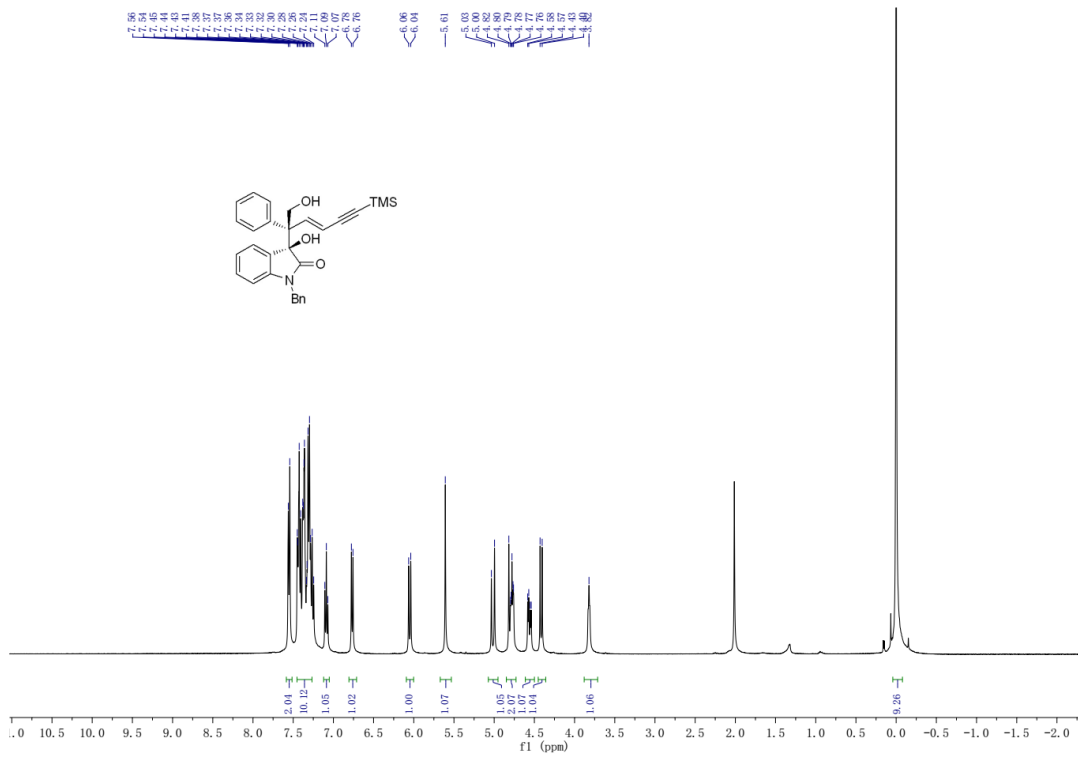


Figure S77. ^1H NMR (400 MHz, CDCl_3) spectrum for **7c**, related to **Figure 3**.

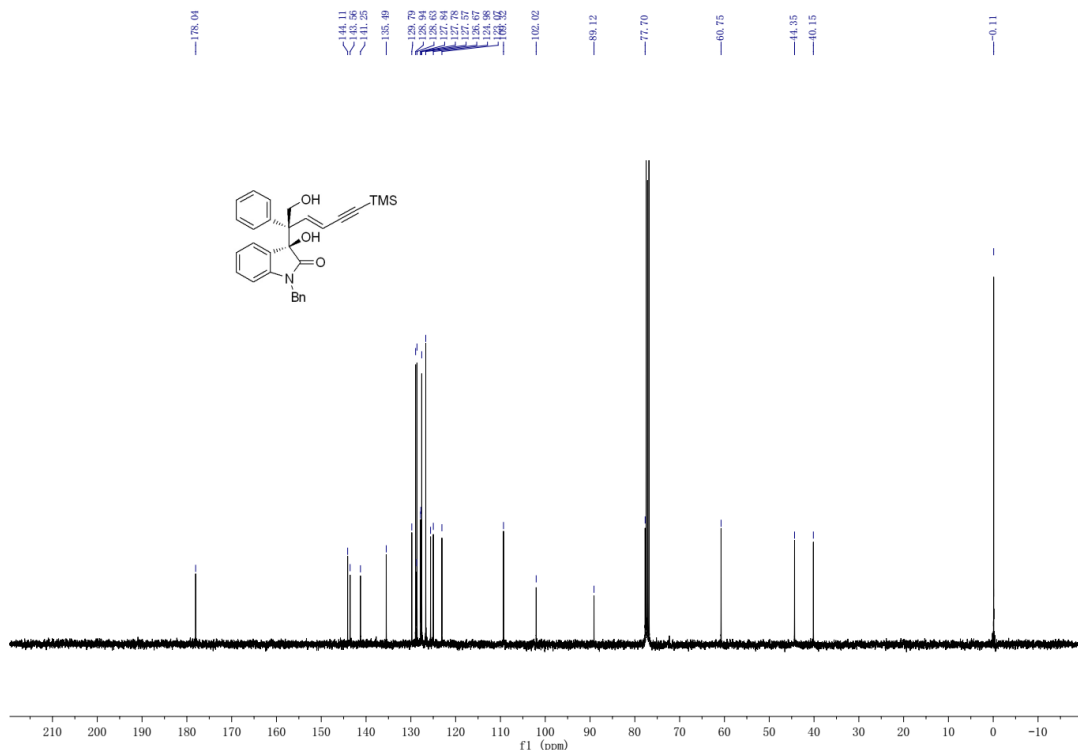


Figure S78. ^{13}C NMR (100 MHz, CDCl_3) spectrum for **7c**, related to **Figure 3**.

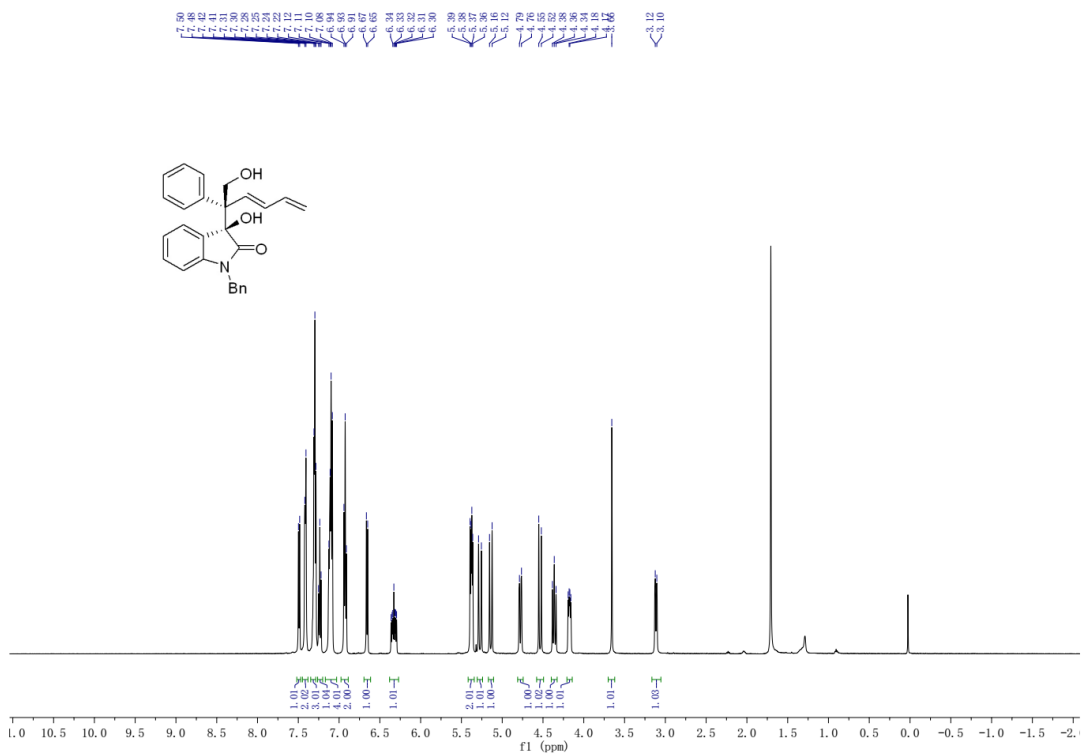


Figure S79. ^1H NMR (400 MHz, CDCl_3) spectrum for **7d**, related to Figure 3.

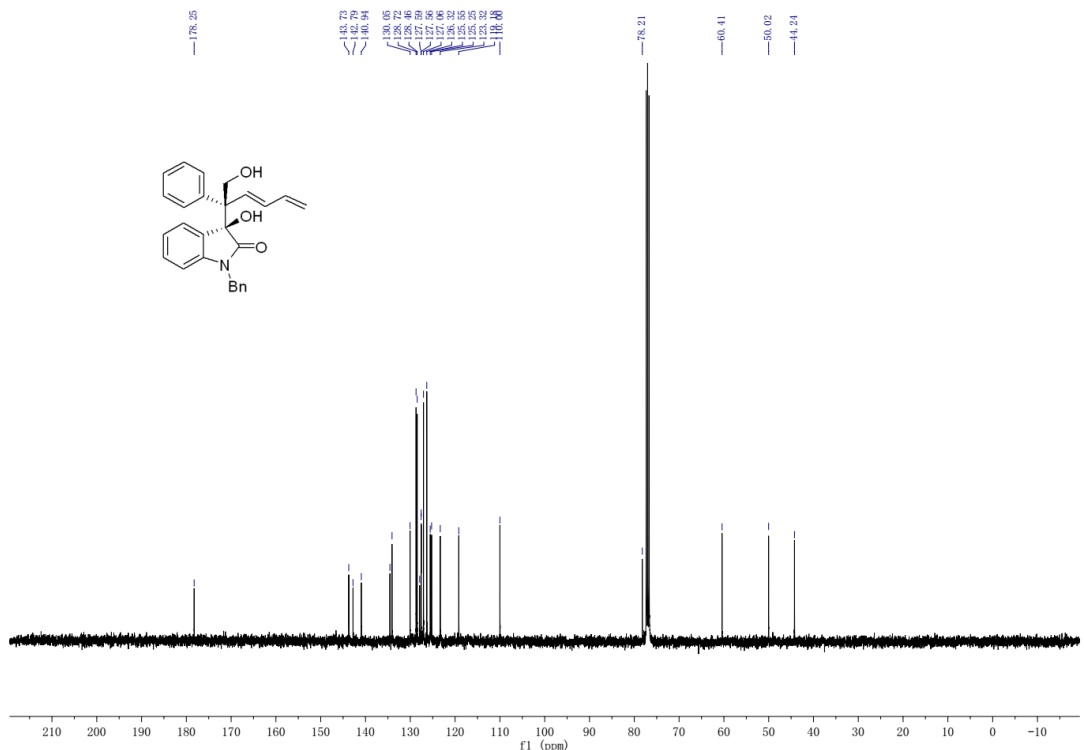


Figure S80. ^{13}C NMR (100 MHz, CDCl_3) spectrum for **7d**, related to **Figure 3**.

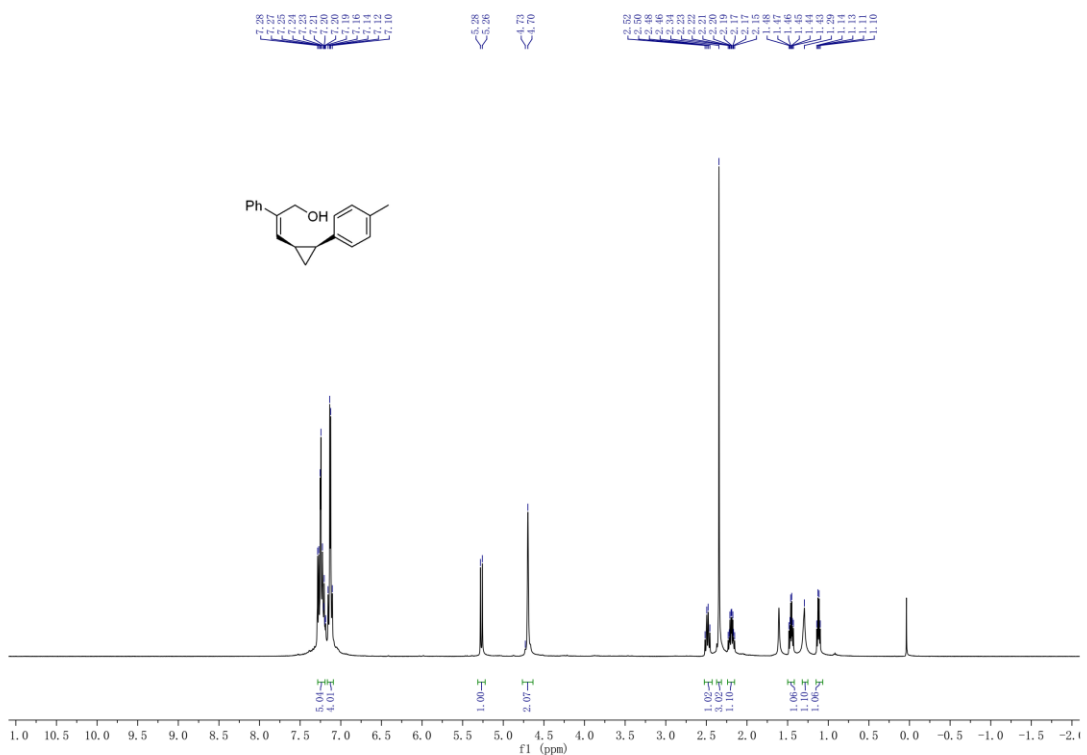


Figure S81. ¹H NMR (400 MHz, CDCl₃) spectrum for Z-5, related to **Figure 4**.

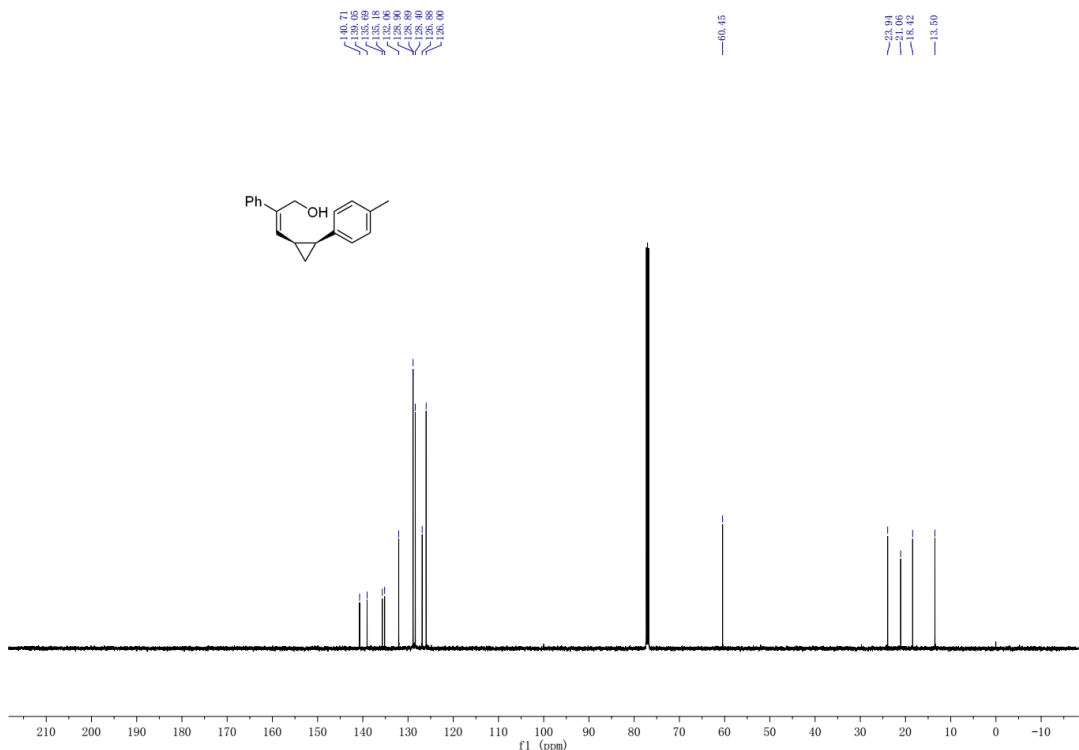


Figure S82. ¹³C NMR (100 MHz, CDCl₃) spectrum for Z-5, related to **Figure 4**.

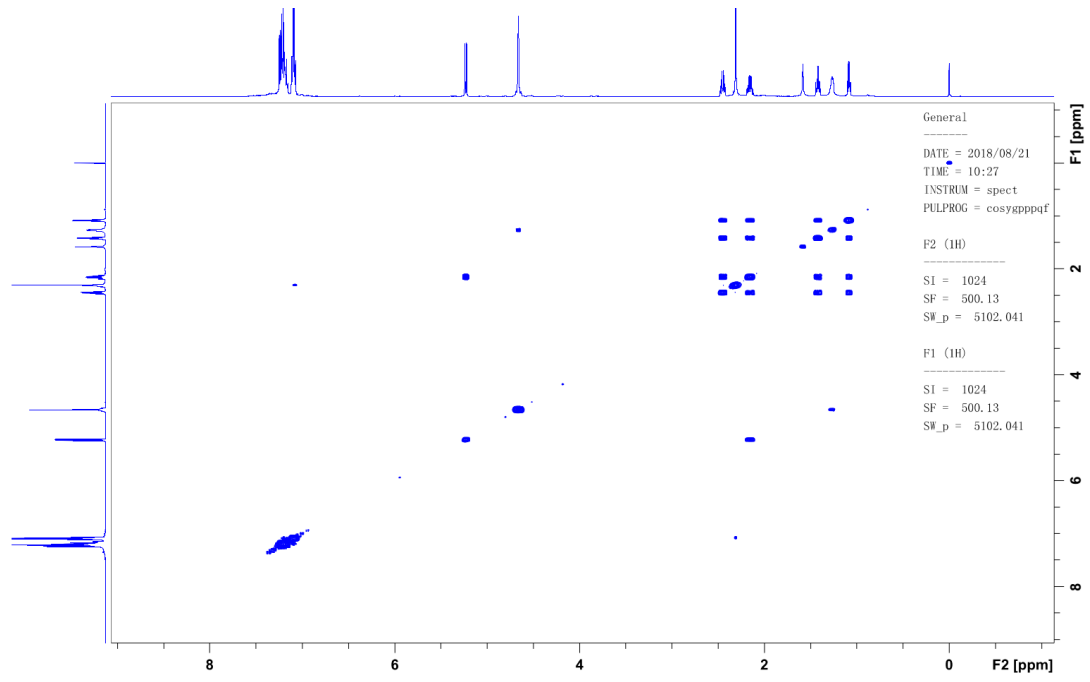


Figure S83. COSY spectrum for Z-5, related to **Figure 4**.

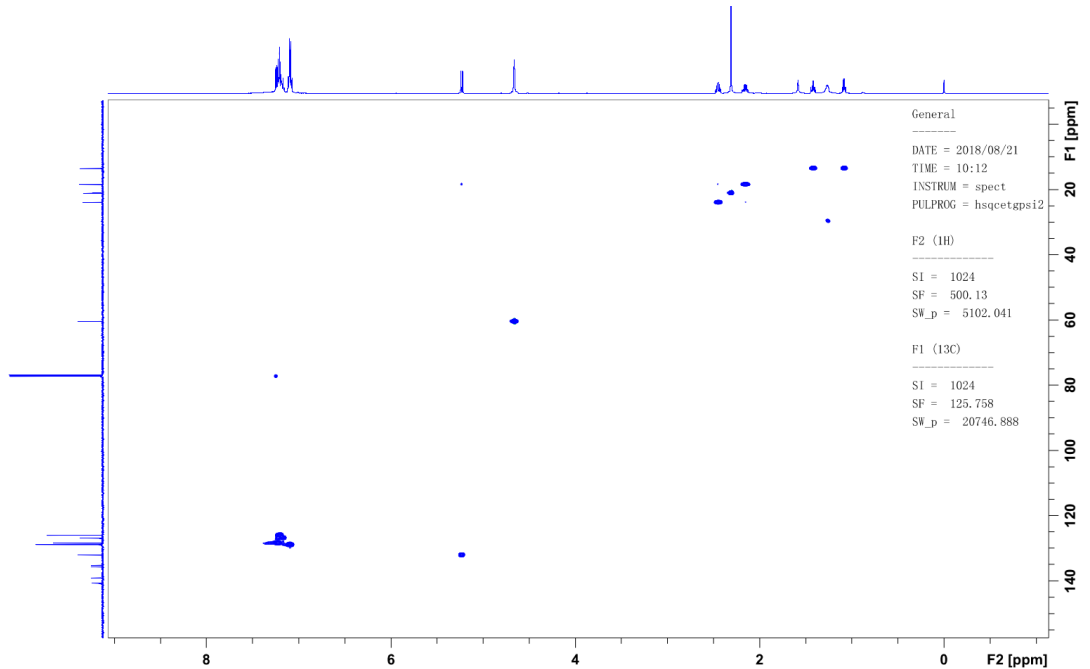


Figure S84. COSY spectrum for Z-5, related to **Figure 4**.

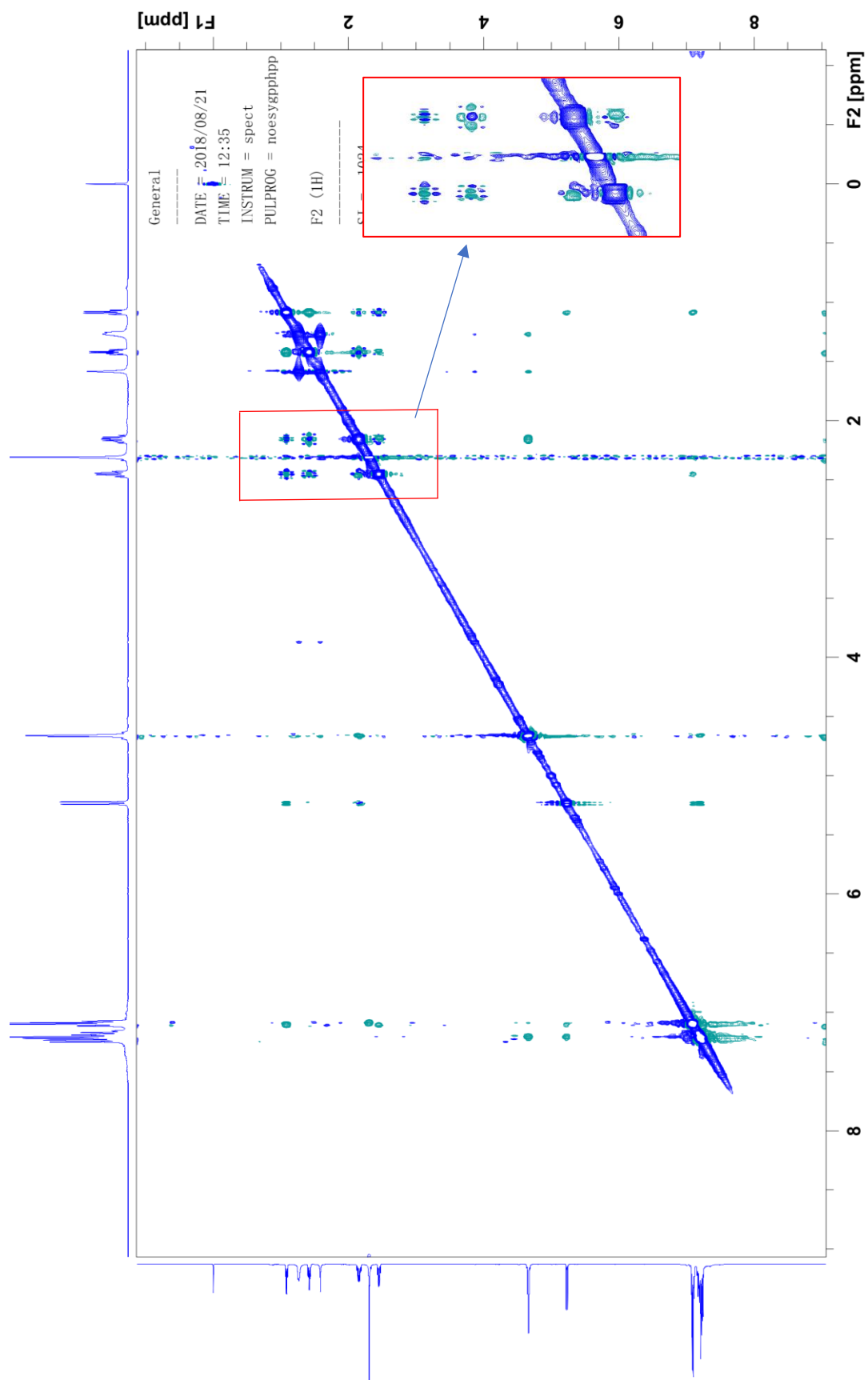


Figure S85. COSY spectrum for Z-5, related to **Figure 4**.

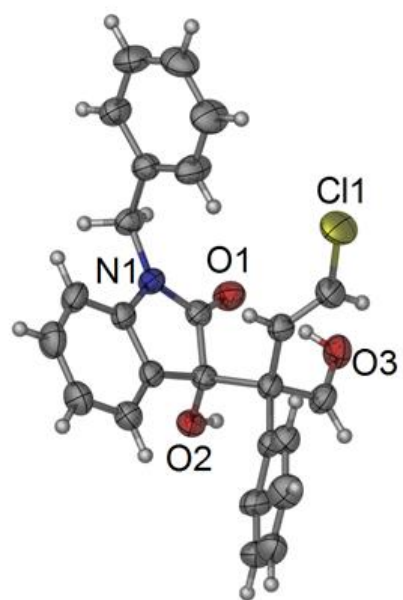


Figure S86. Single X-ray structure of **3a**, related to **Figure 2**.



Figure S87. Single X-ray structure of **3n**, related to **Figure 2**.

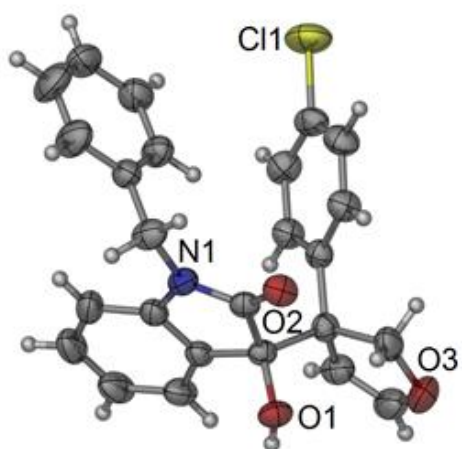


Figure S88. Single X-ray structure of **4b**, related to **Figure 2**.

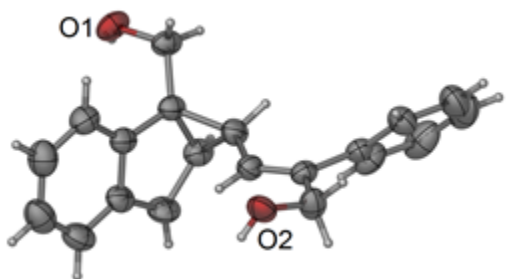


Figure S89. Single X-ray structure of **6**, related to **Figure 2**.

TRANSPARENT METHODS

General

NMR spectra: ^1H NMR (400 MHz, 500 MHz), ^{13}C NMR (100 MHz) and ^{19}F NMR (376 MHz) spectra were recorded on Bruker Ascend 400 or 500 spectrometers. Data is reported as follows: s = singlet, d = doublet, t = triplet, q = quartet, m = multiplet, brs = broad singlet, dd =doublet of doublets, td =triplet of doublets; coupling constants in Hz; integration. High-resolution mass spectrometry (HRMS) was performed on a Waters Micromass Q-TOF micro Synapt High Definition Mass Spectrometer. Single crystal X-ray diffraction data were recorded on a Bruker-AXS SMART APEX II single crystal X-ray diffractometer. Zinc chloride, zinc bromide, and zinc iodide were purchased from Energy Chemical and used directly. $\text{Rh}_2(\text{esp})_2$ was purchased from Sigma Aldrich.

Experimental Procedures

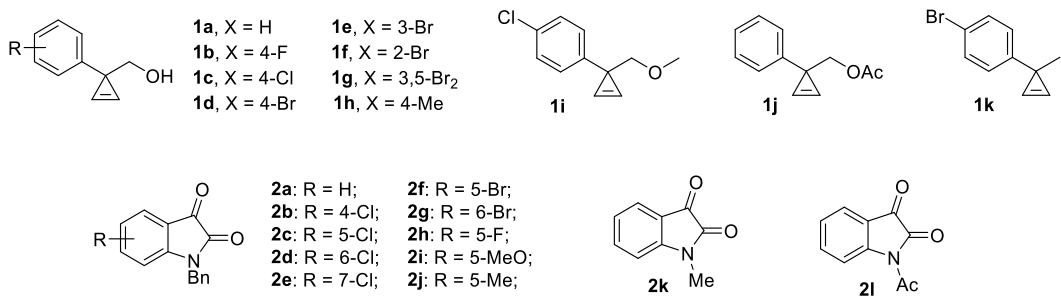
Procedure A: zinc halide-promoted reaction of 3-hydroxymethyl-3-arylidenecyclopropenes with isatins.

To an oven-dried test tube with a septum was added zinc halide (0.4 mmol), **1** (0.4 mmol), and **2** (0.2 mmol). CH_2Cl_2 (2.5 mL) was then added, and the reaction was stirred for 10 min at 25 °C. The reaction was quenched with 0.4 mL H_2O and stirred for 10 min until the solid disappeared. The mixture was extracted with CH_2Cl_2 , dried over Na_2SO_4 , filtered and concentrated to give a residue, which was subjected to ^1H NMR spectroscopy analysis for the determination of diastereoselectivity. Purification of the crude products by flash chromatography on silica gel (eluent: EtOAc/petroleum ether/ CH_2Cl_2 , 1/10/1~1/3/1) afforded pure product **3**.

Procedure B: $\text{Rh}_2(\text{esp})_2$ -catalysed reaction of 3-hydroxymethyl-3-arylidenecyclopropenes with isatins.

To an oven-dried test tube with a septum was added $\text{Rh}_2(\text{esp})_2$ (3.8 mg, 0.005 mmol), **1** (0.3 mmol), and **2** (0.2 mmol). MTBE (2 mL) was then added, and the reaction was stirred for 3 h at 25 °C. The mixture was concentrated to give a residue, and the residue was dissolved in dried tetrahydrofuran (THF) (2 mL). NaH and MeI were then added, and the mixture was stirred for 1 h at room temperature (rt). The reaction was quenched with water, extracted with CH_2Cl_2 , dried over Na_2SO_4 , filtered and concentrated to give a residue, which was subjected to ^1H NMR spectroscopy analysis for the determination of the dr. Purification by flash chromatography on silica gel (eluent: EtOAc/petroleum ether/ CH_2Cl_2 , 1/50/1~1/10/1) gave **4'**.

Starting Materials



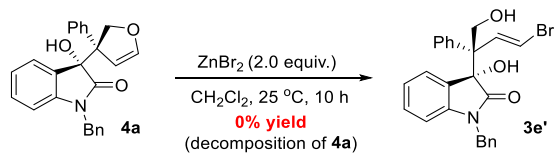
Cyclopropenes **1a**-**1h** were synthesized according to references (see main text: Rubina et al., 2004; Selvaraj et al., 2014). **1i** was obtained by methylation of **1c** with MeI/NaH (Phan et al. 2010). **1j** was prepared from 4'-bromoacetophenone according to reference (Phan et al. 2010). The N-protected isatins were prepared from corresponding N-H isatin by the following methods: benzylated isatins **2a**-**2j** were achieved with BnBr/K₂CO₃ in CH₃CN at reflux, N-Me isatin **2k** was obtained from MeI/NaH in THF at rt, and the Ac-protected isatin **2l** was formed in Ac₂O under reflux for 3 h (Allous et al. 2010).

Competing Reaction, related to Figure 4



To an oven-dried test tube with a septum were loaded with **1** (29.2 mg, 0.2 mmol), **2a** (23.7 mg, 0.1 mmol) and 4-methylstyrene (11.8 mg, 0.1 mmol) in 1 mL DCM was added zinc bromide (45 mg, 0.2 mmol). The reaction was stirred for 10 min at 25 °C and then quenched with 0.2 mL H₂O. The mixture was diluted with 5 mL CH₂Cl₂, dried over Na₂SO₄, filtered and concentrated to give a residue, which was subjected to ¹H NMR spectroscopy analysis for the determination of diastereoselectivity and ratio of **3b**/**6**. Purification of the crude products by flash chromatography on silica gel (eluent: EtOAc/petroleum ether/CH₂Cl₂, 1/20/1~1/5/1) afforded **3b** (29.4 mg, 63%) and **Z-5** (8.2 mg, 31%).

Conversion of **4a** under the standard conditions of zinc catalysis



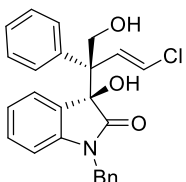
To an oven-dried test tube with a septum were loaded with **4a** (38 mg, 0.1 mmol) in 1 mL DCM was added zinc bromide (45 mg, 0.2 mmol). The reaction was stirred for 10 h at 25 °C. During stirring, **4a** disappeared and messy mixture was appeared. No **3e'**, the ring-opening product, was detected by TLC or LC-MS.

Supplemental References

Allous, I., Comesse, S., Sanselme, M. & Daïch, A. (2011). Diastereoselective Access to Tri- and Pentacyclic Spiro- γ -lactam-oxindole Cores through a Tandem Aza-Michael Initiated Ring Closure Sequence. *Eur. J. Org. Chem.* 2011, 5303.

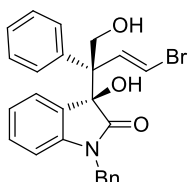
Phan, D. H. T., Kou, K. G. M., and Dong, V. M. (2010). Enantioselective Desymmetrization of Cyclopropenes by Hydroacylation. *J. Am. Chem. Soc.* 32, 16354.

Characterization of All Compounds



(S*)-1-benzyl-3-((S*,E)-4-chloro-1-hydroxy-2-phenylbut-3-en-2-yl)-3-hydroxyindolin-2-one (3a)

According to the procedure A, the reaction of **1a** (58.5 mg, 0.4 mmol), **2a** (47.5 mg, 0.2 mmol) and $ZnCl_2$ (55 mg, 0.4 mmol) gave three-component product **3a** (70 mg, 84%). 1H NMR (400 MHz, $CDCl_3$) δ 7.47 – 7.37 (m, 2H), 7.35 – 7.22 (m, 6H), 7.19 – 7.06 (m, 3H), 6.82 (t, J = 7.4 Hz, 1H), 6.58 (d, J = 7.8 Hz, 1H), 6.49 (d, J = 13.7 Hz, 2H), 6.17 (d, J = 13.3 Hz, 1H), 5.05 (d, J = 15.7 Hz, 1H), 4.68 (dd, J = 11.8, 4.4 Hz, 1H), 4.43 (d, J = 15.7 Hz, 1H), 4.39 – 4.27 (m, 2H), 3.79 (br, 1H). ^{13}C NMR (100 MHz, $CDCl_3$) δ 177.4, 143.2, 139.3, 134.9, 131.4, 130.2, 129.0, 128.7, 128.2, 128.0, 127.7, 127.1, 126.2, 123.6, 123.0, 109.5, 81.2, 65.9, 54.3, 44.2. HRMS (ESI) m/z : calcd. for $C_{25}H_{23}NO_3Cl$ ($M+H$)⁺ 420.1366, found 420.1349.



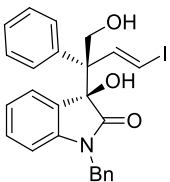
(S*)-1-benzyl-3-((S*,E)-4-bromo-1-hydroxy-2-phenylbut-3-en-2-yl)-3-hydroxyindolin-2-one (3b)

According to procedure A, the reaction of **1a** (58.5 mg, 0.4 mmol), **2a** (47.5 mg, 0.2 mmol) and $ZnBr_2$ (90 mg, 0.4 mmol) gave three-component product **3b** (76 mg, 82%).

1H NMR (400 MHz, $CDCl_3$) δ = 7.46 – 7.36 (m, 2H), 7.35 – 7.21 (m, 6H), 7.19 – 7.04 (m, 3H), 6.83 (dd, 1H), 6.66 – 6.42 (m, 4H), 5.02 (d, J =15.7, 1H), 4.67 (dd, J =11.9, 4.1, 1H), 4.45 (d, J =15.8, 1H), 4.38 (s, 1H), 4.33 (dd, J =11.9, 6.9, 1H), 3.78 (s, 1H).

^{13}C NMR (100 MHz, $CDCl_3$) δ = 177.3, 143.1, 139.0, 135.4, 134.9, 130.2, 129.0, 128.6, 128.2, 128.01, 127.95, 127.7, 127.1, 126.2, 123.1, 111.4, 109.6, 81.0, 65.7, 55.7, 44.2.

HRMS (ESI) m/z : calcd. for $C_{25}H_{22}NO_3NaBr$ ($M+Na$)⁺ 486.0681, found 486.0673.



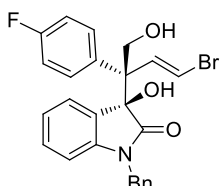
(S*)-1-benzyl-3-hydroxy-3-((S*,E)-1-hydroxy-4-iodo-2-phenylbut-3-en-2-yl)indolin-2-one (3c)

According to procedure A, the reaction of **1a** (58.5 mg, 0.4 mmol), **2a** (47.5 mg, 0.2 mmol) and ZnI_2 (128 mg, 0.4 mmol) gave three-component product **3c** (91 mg, 89%).

1H NMR (400 MHz, $CDCl_3$) δ = 7.41 – 7.22 (m, 8H), 7.16 (dd, J =7.8, 1H), 7.08 (d, J =7.2, 2H), 6.99 – 6.80 (m, 2H), 6.73 – 6.51 (m, 3H), 4.97 (d, J =15.7, 1H), 4.64 (dd, J =11.9, 4.7, 1H), 4.50 (d, J =15.7, 1H), 4.39 (dd, J =11.6, 6.8, 1H), 4.31 – 4.22 (m, 1H), 3.59 (d, J =5.0, 1H).

^{13}C NMR (100 MHz, $CDCl_3$) δ = 177.3, 143.5, 143.1, 138.9, 134.9, 130.2, 129.1, 128.7, 128.2, 128.1, 127.9, 127.6, 127.2, 126.2, 123.1, 109.6, 82.2, 81.0, 65.7, 57.6, 44.3.

HRMS (ESI) m/z : calcd. for $C_{25}H_{22}NO_3NaI$ ($M+Na$)⁺ 534.0542, found 534.0529.



(S*)-1-benzyl-3-((S*,E)-4-bromo-2-(4-fluorophenyl)-1-hydroxybut-3-en-2-yl)-3-hydroxyindolin-2-one (3d)

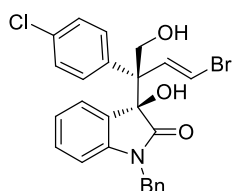
According to procedure A, the reaction of **1b** (65.7 mg, 0.4 mmol), **2a** (47.5 mg, 0.2 mmol) and $ZnBr_2$ (90 mg, 0.4 mmol) gave three-component product **3d** (88 mg, 91%).

1H NMR (400 MHz, $CDCl_3$) δ 7.39 – 7.25 (m, 5H), 7.18 (td, J = 7.8, 1.2 Hz, 1H), 7.09 (d, J = 6.9 Hz, 2H), 6.95 (t, J = 8.7 Hz, 2H), 6.88 (td, J = 7.6, 0.7 Hz, 1H), 6.65 – 6.44 (m, 4H), 5.03 (d, J = 15.7 Hz, 1H), 4.62 (dd, J = 11.9, 4.6 Hz, 1H), 4.44 (d, J = 15.7 Hz, 1H), 4.39 (s, 1H), 4.29 (dd, J = 11.9, 7.2 Hz, 1H), 3.85 – 3.74 (m, 1H).

^{13}C NMR (100 MHz, $CDCl_3$) δ 177.2, 162.3 (d, J = 247.9 Hz), 143.1, 135.2, 134.8, 130.43, 130.40, 130.35, 129.0, 127.8, 127.2, 126.1, 123.1, 115.1, 114.9, 111.7, 109.7, 81.0, 65.9, 55.2, 44.3.

^{19}F NMR (376 MHz, $CDCl_3$) δ -113.96.

HRMS (ESI) m/z : calcd. for $C_{25}H_{21}NO_3BrFNa$ ($M+Na$)⁺ 504.0587, found 504.0588.



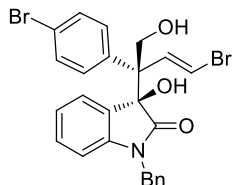
(S*)-1-benzyl-3-((S*,E)-4-bromo-2-(4-chlorophenyl)-1-hydroxybut-3-en-2-yl)-3-hydroxyindolin-2-one (3e)

According to procedure A, the reaction of **1c** (72 mg, 0.4 mmol), **2a** (47.5 mg, 0.2 mmol) and $ZnBr_2$ (90 mg, 0.4 mmol) gave three-component product **3e** (92 mg, 92%).

¹H NMR (400 MHz, CDCl₃) δ 7.35 – 7.16 (m, 8H), 7.09 (d, J = 7.2 Hz, 2H), 6.90 (t, J = 7.6 Hz, 1H), 6.68 – 6.55 (m, 3H), 6.50 (d, J = 13.7 Hz, 1H), 5.05 (d, J = 15.7 Hz, 1H), 4.60 (dd, J = 11.9, 4.6 Hz, 1H), 4.44 (d, J = 15.7 Hz, 1H), 4.34 – 4.25 (m, 2H), 3.75 – 3.65 (m, 1H).

¹³C NMR (100 MHz, CDCl₃) δ 177.1, 143.1, 137.6, 135.0, 134.8, 134.0, 130.4, 130.1, 129.0, 128.3, 127.8, 127.2, 126.1, 123.2, 111.8, 109.7, 80.9, 65.8, 55.3, 44.3.

HRMS (ESI) *m/z*: calcd. for C₂₅H₂₁NO₃BrClNa (M+Na)⁺ 520.0291, found 520.0310.



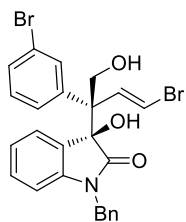
(S*)-1-benzyl-3-((S*,E)-4-bromo-2-(4-bromophenyl)-1-hydroxybut-3-en-2-yl)-3-hydroxyindolin-2-one (3f)

According to procedure A, the reaction of **1d** (90 mg, 0.4 mmol), **2a** (47.5 mg, 0.2 mmol) and ZnBr₂ (90 mg, 0.4 mmol) gave three-component product **3f** (83 mg, 76%).

¹H NMR (400 MHz, CDCl₃) δ 7.42 – 7.30 (m, 4H), 7.29 – 7.23 (m, 3H), 7.19 (td, J = 7.8, 1.1 Hz, 1H), 7.09 (d, J = 7.2 Hz, 2H), 6.90 (t, J = 7.4 Hz, 1H), 6.71 – 6.56 (m, 3H), 6.49 (d, J = 13.3 Hz, 1H), 5.05 (d, J = 15.7 Hz, 1H), 4.60 (dd, J = 11.9, 4.6 Hz, 1H), 4.45 (d, J = 15.7 Hz, 1H), 4.37 – 4.26 (m, 2H), 3.75 – 3.65 (m, 1H).

¹³C NMR (100 MHz, CDCl₃) δ 177.0, 143.2, 138.2, 134.9, 134.8, 131.3, 130.5, 130.4, 129.1, 127.8, 127.6, 127.1, 126.1, 123.2, 122.3, 111.8, 109.7, 80.8, 65.9, 55.4, 44.3.

HRMS (ESI) *m/z*: calcd. for C₂₅H₂₂NO₃Br₂ (M+Na)⁺ 541.9966, found 541.9966.



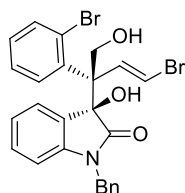
(S*)-1-benzyl-3-((S*,E)-4-bromo-2-(3-bromophenyl)-1-hydroxybut-3-en-2-yl)-3-hydroxyindolin-2-one (3g)

According to procedure A, the reaction of **1e** (90 mg, 0.4 mmol), **2a** (47.5 mg, 0.2 mmol) and ZnBr₂ (90 mg, 0.4 mmol) gave three-component product **3g** (106 mg, 98%).

¹H NMR (400 MHz, MeOD) δ 7.56 (s, 1H), 7.45 (d, J = 7.8 Hz, 1H), 7.37 – 7.12 (m, 8H), 6.89 (t, J = 7.5 Hz, 1H), 6.67 (d, J = 7.9 Hz, 1H), 6.64 – 6.45 (m, 3H), 4.81 (d, J = 11.6 Hz, 1H), 4.72 (t, J = 14.5 Hz, 2H), 4.51 (d, J = 11.6 Hz, 1H).

¹³C NMR (100 MHz, MeOD) δ 178.7, 144.3, 143.0, 137.3, 136.9, 133.4, 131.5, 131.0, 130.3, 129.9, 129.2, 128.6, 128.4, 127.0, 123.7, 122.8, 111.6, 110.6, 81.5, 63.6, 58.0, 44.8.

HRMS (ESI) *m/z*: calcd. for C₂₅H₂₂NO₃Br₂ (M+H)⁺ 541.9966, found 541.9962.



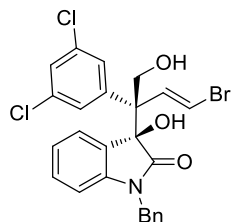
(S*)-1-benzyl-3-((S*,E)-4-bromo-2-(2-bromophenyl)-1-hydroxybut-3-en-2-yl)-3-hydroxyindolin-2-one (3h)

According to procedure A, the reaction of **1f** (90 mg, 0.4 mmol), **2a** (47.5 mg, 0.2 mmol) and ZnBr₂ (90 mg, 0.4 mmol) gave three-component product **3h** (58 mg, 53%).

¹H NMR (400 MHz, MeOD) δ 7.59 (d, *J* = 7.3 Hz, 1H), 7.51 (d, *J* = 7.9 Hz, 1H), 7.38 (d, *J* = 6.7 Hz, 2H), 7.31 – 7.19 (m, 5H), 7.15 (t, *J* = 7.7 Hz, 1H), 7.09 (t, *J* = 7.5 Hz, 1H), 6.92 (d, *J* = 7.7 Hz, 2H), 5.76 (d, *J* = 1.4 Hz, 1H), 5.43 – 5.36 (m, 1H), 5.00 (d, *J* = 15.6 Hz, 1H), 4.97 – 4.91 (m, 1H), 4.87 (d, *J* = 15.6 Hz, 1H), 4.76 (ddd, *J* = 12.2, 6.2, 1.8 Hz, 1H).

¹³C NMR (100 MHz, MeOD) δ 178.1, 144.3, 143.1, 137.3, 135.3, 134.3, 131.3, 130.7, 130.7, 130.3, 129.7, 128.7, 128.7, 128.5, 126.3, 124.8, 124.3, 122.8, 110.6, 93.3, 80.2, 78.6, 44.4.

HRMS (ESI) *m/z*: calcd. for C₂₅H₂₂NO₃Br₂ (M+H)⁺ 541.9966, found 541.9963.



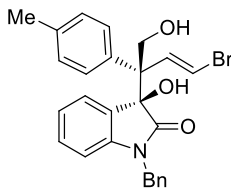
(S*)-1-benzyl-3-((S*,E)-4-bromo-2-(3,5-dichlorophenyl)-1-hydroxybut-3-en-2-yl)-3-hydroxyindolin-2-one (3i)

According to procedure A, the reaction of **1g** (86 mg, 0.4 mmol), **2a** (47.5 mg, 0.2 mmol) and ZnBr₂ (90 mg, 0.4 mmol) gave three-component product **3i** (101 mg, 95%).

¹H NMR (400 MHz, MeOD) δ 7.54 (s, 1H), 7.39 – 7.17 (m, 8H), 6.91 (td, *J* = 7.6, 0.7 Hz, 1H), 6.71 (d, *J* = 7.8 Hz, 1H), 6.66 – 6.49 (m, 3H), 4.87 (d, *J* = 15.9 Hz, 1H), 4.71 (d, *J* = 11.7 Hz, 2H), 4.69 (d, *J* = 15.7 Hz, 2H), 4.53 (d, *J* = 11.7 Hz, 1H).

¹³C NMR (100 MHz, MeOD) δ 178.6, 144.4, 141.3, 137.0, 136.8, 132.6, 132.6, 132.4, 131.2, 130.6, 130.4, 130.0, 129.9, 128.6, 128.4, 126.9, 123.8, 112.0, 110.7, 81.2, 63.3, 57.8, 44.8.

HRMS (ESI) *m/z*: calcd. for C₂₅H₂₁NO₃BrCl₂ (M+H)⁺ 532.0082, found 532.0105.



(S*)-1-benzyl-3-((S*,E)-4-bromo-1-hydroxy-2-(p-tolyl)but-3-en-2-yl)-3-hydroxyindolin-2-one (3j)

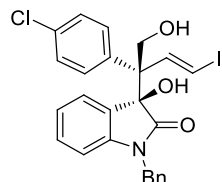
According to procedure A, the reaction of **1h** (64 mg, 0.4 mmol), **2a** (47.5 mg, 0.2 mmol) and ZnBr₂ (90 mg, 0.4 mmol) gave three-component product **3j** (89 mg, 93%).

¹H NMR (400 MHz, CDCl₃) δ 7.31 – 7.22 (m, 5H), 7.15 (td, *J* = 7.8, 1.2 Hz, 1H), 7.11 – 7.04 (m,

4H), 6.86 (t, J = 7.6 Hz, 1H), 6.68 – 6.47 (m, 4H), 5.04 (d, J = 15.8 Hz, 1H), 4.63 (dd, J = 11.9, 4.7 Hz, 1H), 4.43 (d, J = 15.8 Hz, 1H), 4.34 (s, 1H), 4.31 (dd, J = 12.0, 7.0 Hz, 1H), 3.75 – 3.66 (m, 1H), 2.34 (s, 3H).

^{13}C NMR (100 MHz, CDCl_3) δ 177.3, 143.2, 137.6, 135.9, 135.6, 134.9, 130.2, 129.0, 128.9, 128.5, 128.0, 127.6, 127.2, 126.2, 123.0, 111.2, 109.5, 81.0, 65.9, 55.4, 44.2, 21.1.

HRMS (ESI) m/z : calcd. for $\text{C}_{26}\text{H}_{24}\text{NO}_3\text{BrNa}$ ($\text{M}+\text{Na}$) $^+$ 500.0837, found 500.0863.



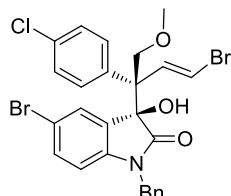
(S*)-1-benzyl-3-((S*,E)-2-(4-chlorophenyl)-1-hydroxy-4-iodobut-3-en-2-yl)-3-hydroxyindolin-2-one (3k)

According to procedure A, the reaction of **1h** (72 mg, 0.4 mmol), **2a** (47.5 mg, 0.2 mmol) and ZnBr_2 (90 mg, 0.4 mmol) gave three-component product **3k** (99 mg, 91%).

^1H NMR (400 MHz, MeOD) δ 7.37 – 7.15 (m, 10H), 7.00 (d, J = 14.6 Hz, 1H), 6.90 (t, J = 7.6 Hz, 1H), 6.72 – 6.53 (m, 3H), 4.81 (d, J = 15.8 Hz, 1H), 4.76 – 4.67 (m, 2H), 4.49 (d, J = 11.7 Hz, 1H).

^{13}C NMR (100 MHz, MeOD) δ 178.8, 145.7, 144.3, 139.0, 136.9, 134.4, 132.0, 131.0, 130.3, 129.9, 128.7, 128.6, 128.4, 127.0, 123.7, 110.6, 81.7, 81.4, 63.5, 59.7, 44.8.

HRMS (ESI) m/z : calcd. for $\text{C}_{25}\text{H}_{21}\text{NO}_3\text{ClNa}$ ($\text{M}+\text{Na}$) $^+$ 568.0152, found 568.0150.



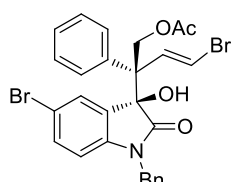
(S*)-1-benzyl-5-bromo-3-((S*,E)-4-bromo-2-(4-chlorophenyl)-1-methoxybut-3-en-2-yl)-3-hydroxyindolin-2-one (3l)

According to procedure A, the reaction of **1i** (96 mg, 0.4 mmol), **2f** (63.2 mg, 0.2 mmol) and ZnBr_2 (90 mg, 0.4 mmol) gave three-component product **3l** (114 mg, 96%).

^1H NMR (400 MHz, CDCl_3) δ 7.34 – 7.17 (m, 8H), 7.04 – 6.71 (m, 4H), 6.43 (d, J = 8.3 Hz, 1H), 6.36 (d, J = 14.3 Hz, 1H), 5.14 (s, 1H), 4.93 (d, J = 15.8 Hz, 1H), 4.39 (d, J = 15.8 Hz, 1H), 4.29 (d, J = 9.0 Hz, 1H), 4.08 (d, J = 9.4 Hz, 1H), 3.54 (s, 3H).

^{13}C NMR (100 MHz, CDCl_3) δ 175.1, 142.5, 136.9, 135.7, 134.6, 134.1, 133.0, 130.1, 130.0, 129.1, 129.0, 128.2, 127.8, 127.0, 115.5, 110.9, 110.0, 80.9, 75.8, 59.6, 54.0, 44.1.

HRMS (ESI) m/z : calcd. for $\text{C}_{26}\text{H}_{22}\text{NO}_3\text{Br}_2\text{ClNa}$ ($\text{M}+\text{Na}$) $^+$ 611.9553, found 611.9535.



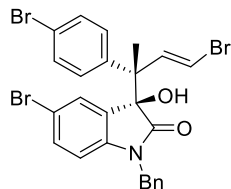
(S*,E)-2-((S*)-1-benzyl-5-bromo-3-hydroxy-2-oxoindolin-3-yl)-4-bromo-2-phenylbut-3-en-1-yl acetate (3m)

According to procedure A (reaction time: 12 h), the reaction of **1j** (75 mg, 0.4 mmol), **2f** (63.2 mg, 0.2 mmol) and ZnBr₂ (90 mg, 0.4 mmol) gave three-component product **3m** (89 mg, 76%), with 11 mg of **2f** recovered.

¹H NMR (400 MHz, CDCl₃) δ 7.46 – 7.21 (m, 9H), 7.18 – 7.08 (m, 2H), 6.57 – 6.33 (m, 4H), 5.33 (d, *J* = 11.9 Hz, 1H), 5.03 (d, *J* = 11.9 Hz, 1H), 4.91 (d, *J* = 15.7 Hz, 1H), 4.53 (d, *J* = 15.8 Hz, 1H), 3.70 (s, 1H), 1.89 (s, 3H).

¹³C NMR (100 MHz, CDCl₃) δ 175.7, 170.9, 142.2, 137.1, 134.8, 134.5, 133.0, 129.4, 129.1, 128.6, 128.08, 128.05, 127.8, 127.2, 115.5, 111.2, 110.9, 79.86, 63.6, 55.6, 44.3, 20.9.

HRMS (ESI) *m/z*: calcd. for C₂₇H₂₃NO₄Br₂Na (M+Na)⁺ 605.9886, found 605.9888.



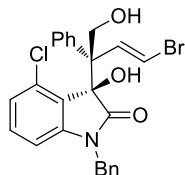
(R*)-1-benzyl-5-bromo-3-((S*,E)-4-bromo-2-(4-bromophenyl)but-3-en-2-yl)-3-hydroxyindolin-2-one (3n)

According to procedure A (reaction time: 12 h), the reaction of **1k** (84 mg, 0.4 mmol), **2f** (63.2 mg, 0.2 mmol) and ZnBr₂ (90 mg, 0.4 mmol) gave three-component product **3n** (117 mg, 97%).

¹H NMR (400 MHz, CDCl₃) δ 7.39 – 7.25 (m, 6H), 7.16 – 6.85 (m, 6H), 6.49 – 6.38 (m, 2H), 4.92 (d, *J* = 15.8 Hz, 1H), 4.43 (d, *J* = 15.8 Hz, 1H), 3.10 (s, 1H), 1.74 (s, 3H).

¹³C NMR (100 MHz, CDCl₃) δ 176.3, 142.4, 140.0, 138.0, 134.5, 132.9, 131.1, 129.7, 129.5, 129.2, 129.0, 127.9, 127.1, 121.8, 115.4, 110.9, 110.2, 79.6, 51.7, 44.3, 18.7.

HRMS (ESI) *m/z*: calcd. for C₂₅H₂₀NO₂Br₃Na (M+Na)⁺ 625.8936, found 625.8955.



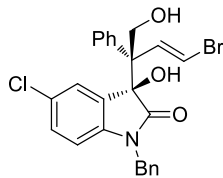
(R*)-1-benzyl-3-((S*,E)-4-bromo-1-hydroxy-2-phenylbut-3-en-2-yl)-4-chloro-3-hydroxyindolin-2-one (3o)

According to procedure A, the reaction of **1a** (58.5 mg, 0.4 mmol), **2b** (54.3 mg, 0.2 mmol) and ZnBr₂ (90 mg, 0.4 mmol) gave three-component product **3o** (65 mg, 65%).

¹H NMR (400 MHz, CDCl₃) δ 7.46 (d, *J* = 14.2 Hz, 1H), 7.24 – 7.16 (m, 4H), 7.11 (t, *J* = 7.7 Hz, 2H), 7.07 – 6.96 (m, 4H), 6.92 (dd, *J* = 6.5, 2.7 Hz, 2H), 6.58 (d, *J* = 14.2 Hz, 1H), 6.23 (d, *J* = 7.6 Hz, 1H), 4.88 (d, *J* = 11.9 Hz, 1H), 4.53 (d, *J* = 15.8 Hz, 1H), 4.43 (br, 1H), 4.29 (d, *J* = 11.9 Hz, 1H), 4.20 (d, *J* = 15.8 Hz, 1H), 2.37 (br, 1H).

¹³C NMR (100 MHz, CDCl₃) δ 175.6, 145.1, 137.5, 135.8, 134.5, 131.9, 131.0, 128.8, 128.1, 128.0, 127.9, 127.7, 127.2, 125.0, 124.7, 111.4, 107.8, 83.8, 66.8, 58.9, 44.2.

HRMS (ESI) *m/z*: calcd. for C₂₅H₂₁NO₃BrClNa (M+Na)⁺ 520.0291, found 520.0310.



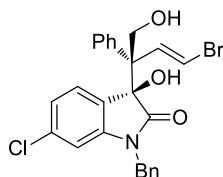
(S*)-1-benzyl-3-((S*,E)-4-bromo-1-hydroxy-2-phenylbut-3-en-2-yl)-5-chloro-3-hydroxyindolin-2-one (3p)

According to procedure A, the reaction of **1a** (58.5 mg, 0.4 mmol), **2c** (54.3 mg, 0.2 mmol) and ZnBr₂ (90 mg, 0.4 mmol) gave three-component product **3p** (81 mg, 81%).

¹H NMR (400 MHz, CDCl₃) δ = 7.42 – 7.23 (m, 8H), 7.12 (dd, J=8.4, 2.1, 1H), 7.06 (d, J=6.7, 2H), 6.60 (d, J=14.1, 1H), 6.56 – 6.41 (m, 3H), 4.99 (d, J=15.8, 1H), 4.63 (dd, J=11.9, 5.0, 1H), 4.54 (s, 1H), 4.45 (d, J=15.8, 1H), 4.42 (dd, J=11.9, 6.8, 1H), 3.55 (t, J=5.8, 1H).

¹³C NMR (100 MHz, CDCl₃) δ = 176.8, 141.6, 138.5, 135.2, 134.4, 130.1, 129.6, 129.1, 128.6, 128.5, 128.3, 128.2, 127.8, 127.1, 126.8, 111.5, 110.5, 81.1, 65.8, 55.5, 44.3.

HRMS (ESI) *m/z*: calcd. for C₂₅H₂₁NO₃BrClNa (M+Na)⁺ 520.0291, found 520.0310.



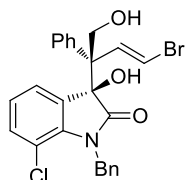
(S*)-1-benzyl-3-((S*,E)-4-bromo-1-hydroxy-2-phenylbut-3-en-2-yl)-6-chloro-3-hydroxyindolin-2-one (3q)

According to procedure A, the reaction of **1a** (58.5 mg, 0.4 mmol), **2d** (54.3 mg, 0.2 mmol) and ZnBr₂ (90 mg, 0.4 mmol) gave three-component product **3q** (83 mg, 83%).

¹H NMR (400 MHz, CDCl₃) δ 7.41 (d, J = 7.0 Hz, 2H), 7.37 – 7.26 (m, 6H), 7.10 (d, J = 6.9 Hz, 2H), 6.83 (dd, J = 8.1, 1.8 Hz, 1H), 6.64 – 6.55 (m, 2H), 6.54 – 6.35 (m, 2H), 5.01 (d, J = 15.8 Hz, 1H), 4.60 (dd, J = 11.9, 5.2 Hz, 1H), 4.45 (d, J = 15.4 Hz, 2H), 4.43 (dd, J = 12.3, 6.7 Hz, 2H), 4.36 (s, 1H), 3.41 (dd, J = 6.4, 5.6 Hz, 1H).

¹³C NMR (100 MHz, CDCl₃) δ 177.2, 144.4, 138.8, 136.1, 135.2, 134.3, 129.2, 128.6, 128.3, 128.1, 127.9, 127.2, 127.1, 126.4, 123.0, 111.5, 110.1, 80.7, 65.8, 55.5, 44.3.

HRMS (ESI) *m/z*: calcd. for C₂₅H₂₁NO₃BrClNa (M+Na)⁺ 520.0291, found 520.0310.



(S*)-1-benzyl-3-((S*,E)-4-bromo-1-hydroxy-2-phenylbut-3-en-2-yl)-7-chloro-3-hydroxyindolin-2-one (3r)

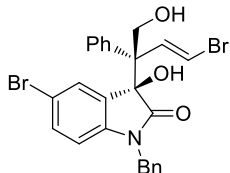
According to procedure A, the reaction of **1a** (58.5 mg, 0.4 mmol), **2e** (54.3 mg, 0.2 mmol) and ZnBr₂ (90 mg, 0.4 mmol) gave three-component product **3r** (91 mg, 91%).

¹H NMR (400 MHz, CDCl₃) δ 7.36 – 7.15 (m, 9H), 7.03 (d, J=7.1, 2H), 6.82 (t, J=7.9, 1H), 6.66 – 6.48 (m, 3H), 5.16 (d, J=16.3, 1H), 5.09 (d, J=16.3, 1H), 4.62 – 4.50 (m, 2H), 4.39 (dd, J=11.8,

6.6, 1H), 3.39 (t, $J=5.9$, 1H).

^{13}C NMR (100 MHz, CDCl_3) δ 177.8, 139.3, 138.5, 136.7, 135.2, 132.8, 130.9, 128.7, 128.7, 128.3, 128.2, 127.1, 126.3, 124.8, 123.8, 115.7, 111.5, 80.4, 65.9, 55.6, 45.4.

HRMS (ESI) m/z : calcd. for $\text{C}_{25}\text{H}_{21}\text{NO}_3\text{BrClNa}$ ($\text{M}+\text{Na}$) $^+$ 520.0291, found 520.0310.



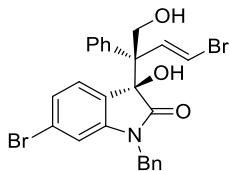
(S*)-1-benzyl-5-bromo-3-((S*,E)-4-bromo-1-hydroxy-2-phenylbut-3-en-2-yl)-3-hydroxyindolin-2-one (3s)

According to procedure A, the reaction of **1a** (58.5 mg, 0.4 mmol), **2f** (63.2 mg, 0.2 mmol) and ZnBr_2 (90 mg, 0.4 mmol) gave three-component product **3s** (99 mg, 91%).

^1H NMR (400 MHz, CDCl_3) δ 7.42 – 7.23 (m, 9H), 7.06 (d, $J=6.7$ Hz, 2H), 6.70 – 6.56 (m, 2H), 6.51 (d, $J=14.2$ Hz, 1H), 6.44 (d, $J=8.3$ Hz, 1H), 4.98 (d, $J=15.8$ Hz, 1H), 4.64 (d, $J=11.9$ Hz, 1H), 4.56 (br, 1H), 4.45 (d, $J=16.1$ Hz, 2H), 4.41 (d, $J=12.5$ Hz, 1H), 3.57 (br, 1H).

^{13}C NMR (100 MHz, CDCl_3) δ 176.6, 142.1, 138.5, 135.1, 134.4, 133.0, 129.9, 129.5, 129.1, 128.6, 128.3, 128.2, 127.9, 127.1, 115.8, 111.5, 111.0, 81.0, 65.9, 55.5, 44.3.

HRMS (ESI) m/z : calcd. for $\text{C}_{25}\text{H}_{22}\text{NO}_3\text{Br}_2$ ($\text{M}+\text{H}$) $^+$ 541.9966, found 541.9966.



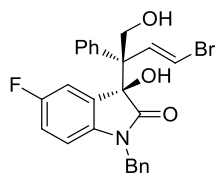
(S*)-1-benzyl-6-bromo-3-((S*,E)-4-bromo-1-hydroxy-2-phenylbut-3-en-2-yl)-3-hydroxyindolin-2-one (3t)

According to procedure A, the reaction of **1a** (58.5 mg, 0.4 mmol), **2g** (63.2 mg, 0.2 mmol) and ZnBr_2 (90 mg, 0.4 mmol) gave three-component product **3t** (98 mg, 91%).

^1H NMR (400 MHz, CDCl_3) δ = 7.41 (d, $J=7.0$, 2H), 7.37 – 7.24 (m, 6H), 7.10 (d, $J=6.9$, 2H), 6.99 (dd, $J=8.1$, 1.6, 1H), 6.73 (d, $J=1.6$, 1H), 6.60 (d, $J=14.2$, 1H), 6.52 – 6.29 (m, 2H), 5.00 (d, $J=15.8$, 1H), 4.60 (dd, $J=11.9$, 4.4, 1H), 4.49 – 4.34 (m, 3H), 3.44 (s, 1H).

^{13}C NMR (100 MHz, CDCl_3) δ = 177.1, 144.5, 138.8, 135.1, 134.3, 129.2, 128.6, 128.3, 128.2, 127.9, 127.5, 127.1, 126.9, 126.0, 124.1, 112.9, 111.6, 80.7, 65.8, 55.4, 44.3.

HRMS (ESI) m/z : calcd. for $\text{C}_{25}\text{H}_{22}\text{NO}_3\text{Br}_2$ ($\text{M}+\text{H}$) $^+$ 541.9966, found 541.9966.



(S*)-1-benzyl-3-((S*,E)-4-bromo-1-hydroxy-2-phenylbut-3-en-2-yl)-5-fluoro-3-hydroxyindolin-2-one (3u)

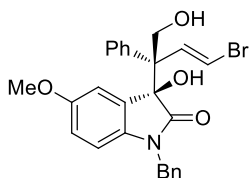
According to procedure A, the reaction of **1a** (58.5 mg, 0.4 mmol), **2h** (51 mg, 0.2 mmol) and ZnBr₂ (90 mg, 0.4 mmol) gave three-component product **3u** (91 mg, 94%).

¹H NMR (400 MHz, CDCl₃) δ 7.43 (d, *J* = 7.2 Hz, 2H), 7.38 – 7.22 (m, 6H), 7.09 (d, *J* = 6.9 Hz, 2H), 6.85 (td, *J* = 8.7, 2.6 Hz, 1H), 6.60 (d, *J* = 14.1 Hz, 1H), 6.54 – 6.41 (m, 2H), 6.27 (d, *J* = 6.7 Hz, 1H), 5.02 (d, *J* = 15.8 Hz, 1H), 4.67 (s, 1H), 4.63 (dd, *J* = 12.0, 4.3 Hz, 1H), 4.50 – 4.36 (m, 2H), 3.81 – 3.70 (m, 1H).

¹³C NMR (100 MHz, CDCl₃) δ 177.1, 160.2, 157.8, 139.02, 139.00, 138.7, 135.2, 134.6, 129.7, 129.6, 129.1, 128.6, 128.3, 128.2, 127.8, 127.1, 116.6, 116.4, 114.6, 114.4, 111.5, 110.2, 110.1, 81.20, 81.19, 65.9, 55.5, 44.4.

¹⁹F NMR (376 MHz, CDCl₃) δ -118.8.

HRMS (ESI) *m/z*: calcd. for C₂₅H₂₁NO₃BrFNa (M+Na)⁺ 504.0587, found 504.0588.



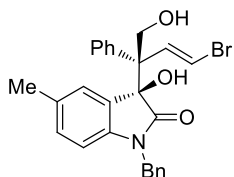
(S*)-1-benzyl-3-((S*,E)-4-bromo-1-hydroxy-2-phenylbut-3-en-2-yl)-3-hydroxy-5-methoxyindolin-2-one (3v)

According to procedure A, the reaction of **1a** (58.5 mg, 0.4 mmol), **2i** (53.5 mg, 0.2 mmol) and ZnBr₂ (90 mg, 0.4 mmol) gave three-component product **3v** (84 mg, 85%).

¹H NMR (400 MHz, CDCl₃) δ 7.53 – 7.42 (m, 2H), 7.34 – 7.23 (m, 6H), 7.14 (d, *J* = 7.1 Hz, 2H), 6.68 – 6.58 (m, 2H), 6.47 (d, *J* = 8.6 Hz, 1H), 6.33 (d, *J* = 13.9 Hz, 1H), 5.96 (s, 1H), 5.04 (d, *J* = 15.7 Hz, 1H), 4.71 (dd, *J* = 11.9, 4.0 Hz, 1H), 4.57 (s, 1H), 4.43 (d, *J* = 15.7 Hz, 1H), 4.29 (dd, *J* = 11.9, 7.5 Hz, 1H), 4.23 – 4.09 (m, 1H), 3.45 (d, *J* = 11.1 Hz, 3H).

¹³C NMR (100 MHz, CDCl₃) δ 177.4, 155.8, 139.4, 136.3, 135.3, 134.9, 129.1, 129.0, 128.8, 128.2, 128.0, 127.7, 127.2, 115.6, 112.6, 111.5, 110.28, 81.2, 65.8, 55.7, 55.4, 44.4.

HRMS (ESI) *m/z*: calcd. for C₂₆H₂₅NO₄Br (M+H)⁺ 494.0967, found 494.0957.



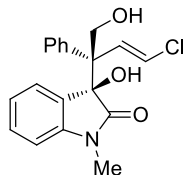
(S*)-1-benzyl-3-((S*,E)-4-bromo-1-hydroxy-2-phenylbut-3-en-2-yl)-3-hydroxy-5-methylindolin-2-one (3w)

According to procedure A, the reaction of **1a** (58.5 mg, 0.4 mmol), **2j** (50.3 mg, 0.2 mmol) and ZnBr₂ (90 mg, 0.4 mmol) gave three-component product **3w** (86 mg, 90%).

¹H NMR (400 MHz, CDCl₃) δ 7.41 – 7.23 (m, 8H), 7.13 – 7.05 (m, 2H), 6.97 – 6.92 (m, 1H), 6.63 (d, *J* = 14.1 Hz, 1H), 6.51 (d, *J* = 14.0 Hz, 1H), 6.47 (d, *J* = 8.0 Hz, 1H), 6.28 (s, 1H), 5.01 (d, *J* = 15.7 Hz, 1H), 4.70 (dd, *J* = 12.0, 4.1 Hz, 1H), 4.45 (d, *J* = 15.7 Hz, 1H), 4.33 (dd, *J* = 12.0, 7.0 Hz, 1H), 4.12 (s, 1H), 3.81 – 3.71 (m, 1H), 2.10 (s, 3H).

¹³C NMR (100 MHz, CDCl₃) δ 177.3, 140.7, 139.1, 135.4, 135.0, 132.6, 130.4, 129.0, 128.7, 128.1, 127.9, 127.8, 127.6, 127.1, 127.1, 111.4, 109.3, 81.1, 65.8, 55.8, 44.3, 21.0.

HRMS (ESI) *m/z*: calcd. for C₂₆H₂₄NO₃BrNa (M+Na)⁺ 500.0837, found 500.0863.

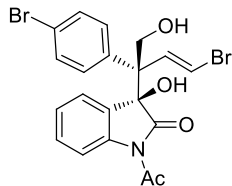


(S*)-3-((S*,E)-4-chloro-1-hydroxy-2-phenylbut-3-en-2-yl)-3-hydroxy-1-methylindolin-2-one (3x) According to procedure A, the reaction of **1a** (58.5 mg, 0.4 mmol), **2k** (32.2 mg, 0.2 mmol) and ZnBr₂ (90 mg, 0.4 mmol) gave three-component product **3x** (53.6 mg, 78%).

¹H NMR (400 MHz, CDCl₃) δ 7.43 – 7.35 (m, 2H), 7.31 – 7.26 (m, 4H), 6.88 (td, *J* = 7.6, 0.9 Hz, 1H), 6.72 (d, *J* = 7.8 Hz, 1H), 6.59 (d, *J* = 7.3 Hz, 1H), 6.39 (d, *J* = 13.8 Hz, 1H), 6.11 (d, *J* = 13.9 Hz, 1H), 4.60 (dd, *J* = 11.9, 5.3 Hz, 1H), 4.35 (dd, *J* = 11.9, 7.2 Hz, 1H), 4.01 (s, 1H), 3.40 (dd, *J* = 6.8, 5.5 Hz, 1H), 3.05 (s, 3H).

¹³C NMR (100 MHz, CDCl₃) δ 177.1, 143.7, 139.0, 131.3, 130.3, 128.6, 128.0, 127.9, 127.7, 126.0, 123.2, 122.9, 108.3, 81.5, 65.8, 54.5, 26.1.

HRMS (ESI) *m/z*: calcd. for C₁₉H₁₈NO₃ClNa (M+Na)⁺ 366.0867, found 366.0867



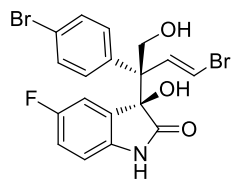
(S*)-1-acetyl-3-((S*,E)-4-bromo-2-(4-bromophenyl)-1-hydroxybut-3-en-2-yl)-3-hydroxyindolin-2-one (3y)

According to procedure A, the reaction of **1a** (58.5 mg, 0.4 mmol), **2l** (37.8 mg, 0.2 mmol) and ZnBr₂ (90 mg, 0.4 mmol) gave three-component product **3y** (77 mg, 78%).

¹H NMR (400 MHz, CDCl₃) δ 8.93 (s, 1H), 8.17 (d, *J* = 8.0 Hz, 1H), 7.58 (d, *J* = 8.6 Hz, 2H), 7.46 (t, *J* = 7.5 Hz, 1H), 7.25 (s, 1H), 7.17 (t, *J* = 7.6 Hz, 1H), 7.03 (d, *J* = 7.5 Hz, 1H), 6.10 (d, *J* = 13.9 Hz, 1H), 6.00 (d, *J* = 13.9 Hz, 1H), 4.74 (d, *J* = 10.3 Hz, 1H), 4.19 (d, *J* = 10.3 Hz, 1H), 4.01 (s, 1H), 2.11 (s, 3H).

¹³C NMR (100 MHz, CDCl₃) δ 175.5, 167.9, 137.9, 135.0, 132.9, 131.9, 131.2, 130.5, 126.8, 125.3, 124.6, 123.6, 123.1, 112.2, 84.3, 70.5, 59.5, 24.9.

HRMS (ESI) *m/z*: calcd. for C₂₀H₁₇NO₄Br₂Na (M+Na)⁺ 515.9422, found 515.9458.



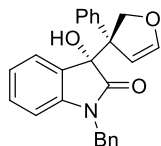
(S*)-3-((S*,E)-4-bromo-2-(4-bromophenyl)-1-hydroxybut-3-en-2-yl)-5-fluoro-3-hydroxyindolin-2-one (3z)

According to procedure A, the reaction of **1a** (58.5 mg, 0.4 mmol), 5-fluoroisatin (33 mg, 0.2 mmol) and ZnBr₂ (90 mg, 0.4 mmol) gave three-component product **3z** (73.5 mg, 85%).

¹H NMR (400 MHz, MeOD) δ 7.51 – 7.30 (m, 4H), 6.96 (td, *J* = 8.9, 2.6 Hz, 1H), 6.74 (dd, *J* = 8.5, 4.3 Hz, 1H), 6.55 (d, *J* = 14.0 Hz, 1H), 6.45 (d, *J* = 13.8 Hz, 1H), 6.15 (d, *J* = 6.7 Hz, 1H), 4.68 (d, *J* = 11.7 Hz, 1H), 4.45 (d, *J* = 11.7 Hz, 1H).

¹³C NMR (100 MHz, MeOD) δ 180.7, 159.8 (d, *J* = 239.2 Hz), 139.5, 139.3 (d, *J* = 1.8 Hz), 137.0, 132.4, 132.3, 131.8, 122.6, 117.2 (d, *J* = 23.6 Hz), 114.9 (d, *J* = 25.6 Hz), 111.6 (d, *J* = 7.9 Hz), 111.4, 82.0, 63.1, 57.7.

HRMS (ESI) *m/z*: calcd. for C₁₈H₁₄NO₃Br₂FNa (M+Na)⁺ 491.9222, found 491.9196.



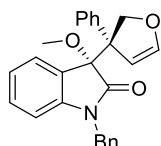
(R*)-1-benzyl-3-hydroxy-3-((S*)-3-phenyl-2,3-dihydrofuran-3-yl)indolin-2-one (4a)

According to procedure B, the Rh₂(esp)₂-catalyzed reaction of **1a** (44 mg, 0.3 mmol), **2a** (47.5 mg, 0.2 mmol) provided **4a** (60%, determined by ¹H NMR). Scale-up reaction (with 1 mmol **2a**) gave isolated major isomer of **4a** in 30% yield (115 mg).

¹H NMR (500 MHz, CDCl₃) δ 7.53 (d, *J* = 7.0 Hz, 1H), 7.23 – 7.14 (m, 3H), 7.14 – 6.98 (m, 5H), 6.90 – 6.71 (m, 5H), 6.30 (d, *J* = 7.4 Hz, 1H), 5.97 (d, *J* = 10.0 Hz, 1H), 5.65 (s, 1H), 4.63 (d, *J* = 9.9 Hz, 1H), 4.55 (d, *J* = 15.9 Hz, 1H), 4.48 (d, *J* = 15.9 Hz, 1H), 3.15 (s, 1H).

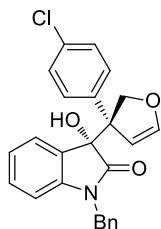
¹³C NMR (125 MHz, CDCl₃) δ 176.6, 149.8, 142.6, 140.2, 134.9, 129.7, 129.0, 128.6, 127.9, 127.9, 127.4, 127.00, 126.98, 124.2, 122.6, 109.3, 100.2, 79.2, 75.5, 62.4, 43.8.

HRMS (ESI) *m/z*: calcd. for C₂₅H₂₂NO₃ (M+H)⁺ 384.1594, found 384.1593.



(R*)-1-benzyl-3-methoxy-3-((S*)-3-phenyl-2,3-dihydrofuran-3-yl)indolin-2-one (4a')

According to the Procedure B, major isomer of **4a'** was obtained (41 mg, 52%). ¹H NMR (400 MHz, CDCl₃) δ 7.40 – 7.17 (m, 12H), 6.93 (t, *J* = 7.5 Hz, 1H), 6.70 (d, *J* = 7.8 Hz, 1H), 6.37 (d, *J* = 1.9 Hz, 1H), 5.54 – 5.48 (m, 1H), 5.14 (d, *J* = 15.8 Hz, 1H), 4.85 (d, *J* = 16.0 Hz, 1H), 4.83 – 4.77 (m, 1H), 4.32 (ddd, *J* = 11.9, 5.9, 2.2 Hz, 1H), 3.17 (s, 3H). ¹³C NMR (125 MHz, CDCl₃) δ 175.0, 144.3, 142.4, 135.6, 131.9, 129.9, 128.73, 128.69, 128.5, 127.5, 127.2, 126.0, 125.5, 124.1, 122.3, 119.1, 109.3, 90.4, 85.1, 76.0, 53.5, 43.9. HRMS (ESI) *m/z*: calcd. for C₂₆H₂₃NO₃Na (M+Na)⁺ 420.1570, found 420.1575.



(R*)-1-benzyl-3-((S*)-3-(4-chlorophenyl)-2,3-dihydrofuran-3-yl)-3-hydroxyindolin-2-one (4b)

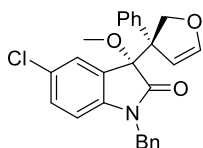
According to procedure B, the Rh₂(esp)₂-catalyzed reaction of **1a** (44 mg, 0.3 mmol), **2a** (47.5

mg, 0.2 mmol) provided **4c** (55%, determined by ^1H NMR). Rapid purification on silica gel and recrystallization (hexane/DCM) gave pure major isomer of **4b** in 28% yield (24 mg).

^1H NMR (400 MHz, CDCl_3) δ 7.53 (dd, $J = 7.4, 0.8$ Hz, 1H), 7.26 – 7.21 (m, 3H), 7.14 (td, $J = 7.7, 1.3$ Hz, 1H), 7.05 (td, $J = 7.6, 1.0$ Hz, 1H), 7.01 – 6.92 (m, 2H), 6.80 (dd, $J = 7.2, 2.1$ Hz, 2H), 6.78 – 6.66 (m, 3H), 6.39 (d, $J = 7.6$ Hz, 1H), 5.94 (d, $J = 10.1$ Hz, 1H), 5.59 (d, $J = 2.8$ Hz, 1H), 4.71 (d, $J = 15.8$ Hz, 1H), 4.56 (d, $J = 10.1$ Hz, 1H), 4.44 (d, $J = 15.8$ Hz, 1H), 3.05 (s, 1H).

^{13}C NMR (100 MHz, CDCl_3) δ 176.4, 150.1, 142.7, 138.8, 134.7, 133.0, 129.9, 129.3, 128.7, 128.7, 128.0, 127.6, 127.0, 124.2, 122.7, 109.5, 99.8, 78.9, 75.4, 62.0, 43.9.

HRMS (ESI) m/z : calcd. for $\text{C}_{25}\text{H}_{20}\text{NO}_3\text{ClNa} (\text{M}+\text{Na})^+$ 440.1029, found 440.1015.



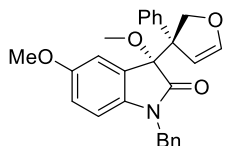
(R*)-1-benzyl-6-chloro-3-methoxy-3-((S*)-3-phenyl-2,3-dihydrofuran-3-yl)indolin-2-one (4c')

According to procedure B, after completion of $\text{Rh}_2(\text{esp})_2$ -catalyzed reaction of **1a** (44 mg, 0.3 mmol), **2d** (54.3 mg, 0.2 mmol), the mixture was concentrated, resolved in dried THF (2 mL), and treated with NaH (25 mg) and MeI (52 μL) for 1 h. Work-up and purification provided **4c'** (41 mg, 50%).

^1H NMR (400 MHz, CDCl_3) δ 7.40 – 7.27 (m, 10H), 7.14 (d, $J = 7.9$ Hz, 1H), 6.91 (dd, $J = 7.9, 1.6$ Hz, 1H), 6.69 (d, $J = 1.7$ Hz, 1H), 6.39 (d, $J = 1.9$ Hz, 1H), 5.52 – 5.45 (m, 1H), 5.12 (d, $J = 15.9$ Hz, 1H), 4.87 – 4.77 (m, 2H), 4.34 (ddd, $J = 12.0, 5.9, 2.2$ Hz, 1H), 3.15 (s, 3H).

^{13}C NMR (100 MHz, CDCl_3) δ 175.1, 145.6, 142.6, 135.8, 135.0, 131.7, 128.9, 128.8, 128.7, 127.8, 127.1, 126.4, 126.0, 122.5, 122.3, 118.8, 109.9, 90.3, 84.8, 76.1, 53.5, 44.0.

HRMS (ESI) m/z : calcd. for $\text{C}_{26}\text{H}_{22}\text{NO}_3\text{ClNa} (\text{M}+\text{Na})^+$ 454.1180, found 454.1170.



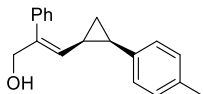
(R*)-1-benzyl-3,5-dimethoxy-3-((S*)-3-phenyl-2,3-dihydrofuran-3-yl)indolin-2-one (4d')

According to procedure B, after completion of $\text{Rh}_2(\text{esp})_2$ -catalyzed reaction of **1a** (44 mg, 0.3 mmol), **2i** (53.4 mg, 0.2 mmol), the mixture was concentrated, resolved in dried THF (3 mL), and treated with NaH (25 mg) and MeI (50 μL) for 1 h. Work-up and purification provided **4d'** (68 mg, 77%).

^1H NMR (500 MHz, CDCl_3) δ 7.36 – 7.27 (m, 7H), 7.25 – 7.20 (m, 3H), 6.83 (d, $J = 2.6$ Hz, 1H), 6.71 (dd, $J = 8.5, 2.6$ Hz, 1H), 6.56 (d, $J = 8.5$ Hz, 1H), 6.34 (q, $J = 2.0$ Hz, 1H), 5.50 – 5.44 (m, 1H), 5.09 (d, $J = 15.8$ Hz, 1H), 4.85 – 4.75 (m, 2H), 4.35 (ddd, $J = 11.9, 5.9, 2.3$ Hz, 1H), 3.51 (s, 3H), 3.15 (s, 3H).

^{13}C NMR (125 MHz, CDCl_3) δ 174.7, 155.5, 142.5, 137.6, 135.7, 131.9, 128.7, 128.5, 127.5, 127.2, 125.9, 125.4, 119.1, 115.3, 111.9, 109.8, 90.4, 85.4, 76.0, 55.6, 53.5, 44.0.

LC-MS (ESI) m/z : C₂₇H₂₅NO₄Na (M+Na)⁺ 450.19.



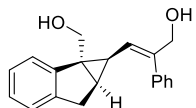
(E)-2-phenyl-3-((1R*,2R*)-2-(p-tolyl)cyclopropyl)prop-2-en-1-ol (5)

According to procedure B, **5** was obtained as a colourless liquid (34 mg, 65%).

¹H NMR (500 MHz, CDCl₃) δ 7.41 – 7.33 (m, 4H), 7.32 – 7.26 (m, 1H), 7.15 – 7.07 (m, 4H), 5.01 (d, J = 10.1 Hz, 1H), 4.22 – 4.09 (m, 2H), 2.33 (s, 3H), 2.27 (dd, J = 15.1, 8.5 Hz, 1H), 1.83 (td, J = 10.0, 8.6, 5.6 Hz, 1H), 1.29 (s, 1H), 1.25 – 1.19 (m, 1H), 1.03 (dd, J = 11.6, 5.4 Hz, 1H).

¹³C NMR (125 MHz, CDCl₃) δ 140.1, 138.7, 135.6, 135.5, 129.1, 128.93, 128.91, 128.86, 128.4, 127.1, 67.9, 23.8, 21.1, 19.0, 13.2.

LC-MS (ESI) m/z : C₁₉H₂₀ONa (M+Na)⁺ 287.07.



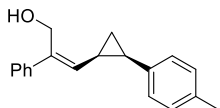
(E)-3-((1S*,1aS*,6aR*)-1a-(hydroxymethyl)-1,1a,6,6a-tetrahydrocyclopropa[a]inden-1-yl)-2-phenylprop-2-en-1-ol (6)

To an oven-dried test tube with a septum were loaded with Rh₂(esp)₂ (7.6 mg, 0.01 mmol) and **1a** (58 mg, 0.4 mmol). CH₂Cl₂ (2 mL) was then added and the reaction was stirred for 1 h at 25 °C. The mixture was concentrated to give a residue, and purified on silica gel to provide **6** (46 mg, 78%, >95:5 dr).

¹H NMR (400 MHz, CDCl₃) δ 7.43 – 7.35 (m, 3H), 7.35 – 7.27 (m, 3H), 7.24 – 7.14 (m, 3H), 4.82 (d, J = 8.7 Hz, 1H), 4.17 (dd, J = 13.0, 5.4 Hz, 1H), 4.12 – 4.02 (m, 2H), 3.80 (dd, J = 11.6, 6.8 Hz, 1H), 3.21 (dd, J = 17.5, 6.7 Hz, 1H), 2.92 (d, J = 17.5 Hz, 1H), 2.02 (t, J = 7.6 Hz, 1H), 1.93 (t, J = 8.7 Hz, 1H), 1.33 (s, 1H), 1.22 (t, J = 6.0 Hz, 1H).

¹³C NMR (100 MHz, CDCl₃) δ 144.2, 143.4, 142.2, 138.7, 128.7, 128.5, 127.4, 126.6, 124.4, 123.9, 123.0, 67.8, 65.8, 44.6, 31.6, 29.1, 26.7.

See **Fig. Suppl. 89** for x-ray structure.

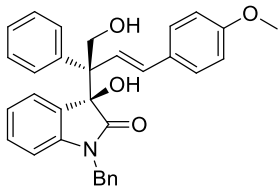


(Z)-2-phenyl-3-((1R*,2R*)-2-(p-tolyl)cyclopropyl)prop-2-en-1-ol (Z-5)

¹H NMR (400 MHz, CDCl₃) δ 7.30 – 7.18 (m, 5H), 7.17 – 7.09 (m, 4H), 5.27 (d, J = 9.4 Hz, 1H), 4.70 (s, 2H), 2.49 (dd, J = 15.3, 8.4 Hz, 1H), 2.34 (s, 3H), 2.19 (ddd, J = 17.7, 8.8, 5.6 Hz, 1H), 1.29 (s, 1H), 1.46 (td, J = 8.4, 5.1 Hz, 1H), 1.12 (dd, J = 11.5, 5.6 Hz, 1H).

¹³C NMR (125 MHz, CDCl₃) δ 140.7, 139.1, 135.7, 135.2, 132.1, 128.90, 128.89, 128.4, 126.9, 126.0, 60.5, 23.94, 21.1, 18.4, 13.5.

HRMS (ESI) m/z : calcd. for C₁₉H₂₀ONa (M+Na)⁺ 287.1406, found 287.1400.



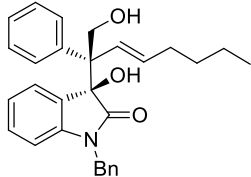
(*S)-1-benzyl-3-hydroxy-3-((*S**,*E*)-1-hydroxy-4-(4-methoxyphenyl)-2-phenylbut-3-en-2-yl)indolin-2-one (7a)**

A mixture of **3c** (102 mg, 0.2 mmol), *p*-methoxyphenylboronic acid (62 mg, 0.4 mmol), Pd(PPh₃)₄ (12 mg, 5 mol%), Na₂CO₃ (2 M, 0.3 mL), CH₃OH (1 mL) and toluene (3 mL) was heated at 50 °C under Ar for 10 h. After dilution and extraction with ethyl acetate, the combined extracts were washed with H₂O and brine successively. After drying over Na₂SO₄, filtration, and evaporation, the residue was purified by column chromatography on silica gel to give **7a** (58.2 mg, 60%).

¹H NMR (400 MHz, CDCl₃) δ 7.60 – 7.51 (m, 2H), 7.43 – 7.30 (m, 3H), 7.20 – 7.16 (m, 2H), 7.13 – 7.08 (m, 2H), 6.86 – 6.78 (m, 3H), 6.65 (d, *J* = 8.3 Hz, 2H), 6.50 (d, *J* = 7.4 Hz, 2H), 6.46 – 6.40 (m, 2H), 5.42 – 5.29 (m, 1H), 5.03 – 4.90 (m, 2H), 4.65 (d, *J* = 11.1 Hz, 1H), 4.55 (d, *J* = 10.8 Hz, 1H), 4.22 (d, *J* = 16.0 Hz, 1H), 3.82 (s, 1H), 3.78 (s, 1H), 3.76 (s, 3H).

¹³C NMR (100 MHz, CDCl₃) δ 178.0, 159.0, 143.4, 142.8, 141.9, 134.8, 130.0, 129.8, 129.22, 129.17, 128.5, 128.4, 127.5, 127.2, 126.6, 126.5, 125.3, 122.9, 116.1, 114.8, 113.9, 109.7, 79.1, 60.6, 55.1, 51.1, 43.9.

HRMS (ESI) *m/z*: calcd. for C₃₂H₂₉NO₄Na (M+Na)⁺ 514.1989, found 514.1982.



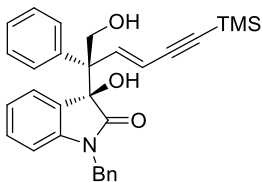
(*S)-1-benzyl-3-hydroxy-3-((*S**,*E*)-1-hydroxy-2-phenyloct-3-en-2-yl)indolin-2-one (7b)**

To a solution of Pd(PPh₃)₄ (6 mg, 5 mol%) and **3c** (51 mg, 0.1 mmol) in 2 mL of anhydrous THF was added n-BuZnBr (1 mL, 0.5 M in THF) and the mixture was stirred at 25 °C for 1 h. After evaporation of solvent, the residue was purified by column chromatography on silica gel to afford **7b** (34.8 mg, 79%) as a white solid.

¹H NMR (500 MHz, CDCl₃) δ 7.66 (dd, *J* = 12.4, 7.6 Hz, 2H), 7.57 – 7.53 (m, 1H), 7.51 (d, *J* = 7.3 Hz, 1H), 7.43 – 7.38 (m, 1H), 7.37 (t, *J* = 7.5 Hz, 2H), 7.29 (d, *J* = 7.3 Hz, 4H), 7.20 (td, *J* = 7.8, 0.9 Hz, 1H), 7.00 (t, *J* = 7.4 Hz, 1H), 6.75 (d, *J* = 7.8 Hz, 1H), 5.86 (d, *J* = 11.0 Hz, 1H), 5.04 (d, *J* = 15.6 Hz, 1H), 4.97 (s, 1H), 4.78 (d, *J* = 11.5 Hz, 1H), 4.67 (d, *J* = 15.6 Hz, 1H), 4.50 (dd, *J* = 11.6, 5.3 Hz, 1H), 3.56 (s, 1H), 3.33 (td, *J* = 10.9, 1.9 Hz, 1H), 1.29 – 1.07 (m, 5H), 0.90 – 0.81 (m, 1H), 0.77 (t, *J* = 6.8 Hz, 3H).

¹³C NMR (125 MHz, CDCl₃) δ 178.5, 144.0, 143.1, 141.8, 135.6, 132.7, 130.8, 129.6, 128.9, 128.8, 128.7, 128.6, 128.5, 127.7, 127.5, 127.4, 126.3, 125.2, 122.9, 109.4, 78.0, 60.8, 46.0, 44.1, 29.7, 29.4, 22.5, 13.9.

HRMS (ESI) *m/z*: calcd. for C₂₉H₃₁NO₃Na (M+Na)⁺ 464.2196, found 464.2194.



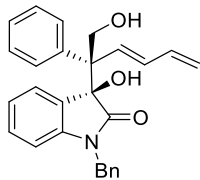
(S*)-1-benzyl-3-hydroxy-3-((S*)-1-hydroxy-2-phenyl-6-(trimethylsilyl)hex-3-en-5-yn-2-yl)indolin-2-one (7c)

A mixture of **3c** (51 mg, 0.1 mmol), TMSC≡CH (30 mg, 0.3 mmol), PdCl₂(PPh₃)₂ (3.5 mg, 5 mol%), CuI (1.9 mg, 10 mol%), Et₃N (0.5 mL) in CH₃CN (3 mL) was stirred at 25 °C under Ar for 5 h. Evaporation and purification by column chromatography on silica gel afforded **7c** (68 mg, 91%) as a white solid.

¹H NMR (400 MHz, CDCl₃) δ 7.55 (d, *J* = 7.3 Hz, 2H), 7.46 – 7.22 (m, 10H), 7.09 (t, *J* = 7.5 Hz, 1H), 6.77 (d, *J* = 7.8 Hz, 1H), 6.05 (d, *J* = 10.5 Hz, 1H), 5.61 (s, 1H), 5.02 (d, *J* = 15.6 Hz, 1H), 4.85 – 4.71 (m, 2H), 4.56 (dd, *J* = 12.2, 5.2 Hz, 1H), 4.42 (d, *J* = 10.4 Hz, 1H), 3.82 (s, 1H), -0.00 (s, 9H).

¹³C NMR (100 MHz, CDCl₃) δ 178.0, 144.1, 143.6, 141.3, 135.5, 129.8, 128.9, 128.7, 128.6, 127.8, 127.8, 127.6, 126.7, 125.6, 125.0, 123.1, 109.3, 102.0, 89.1, 77.7, 60.8, 44.4, 40.2, -0.1.

HRMS (ESI) *m/z*: calcd. for C₃₀H₃₂NO₃Si (M+H)⁺ 482.2146, found 486.2148.



(S*)-1-benzyl-3-hydroxy-3-((S*,E)-1-hydroxy-2-phenylhexa-3,5-dien-2-yl)indolin-2-one (7d)

To a mixture of **3c** (102 mg, 0.2 mmol) and Pd(PPh₃)₂Cl₂ (7 mg, 0.01 mmol) in DMF (4 mL) was added vinyltributyltin (81 mg, 0.4 mmol) and the mixture stirred at 25 °C under Ar for 4 h. The reaction mixture was quenched with water (25 mL) and extracted with CH₂Cl₂ (3×20 mL). The combined organic layer was washed with brine, dried with Na₂SO₄, evaporated under reduced pressure, and purified by silica gel column chromatography (10-30 % EtOAc/hexane) to afford the diene **7d** (58 mg, 70 %).

¹H NMR (500 MHz, CDCl₃) δ 7.49 (d, *J* = 7.4 Hz, 1H), 7.45 – 7.38 (m, 2H), 7.34 – 7.28 (m, 3H), 7.24 (t, *J* = 7.7 Hz, 1H), 7.17 – 7.05 (m, 4H), 6.97 – 6.89 (m, 2H), 6.66 (d, *J* = 7.8 Hz, 1H), 6.37 – 6.27 (m, 1H), 5.42 – 5.33 (m, 2H), 5.27 (d, *J* = 17.4 Hz, 1H), 5.14 (d, *J* = 15.7 Hz, 1H), 4.78 (d, *J* = 12.3 Hz, 1H), 4.54 (d, *J* = 15.7 Hz, 1H), 4.41 – 4.31 (m, 1H), 4.18 (dd, *J* = 10.5, 5.9 Hz, 1H), 3.66 (s, 1H), 3.11 (d, *J* = 9.7 Hz, 1H).

¹³C NMR (100 MHz, CDCl₃) δ 178.3, 143.7, 142.8, 140.9, 134.6, 134.1, 130.1, 128.7, 128.5, 127.9, 127.59, 127.56, 127.1, 126.3, 125.6, 125.3, 123.3, 119.2, 110.0, 78.2, 60.4, 50.0, 44.2. HRMS (ESI) *m/z*: calcd. for C₂₇H₂₅NO₃ (M+Na)⁺ 434.1727, found 432.1727.